3-14-2014

Production Potential of Scandium-47 Using Spallation Neutrons at Los Alamos Isotope Production Facility

Kerriann A. DeLorme

PRODUCTION POTENTIAL OF ^{47}Sc USING SPALLATION NEUTRON FLUX AT THE LOS ALAMOS ISOTOPE PRODUCTION FACILITY

THESIS

K. Austin DeLorme, 1st Lieutenant, United States Air Force

AFIT-ENP-14-M-02

DEPARTMENT OF THE AIR FORCE
AIR UNIVERSITY

AIR FORCE INSTITUTE OF TECHNOLOGY

Wright-Patterson Air Force Base, Ohio

DISTRIBUTION STATEMENT A
APPROVED FOR PUBLIC RELEASE; DISTRIBUTION UNLIMITED

The views expressed in this document are those of the author and do not reflect the official policy or position of the United States Air Force, the United States Department of Defense or the United States Government. This material is declared a work of the U.S. Government and is not subject to copyright protection in the United States.

AFIT-ENP-14-M-02

PRODUCTION POTENTIAL OF ^{47}Sc USING SPALLATION NEUTRON FLUX AT
THE LOS ALAMOS ISOTOPE PRODUCTION FACILITY

THESIS

Presented to the Faculty

Department of Engineering Physics

Graduate School of Engineering and Management

Air Force Institute of Technology

Air University

Air Education and Training Command

in Partial Fulfillment of the Requirements for the

Degree of Master of Science

K. Austin DeLorme, BS

1st Lieutenant, United States Air Force

March 2014

PRODUCTION POTENTIAL OF ^{47}SC USING SPALLATION NEUTRON FLUX AT
THE LOS ALAMOS ISOTOPE PRODUCTION FACILITY

K. Austin DeLorme, BS
1st Lieutenant, United States Air Force

Approved:

//signed//	6 March 2014
Maj Benjamin Kowash, PhD (Chairman)	Date
//signed//	14 March 2014
LTC Stephen McHale, PhD (Member)	Date
//signed//	10 March 2014
Dr. Jonathan Engle, PhD (Member)	Date
//signed//	14 March 2014
Dr. Justin Clinton, PhD (Member)	Date

Abstract

Scandium-47 ($T_{1/2} = 3.41d$) forms stable complexes with aminopolycarboxylic acids, such as folate conjugates, which are useful as tumor biomarkers or antigens. Its therapeutic beta emissions at 441.1 keV ($E_{\beta-,max}$, $I_{\beta-} = 68\%$) and 600.5 keV$_{max}$ ($E_{\beta-,max}$, $I_{\beta-} = 32\%$) are coupled with an imageable 159.4 keV gamma to permit in vivo-tracking of compound biodistribution. Currently, its wider clinical application is hindered by lack of availability, even as interest grows in radioscandium-based pharmaceuticals thanks to the successful development of ^{44}Sc (94.27% $\beta+$; $T_{1/2} = 3.97h$) imaging agents. We have investigated the ^{47}Ti(n,np) ^{47}Sc, ^{50}Ti(n,3p) ^{47}Sc, ^{nat}V(n,x)^{47}Sc, and ^{nat}Ti(n,x)^{47}Sc reactions as potential routes to therapeutically relevant quantities of ^{47}Sc. Targets of ^{nat}V, ^{nat}Ti, and enriched ^{47}Ti (95.7% isotopic abundance) and ^{50}Ti (83.1%) oxide targets were exposed to the spallation neutrons resulting from the proton-irradiation of RbCl and Ga targets at the Los Alamos National Laboratory (LANL) Isotope Production Facility (IPF). Targets were activated for 1 hr using an average proton beam current of 218±14 μAh incident on IPF targets. Derived production rates for ^{47}Sc, expressed as activity created per gram of target material and per Ah of incident proton beam, are 0.146±.005 μCi g^{-1} μAh^{-1} in the ^{nat}V foil, 0.44±0.01 μCi g^{-1} μAh^{-1} in the ^{nat}Ti foil, and 0.21±0.09 μCi g^{-1} μAh^{-1} and 0.34±0.2 μCi g^{-1} μAh^{-1} in the ^{47}Ti and ^{50}Ti-oxide samples, respectively. Radioisotopic purities of ^{47}Sc in excess of 90% are achieved by activation of ^{47}Ti targets, and small yields of ^{47}Ca produce ^{47}Sc with 100% radioisotopic purity from activation of ^{50}Ti. Yields and neutron fluxes predicted by MCNP6 event generators and evaluated nuclear data are also compared with the results of these activation experiments.

Dedicated to the SlaughterHaus. Thanks.

Acknowledgements

As with anything, this work was the product of a lot of effort and assistance from many wonderful people I was fortunate enough to interact with throughout this process. I'd like to start by acknowledging Col John Weidner, my initial advisor whom introduced me to the Isotope Production Facility and opened the door to this great opportunity. I would also like to thank Maj Benjamin Kowash for taking on my project, despite its peculiarity in the AFIT setting, and for his assistance along the way. This goes, as well, to my AFIT committee members, LTC Stephen McHale, and Dr. Justin Clinton.

I would like to give a special thank you to Dr. Jon Engle for all of his time, effort and the exceptional mentorship he provided me with throughout this entire process. The patience and time commitment he put into working with me was beyond my expectations. I'm exceedingly grateful for his persistently thoughtful responses to every phone call and email, as I flooded his inbox regularly.

Along with Jon, I would like to acknowledge the entirety of the Inorganic, Isotope and Actinide Chemistry (C-IIAC) Division at Los Alamos. Meiring Nortier also took a great deal of time to mentor and assist this effort. It was an honor to be able to learn from Meiring's knowledge and vast experience in the field. Dr. Eva Birnbaum was an invaluable asset both programmatically and academically–this experiment would have never gone forward without her efforts. The same may be said for Dr. Kevin John whose oversight ensured the project was properly supported.

There are several individuals at Los Alamos who were invaluable to the experimental process. Wayne Taylor who kept three young physicists from causing too much chaos in our attempts to do black magic (a.k.a. chemistry), and who consistently offered his experience and assistance. Lauren Marus, who spent hours carefully measuring and preparing samples, as well as working on numerous other parts of the experiment. As well, Dr. Kevin Jackman who manned the count room and ensured data was properly

2

and accurately acquired and provided.

Additionally I'd like to thank Dr. Hong Bach, Dave Reass and Michael Connors for their assistance at IPF during preparation, irradiation and target transport. I'd like to acknowledge Luke Daemen for his assistance in mentorship in the art of blowing glass, as well as Art and Dave in the machine shop. I'd also like to thank the entire crew of the Hot Cell Laboratory for all of their efforts. There were numerous other individuals with whom I interacted while in Los Alamos – as a whole, thank you for your time, assistance and kindness.

I would like to thank my older brother, for pausing his life every time I called to help mediate my relationship with my computer. Finally I would like to acknowledge my entire wonderful family for their continued love and support.

Last but not least, I need to extend a special thank you to the Slaughters for everything they have done for me over the last year and a half–from late night talks about "what could possibly be making a mess of these peaks!" to yogurt dates when one more MCNP error would have sent me over the edge. It's a blessing to have a family away from home.

There are never enough words to catch it all - so I'll conclude with a simple, "Thanks."

K. Austin DeLorme

Table of Contents

4

5

6

List of Figures

7

Figure   Page

8

Figure   Page

9

List of Tables

Table   Page

PRODUCTION POTENTIAL OF ^{47}Sc USING SPALLATION NEUTRON FLUX AT
THE LOS ALAMOS ISOTOPE PRODUCTION FACILITY

1. Introduction

1.1   Background

Radioisotopes are an invaluable asset to the medical community. Nuclear medicine
can use radiation for the extraction of diagnostic information and radiotherapy can be
used to treat medical conditions. According to the World Nuclear Association, tens of
millions of procedures requiring radioisotopes are performed annually as a part of an
ever-increasing demand [1].

Currently, leading research in advanced cancer treatment looks to nuclear medicine
as a key. According to census data from the Center for Disease Control and Prevention,
malignant cancer is the second leading cause of death in the United States. In 2010 it
accounted for nearly one in every fourth deaths [2]. The magnitude of its impact on
human life is what drives persistent investigations on new treatments.

There are many treatment options available, including surgery, chemotherapy, im-
munotherapy and radiotherapy options. The method of treatment is generally selected
based on the type, location and progression of a particular case. Ideal cancer therapy
is described by the targeted concept, such that cancer cells are attcked while the nor-
mal, healthy cells are left unscathed [3]. Targeted radiotherapy is one option under
investigation.

Targeted radiotherapy has many advantages over other options. As with targeted
chemotherapy, it results in less severe side effects than its traditional counterpart. This

1

method also allows for the use of more destructive means of radiation as compared to external beam therapy. Alpha and beta particles have a higher linear energy transfer than gamma radiation leading to a larger quality factor, Q, and therefore a larger dose equivalent [3] [4].

The goal of targeted radiotherapy is to attach a radioisotope to biological molecules that naturally seek out rapidly growing cancer cells. The constraints on a beta-emitting isotope include an energy corresponding to a mean free path on the order of μms, and a half-life corresponding to the biological life of the bio-molecule to which it is attached [5] [6] [7]. This work investigates scandium-47 (^{47}Sc), which has uses in both diagnostic imaging, as well as potential for targeted radiotherapy.

1.1.1 Scandium-47.

^{47}Sc is a medium energy beta-emitting isotope with a strong, independent gamma-line. The gamma energy at 159.38 keV makes it an ideal isotope for medical imaging. Due to its similar chemical properties to rare earth elements such as Sm, Lu, Ho, etc, it has the ability to form complexes of reasonable stability to aminopolycarboxylic acids. This coupled with its beta energies of 441.1 keV and 600.5 keV (max) , gives it great potential for endo-radiotherapy [6]. It also has a unique property of having a theragnostic pair in ^{44}Sc, a positron emitting isotope (511 keV) with a 2.4 day half-life. A theragnostic pair is a set of sources, one used for diagnostic imaging, such as ^{44}Sc, and another used for theraputic application, such as ^{47}Sc, which have the same chemical properties. Using a diagnostic source with the same chemical properties of the therapy source allows for proper prediction of biodistribution and dosimetry [25].

2

1.2 Research Objective

The objective of this experiment is to leverage the neutrons generated from the proton irradiation of the Isotope Production Facility's (IPF) primary target stack for the production of ^{47}Sc. IPF is one of the five major facilities powered by the Los Alamos Neutron Science Center (LANSCE) 800 MeV accelerator. IPF is a unique set-up of 100 MeV proton beam irradiating a target stack of RbCl and Ga. Of primary interest for ^{47}SC production is the unique neutron flux that results from this unique beam/target structure [8].

1.3 Summary

The remainder of this document is organized as follows: First, an overview of the LANSCE and IPF Facilities, followed by a review of previous ^{47}Sc production efforts. Next, potential production methods available via the facility resources will be explained. Modeling efforts will then be discussed to include the target selection and expected outcomes. Finally the experimental set up and procedure will be given, followed by an analysis of the resulting data.

3

2. Theory

The utility of the isotope and programmatic constraints were the primary factors considered for isotope selection. From a utility prospective, particularly in the medical community, there are two primary uses to consider: diagnostic imaging and radiotherapy [9] [10].

In regards to programmatic considerations, LANSCE has the ability to allow for production through direct proton irradiation or from residual neutron irradiation. The benefits of neutron irradiation are cost and scheduling, as they can take place without interrupting standard procedures at IPF for an appreciable amount of time. IPF has a regular schedule for production of ^{68}Ge and ^{82}Sr for the medical community. It is the irradiation of RbCl and Ga target stacks that generates the spallation neutrons used in a neutron irradiation experiment, thus avoiding the interruption of the production cycle.

2.0.1 Radioactive Isotopes in Medicine.

Radioactive isotopes are used for both diagnostic imaging and therapeutic applications in medicine. Numerous diagnostic applications exist that include the investigation of cardiac output, pancreatic function studies and tumor localization [9]. The exact use of a radioisotope will be dependent on both nuclear and chemical properties. The chemical and biologic behavior will determine which system may be investigated. Rate of decay, radiations emitted, and total dose absorbed will also contribute to the proper selection of a pharmaceutical [9] [10].

The two most common forms of diagnostic imaging are positron emission tomography (PET) and single-photon emission computed tomography (SPECT). PET requires proton heavy isotopes that decay via positive beta decay, resulting in an annihilation and the subsequent emission of two coincident gamma rays,

4

$$\,^{n}_{m}X = \,^{n}_{m-1}Y + e^{+} + v_{e}. \tag{1}$$

Through this process three-dimensional images may be reconstructed through co-incidence detection of 511 keV gammas released from positron annihilation. SPECT also produces three-dimensional images, in this case, using multiple projections from gamma camera data. SPECT uses internal radionuclides with low energy gamma emission. Two-dimensional imaging may also be accomplished using gamma cameras and non-coincident photon emitters (scintigraphy) [10].

There are also several therapeutic applications for radioactive nuclides, primarily for the reduction of malignant masses. Other applications include thyroid gland disorders, and the treatment of blood dyscrasias [9] [10]. The nuclear characteristics of theraputic isotopes for these applications vary depending on their application.

Considerations to be made in selecting the proper radioactive nuclide for a given medical application include:

- **Characteristics of the emissions** (types, energies and fractionation). For non-PET imaging, 100-400 keV gamma ray emissions are ideal due to the balance between the corresponding mean free path (MFP) and dose rate. Particulate emissions such as beta and alpha particles are generally not preferred for imaging, but have application in targeted radiotherapy [10] [24].

- **Radiological half-life of the nuclide.** Radionuclides that are very short lived ($t_{1/2} < 1hr$) can be very difficult to work with due to complications with storage and chemical manipulation. Long-lived nuclides ($t_{1/2} < 1h$) can often deliver doses too high to administer to patients [10]. For targeted therapy use, it is advisable for the half-life of the nuclide to be around the same length or just longer than the biological half-life of the carrier molecule to which it is attached [7].

- **Chemical Form** Chemical properties of a nuclide are important in order to specify a biological path for a pharmeceutical. The chemistry of the isotope dictates the bio-active substances withwhich it can combine, allowing it concentrates in the area requiring therapy [10].

- **Contaminants** Isotopic impurities may drive up dose rates in patients. An isotopic impurity is the co-existance, generally as a result of production method, of another radioactive isotope of the same element which may have higher energy emissions [10] [11].

Neutron irradiation, such as that conducted in the research, results in neutron heavy isotopes therefore eliminating the possibility of producing PET pharmaceuticals with this method. Work with very heavy nuclei, such as those in the actinide regime are also best for proton irradiation, and can also incite programmatic issues regarding safety of resulting products. With this information, the ideal isotopes include low energy gamma emitting isotopes for gamma imaging, as well as low mid-energy beta emitting particles for targeted therapy. These were the primary characteristics that led to selection of ^{47}Sc as the targeted product.

2.0.2 Dual Purpose Theragnostic Radionuclides.

A growing interest in the field of nuclear medicine is the production of radionuclide pairs that allow for pretherapy imaging at a low dose while maintaining therapy at a high dose. Such pairs would be comprised of separate isotopes of the same element. Because both nuclides have the same chemical and biochemical properties, the imaging results would provide proper insight regarding biodistribution and patient response to particular pharmaceutical prior to injection of the high dose component [25] [4].

Several radionuclide pairs exist and are under investigation. Information regarding nuclide pairs can be seen in Table 1 .

6

Table 1. Theragnostic Radionuclide Pairs. This table has been modified from a publication written by S. C. Srivastava at Brookhaven National Laboratories. It lists potential radioactive nuclide pairs for theragnostic combination, as well as their respective half-lives, Imaging positrons and intensities, and therapeutic particles and energies [25] [4].

Theragnostic Pairs	half-life [d]	Imaging [keV] (I)	Therapeutic ([keV])
Scandium-44/47	2.4/3.5	511(94)	β - (162)
Copper-64/67	0.53/2.6	511(35)	β - (141)
Yttrium-86/90	0.61/2.7	511(66)	β - (935)
Iodine-124/131	4.2/8.0	511(44)	β - (181)

[47]Sc has been selected due to its promising biochemical and nuclear characteristics, as well as its potential for production through neutron irradiation. Biochemically, it has similar properties to, and is often classified as a rare earth element (e.g. Sm, Lu, Dy, etc.) [6]. As such it has been shown to form bonds with various potential carrier isotopes, notably acyclic polyamino-polycarboxylate ligands and folic acid, and other aminopolycarboxylic acids (APCAs) [3] [7] [12]. Scandium's ability to DOTA-form folate conjugates is an especially promising trait due to its use as a tumor biomarker or antigen [12].

2.1 The Isotope Production Facility

The Isotope Production Facility (IPF) at Las Alamos National Loaboratory (LANL) directs a 100 MeV proton beam at the beginning stages of the LANSCE accelerator towards an activation chamber, shown in Figure 1.

At the start of LANSCE, the beam is generated from a duoplasmatron H+ source. Initial acceleration to 750 keV is conducted in a Cockcroft-Walton electrostatic accelerator. The energy is pushed to 100 MeV through accelaration in an Alvarez drift-tube linac [13]. Both positively and negatively charged beams are simultaneously accelerated to a pulsed magnet in the transition region. This allows for the positive beam to be

extracted and redirected to IPF without interrupting negative beam operations [8].

The Isotope Production Facility (IPF) at LANSCE

Figure 1. The Isotope Production Facility at the Los Alamos Neutron Science Center (LANSCE), which houses a 100 MeV proton irradiation cell for the production of medical radio-isotopes [8].

The resulting IPF proton beam parameters are listed in Table 2. It runs with a maximum current of 250 μA. In practice the intensity falls around 230 μA. The nominal energy of the beam is $100 \pm .1$ MeV [22]. In order to reduce power intensity on the IPF targets and mitigate risk of rupture, it is swept in a circle.

Table 2. LANSCE IPF Beam Parameters [13].

Nominal Beam Energy	100 ± 0.1 MeV
Maximum Beam Current	250 μA
Average Power	25 kW
Pulse Duration	625 μ s
Spot Size	12.5 mm
Sweep Radius	625 12.5 mm
Sweep Frequency	5 kHz

IPF is a primary supplier of ^{68}Ge and ^{82}Sr, used for medical imaging. Their standard operation is the proton irradiation of a unique targetry and beam configuration to produce these isotopes. The target stack used in standard production consists of three

8

50 mm diameter pucks. The first two are Inconel-incapsulated RbCl powders, follwed by liquid gallium metal [8]. The targets are separated by 5 mm thick water-based cooling channels, driving the simultaneous irradiation at the nominal incident energies of 90 MeV, 65 MeV, and 30 MeV, respectively [13]. A schematic of this configuration is shown in Figure 2. A by-product of this unique process is the generation of a spallation neutron source exlusive to LANL operations [8].
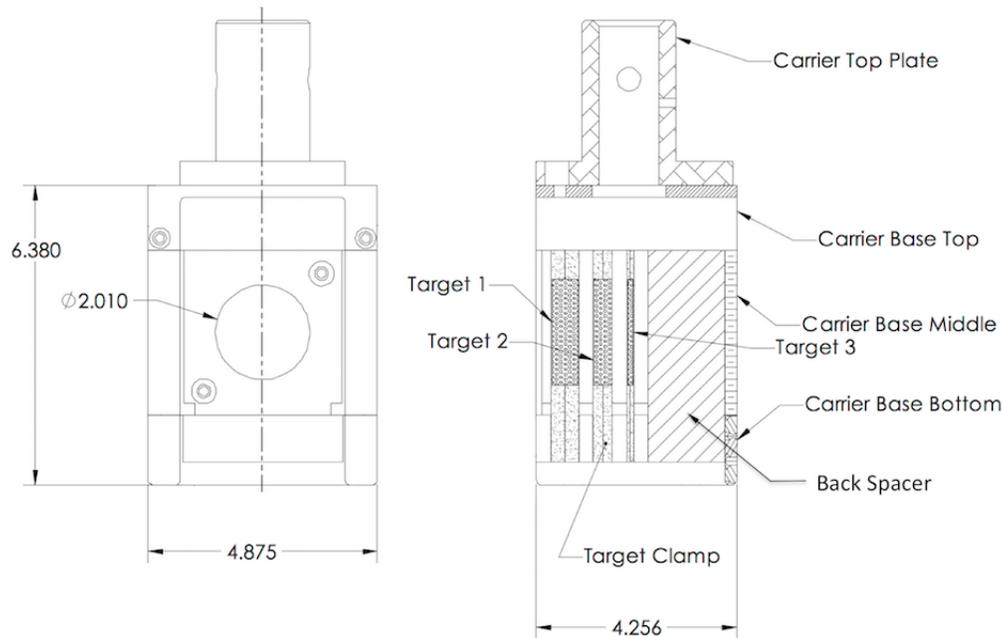
Figure 2. Schematic of IPF target stack showing RbCl powder targets and Ga metal target from the top (left) and side (right), with dimensions in inches. [22].

2.1.1 Spallation Neutron Flux at IPF.

Bombardment of high-energy protons on the Ga/RbCl target stack results in spallation neutrons directed primarily towards the back of the target holder. Recent characterization of the spallation neutrons revealed neutron fluxes peaking as high as $10^{12} n cm^{-2} s^{-1}$. Roughly 50% of the total neutron flux have energies greater 1 MeV. These values result from a proton beam intensity near 200 μA [8]. All previous neutron based production

9

attempts have taken place in nuclear reactor settings with energies peaking near 2 MeV or using comercial cycoltrons with energies peaking below 25 MeV [7].

2.2 Published Production Methods and Results

^{47}Sc has had long standing attention for its potential as a $^{44}Sc/^{47}Sc$ theragnostic pair. There have been many production schemes investigated within the isotope production community, described in Table 3. Proton, neutron, and gamma irradiations as well as deuteron bombardment attempts have all been made, yielding various results of isotopic purity. A clinical-scale production model has yet to be generated and methods of production and separation remain under investigation.

Isotopic purity has been the primary impediment to establishing a method of production. ^{46}Sc is a hindrance in the ability to use ^{47}Sc as a radiotherapy pharmapseutical due it its strong gamma line at 889.28 keV and half-life of 83.8 days. ^{48}Sc poses a similar threat with a 43.7 h half life and gamma lines at 983.3, 1037.52 and 1311.7 keV [6]. ^{44m}Sc ($t_{\frac{1}{2}} = 58.61h$) is undesirable due to its beta decay into ^{44}Sc which has gamma lines at 511 and 1157 keV [7] [11].

Table 3. Previous Sc-47 production attempts. Listed are the reactions leveraged, the facilities utilized and the primary organization [14] [6] [7] [15] [16].

Reaction	Method	Organization
Ti-47(n,p)Sc-47	Pakistan Research Reactor	Isotope Production Division, Pakistan Institute of Nuclear Science and Technology
Ti-47(n,p)Sc-47(geological samples)	Reactor	National Commision of Atomic Energy, Argentina
Ti-48(γ,p)Sc-47	High-Energy Bremsstrahlung-Irradiation via accelerator	Laboratory of Nuclear Science, Tohuku University, Japan
Ti-nat(d,n)Sc-47	Deuteron Bombardment via accelerator	Laboratory for Nuclear Science and Department of Chemistry, Massachusetts Institute of Technology
Ti-48(p,2p)Sc-47	Brookhaven Linac Isotope Producer (accelerator)	Brookhaven National Laboratory
Ti-nat(p,spall)Sc-47	Brookhaven Linac Isotope Producer (accelerator)	Brookhaven National Laboratory
V-51(p,3p2n)Sc-47	Brookhaven Linac Isotope Producer (accelerator)	Brookhaven National Laboratory
Ti-48(p,2p)Sc-47	Brookhaven Linac Isotope Producer (accelerator)	Brookhaven National Laboratory
Ti-47(n,p)Sc-47	High Flux Beam Reactor and High Flux Irradiation Reactor	Brookhaven National Laboratory

2.2.1 Efforts at Brookhaven National Laboratory.

The Isotope Production Facility's counterpart at Brookhaven National Laboratory (BNL) investigated several reactions, using both proton and neutron bombardment. The proton experiments were conducted using the Brookhaven Linac Isotope Producer (BLIP). The reactions investigated in this experiment were $^{48}Ti(p, 2p)$, $^{nat}Ti(p, spall)$, $^{51}V(p, 3p2n)$, and $^{48}Ti(p, 2p)$. Ti and V foils were used, as well as $^{48}TiO_2$ targets (99.8% enriched from Oakridge National Laboratory (ORNL)). The Vanadium target was irra-

11

diated at an energy of $191.1 \pm 0.8 MeV$. The Ti targets were bombarded with varying energies from $48.4 \pm 1.0 MeV$ up to $191.1 \pm 0.8 MeV$. The ^{nat}Ti target was irradiated with proton flux of 50 mA for 3.35 days, at an energy of 192 MeV, resulting in radioimpurity ratios at the end of beam (EoB) of 0.59 ($^{44m}Sc/^{47}Sc$), 0.08 ($^{46}Sc/^{47}Sc$), and 0.02 ($^{48}Sc/^{47}Sc$) [7].

Neutron experiments were performed in high flux beam reactor (HFBM) and high flux irradiation reactor (HFIR) within the fission neutron spectrum. ^{47}Ti (94.53% enrichment) was used as the target material for bombaradment. Several locations within the reactor were selected, utilizing the fast neutron flux ($>$1MeV). For these experiments no ^{44m}Sc was detected and the purity ratios were two orders of magnitude lower, less than 0.4% for both ^{46}Sc and ^{48}Sc at EOB. Based on these results it was determined that 0.03 Ci of the 99.5% purity ^{47}Sc produced could be used to label 1 mg of an IgG antibody [7].

2.2.2 Other $^{47}Ti(n,p)$ Experiments.

Two attempts have been made to utilize the $^{47}Ti(n,p)$ reaction outside of BNL. Both were conducted in reactors, one at the Pakistan Institute of Technology, and one by the National Commission of Atomic Energy in Argentina [6] [14]. The study done in Argentina was investigated geological materials and did not report relative impurities [14]. The results from the Pakistan Institute of Technology reactor reported ^{46}Sc impurites between 3.07% and 5.12% and ^{48}Sc impurites between 19.12 % and 26.72 % depending on the number of length of time the samples were left in the reactor. This experiment used a 100 mg Ti target in a fast neutron flux of 13.6 x 10^{13} $ncm^{-2}s^{-1}$ [6].

2.2.3 Other Efforts.

The final experiments of interest were a high-energy brehmsstrahlung irradiation attempted at Tohuku Universtiy in Japan and deuteron-bombardment attempted at the Massachusettes Instititue of Technology. The high-energy brehmsstrahlung method reported promising results. This method used 99.13 % enriched ^{48}Ti. After a 12 hour irradiation at 60 MeV, the resulting impurites of ^{46}Sc and ^{48}Sc were less than 0.57 % and 0.26 %, respectively [15]. Purities obtained by Massachusettes Institute of Techonology were not reported [16].

3. Modeling Approach

Models are necessary for efficient experiment design. Due to the cost and time constraints of this research, it is ideal to have pre-determined the most promising experiment for the desired outcome. There are multiple software packages that have shown accurate results both qualitatively and quantitatively for experiments involving particle transport and nuclear reactions. Use of these software packages was paramount in determining which isotopes and moderators to investigate for this experiment, as well as regarding timing parameters for irradiation and counting.

3.1 Neutron Flux Characterization

The neutron flux resulting from the proton irradiation has not been precisely characterized through experiment or modeling, as it falls across a broad range of energies, and lacks in sufficient empirical data. In order to investigate production yields, the gap left due to the lack of empirical cross section data available has been filled using the modeling capabilities incorporated into versions X and 6 of the Monte-Carlo N-Particle (MCNPX and MCNP6) code.

3.1.1 MCNP6.

MCNP6 is a Monte Carlo code for particle transport, that allows for high fidelity 3D geometric-modeling, as well as the continuous-energy transport of 36 different particle types plus heavy-ion transport, fuel burn up, and high-fidelity delayed-gamma emission. MCNP6 is a fusion of MCNPX and MCNP5. MCNP5 allows for neutral particle and electron transport, while MCNPX includes other heavy ions and exotic particles [17].

The irradiation scheme for IPF uses a 100 MeV proton beam, with a beam current up to 250 μA, to irradiate the target stack. The beam will attenuate as it passes through

14

the target stacks. With proton energies between 15 and 100 MeV, a range of high-energy neutrons will be generated, causing a neutron flux through the aluminum holder containing the oxides and foils. An MCNP simulation was developed to model the IPF beam and target stacks. The geometry set up for the MCNP run is shown in Figure 3.
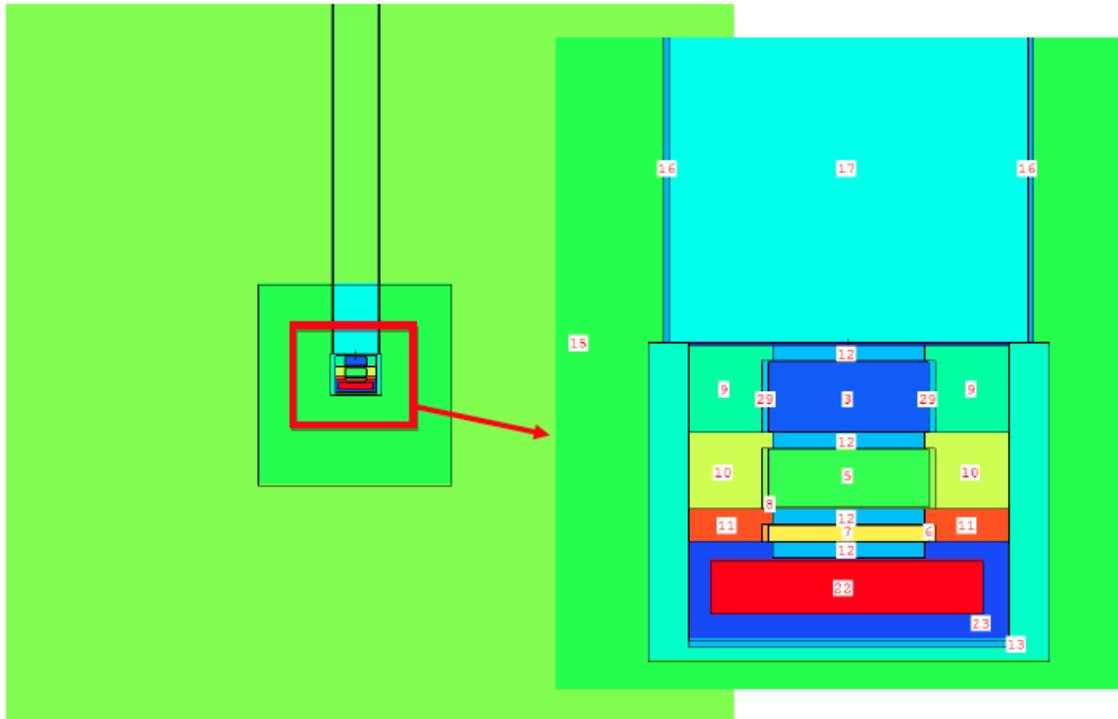
Figure 3. This figure shows the geometry set up using MCNPs Visual Editor, along with the associated script. The foil target of interest is indicated in the image. The image is colored by cell. Cell 22 is the rear spacer, which has been modified to hold targets for neutron spallation irradiation.

This model (Appendix A) can be run to determine the flux of spallation neutrons at a point detector or to determine average neutron flux through a specified cell. Both are given in units of particles/cm^2 normalized per source particle. The nuances between these tally options are described in Section 3.1.3

15

3.1.2 Physics Models.

Modeling neutron flux for the energies up to 100 MeV is challenged by a lack of empirical data beyond 20-25 MeV. The tabulated data used for calculations in MCNP6 are from the ENSDF data libraries, and only extend up to this range. To deal with this disparity, MCNP allows for the use of various physics models in order to generate simulations for which tabulated data is not available. IntraNuclear Cascade, Liege (INCL4), ISABEL, Birtini, and the Cascade-Excitation Model (CEM) of nuclear reactions are the primary codes available. INCL and Bertini may also be combined with either the ALBA or Dresner evaporation-fission models [17].

ISABEL and Bertini are conventional cascade models. These models trace fast particles to a minimum "cut-off" energy, at which point they are deemed to have been absorbed by the nucleus. The CEM model uses a derived term for effective local optical absorptive potential different set of criteria to determine when a particle has left the cascade [18]. IntraNuclear Cascade (INC) is the first stage of CEM. INCL4 was developed by Joseph Cugnon at the University of Liege in Belgium, but with the intended use for modeling within the energy range of 200 MeV to 2 GeV. CEM has been optimized by Los Alamos for the medium energy range between 20 and 400 MeV [17] [19].

In the first stage of CEM, primary particles are allowed to re-scatter and produce secondary particles several times prior to leaving the cascade. This point is determined by a comparison by the effective potential described above to a potential defined by a phenomenological global optical model [18]. Once the cascade is complete, an excited residual remains from which the particle-hole configuration is determined. The model then allows for the relaxation of nuclear excited model as the second stage, concluded with an equilibrium evaporative stage [17].

As a method of comparison, the four model options were run with a number of source particles (nps) set to 10^7 protons, to collect an average cell flux tally in cell 22,

which corresponds to the rear aluminum spacer designed to hold targets for spallation neutrons. All parameters for each model run remained constant. Figure 4 shows the resulting flux. In the region above 25 MeV, where tabulated data is unavailable, all models show similar trends, with the most variant being INCL4.

All models fall within the region of statistical error, for energies below 90 MeV. Above 90 MeV, INCL4 fell outside of the region of statistical error of the other models, while Bertini, ISABEL and CEM3.03 continued to show agreement. All models result in a determined flux within the same order of magnitude of each other.

The most updated version of CEM incorporated into MCNP6 is CEM3.03. This model has been improved by changes motivated by new isotope production data measured at GSI in reversed-kinematics for ^{208}Pb and ^{238}U at 1 GeV/nucleon and ^{197}Au at 800 MeV/nucleon. The updated model was compared to ISABEL and Bertini models and showed closer agreement to measured data within the energy range considered in this experiment [18]. Based on this investigation, the CEM3.03 model was used for the extraction of cross sections and neutron flux modeling.

17
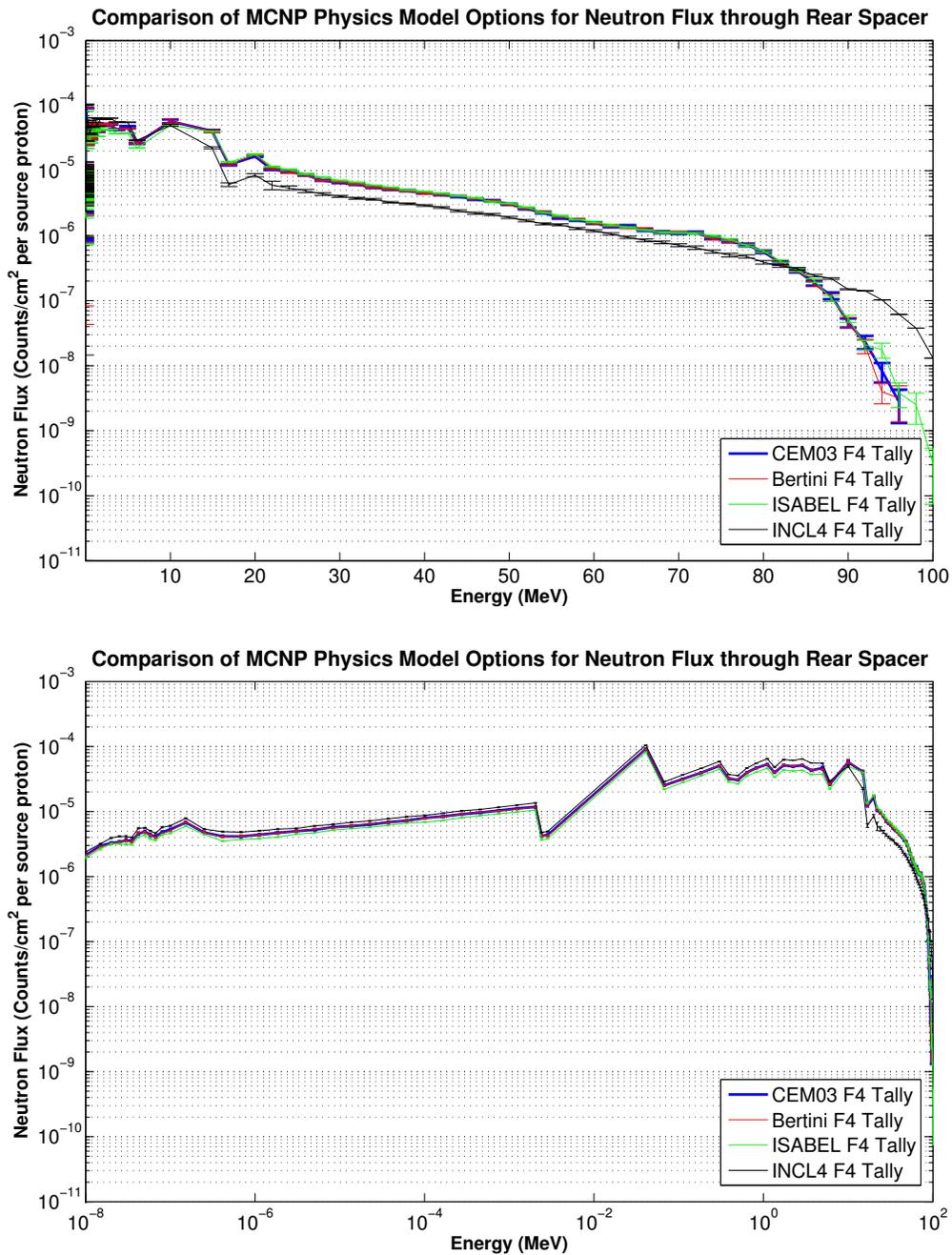
Figure 4. Both plots show a comparison of the neutron flux results for varying physics models in MCNP6 using an F4 Tally, with different scales. The input decks for each run were exactly the same, and considered an average cell flux tally for the rear aluminum spacer (Cell 22). The number of source neutrons specified was 10^7 and proton beam current was set to 220 μA. The error shown is the relative error based on counts statistics of the models.

18

3.1.3 MCNP Flux Tallies.

MCNP6 has three different flux estimators available. Each aims to assess the number of particles per squared centimeter, normalized per source particle [20]. The quantity being estimated is calculated by,

$$\int_t \int_E \Phi(r, E, t) dEdt. \tag{2}$$

The three flux estimation tools are the average surface flux (F2), average cell flux (F4) and next-event (F5). The F2 tally is a surface-crossing estimator, which scores the particle weight crossing the surface within a predetermined range for time and energy. The F4 tally is a track length estimator, which counts the number track-lengths per unit volume.

The F5 tally functions as a point or a ring detector. It differs from the F2 and F4 tallies in that it doesn't require a particle to actually reach the detector. This method tracks each particle and its probability of reaching the detector. It scores a weighted value based on a probability density function. It traces a pseudo particle from its collision point to the detector. MCNP then plays roulette with the pseudo-particles with a cut-off weight of 0.1. The F5 tally is a very powerful tool, and ideal for this modeling technique, which is depended on a high quantity of secondary particles.

There are some concerns with using this method. Though it does reduce computational time, it can also naturally generate biases in the statistical performance of the model. If a collision occurs too close to the detector, an infinite variance. This effort is mitigated with the use of a radius of exclusion, R_0; a very important aspect for proper use of the F5 tally. Usually measured in cm or mean-free paths, this radius reduces the likelihood of skewed statistics. The exclusion radius used in modeling this experiment was 0.15 cm.

19

3.1.4 Neutron Flux Model.

Using the geometry model given in Section 3.1.1, provided in the input deck found in Appendix A, a model of the neutron flux for the IPF target configuration was developed. The script was written into several parts. The first is the geometry set up to include cell, surface and material data cards. The material data cards used a 5-digit ZAID number that corresponds to the Z-number and atomic mass of the isotope. In most cases, materials are not isotopically pure, and the material card serves to provide the isotopic composition of a given cell. This information allows MCNP to extract the correct cross section data when tabulated data is available, as well as to more accurately serve the physics modeling functions of the software [21].

3.1.5 Variance Reduction.

The MCNP model can track secondary particle flux through a point detector. In order to get reasonable statistics on the neutron flux without utilizing any optimization methods, the computational time can take multiple days. In order to speed up this process, stacked importance cells and cell based weight windows were utilized. These processes allowed for acceptable statistical confidence in the model developed while maintaining a reasonable computational time window [21].

MCNP6 automatically runs with criterion for splitting and rouletting optimization techniques. Splitting works by increasing the number or particles to reach a given surface. Whenever a particle crosses from a surface near the source region to a surface near the region being tallied it is split into multiple particles with equivalent fractions of the original particle's weight. These particles each undergo independent random walk simulations, making it more likely that one of them reaches the tally region. With this method, fewer particles can be run in order to draw proper tally statistics, while the true value of the tally remains unaffected, as the particles have been weighted accordingly [21].

20

Rouletting, in particle transport, works to eliminate particles that have ended up in a region in which they are unlikely to arrive in the tally region. In MCNP6, as particles move into regions of lesser importance, or regions farther from the tally region, they are reduced in weight. When a particle's weight falls below a pre-determined threshold, it is killed with a set probability, P. If the particle survives, its weight is increased by $\frac{1}{P}$ and is kept in the simulation.

MCNP6 allows for basic cell importance setting to help control particle tracks. Another option, in lieu of importances, is the cell-based weight window method. This method proved to be most successful in driving down computational time while maintaining statistically sound results for the simulations run for this experiment. The cell-based weight windows provide an importance function to the geometric structure provided based on the cell geometry. It allows for more precise control of severity of splitting and rouletting cutoffs [21].

Weight windows can be generated by MCNP6's built-in weight window generator. The generator can develop a cell-based weight window with input information for the tally bin for which the weight window generator should be optimized and the lower weight window bound. The weight window generator can be re-run multiple times for optimization, and must be re-run when changes are made to the source importance [21].

3.1.6   Modeled Neutron Flux.

The neutron flux model characterization used in the majority of this research is a product of the MCNP6 F5 tally. In cases where the F5 tally could not be used, weight windows were used to draw down the error, along with a source particle count of $2x10^7$ protons. Cross section data up to 25 MeV from Evaluated Nuclear Data File (ENDF) B-V11 (Release Date: 22 Dec 2011) was utilized. For energies beyond 25 MeV, the CEM3.03 model was employed.
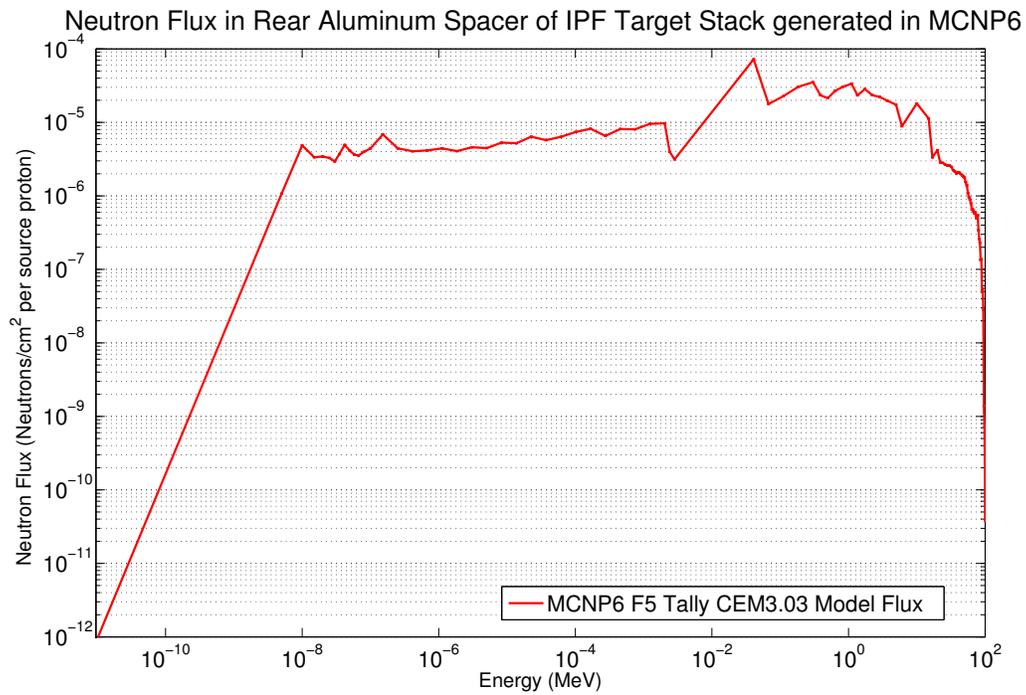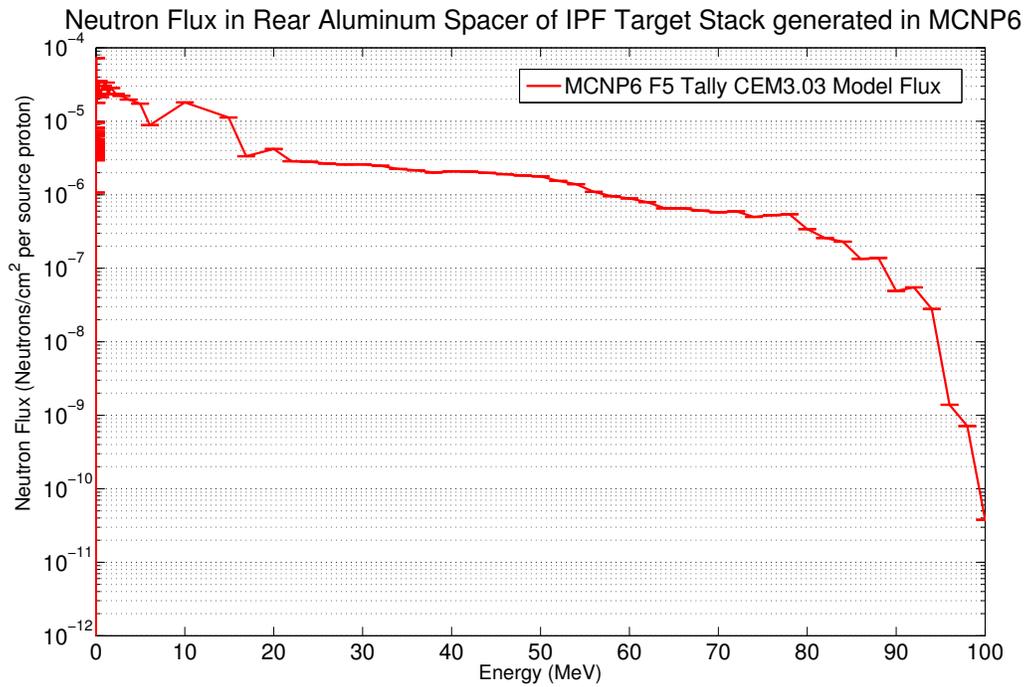
Figure 5. The neutron flux generated using MCNP6 utilizes the F5(point detector) tally and the geometric set up shown in Figure 3. The values for flux are normalized per source proton. Both plots depict the same data with different scaling. The top plot highlights the energies above the tabulated region (25 MeV), and the bottom plot shows the logarithmic trend of the flux characterization model. Error bars are present, and based on count statistics of the Monte Carlo simulation.

22

The proton beam current for this calculation was set to 220 μA. As indicated in the figure, the flux values are normalized per incident proton. Figure 5 displays the flux on both a long and linear scale. The peak of the flux is within the keV region, and the value decays from that point. The neutron energies reaching the target location have energies from eV to 100 MeV. Based on this model only 5.7% of the neutrons have energies over 25 MeV. According to previous investigations, about 50% of the neutrons had energies above 1 MeV. This model showed 41% of neutrons falling above 1 MeV, with 59% in the KeV range and lower.

3.2   Modeled Yield Prediction

With a confident model of the neutron flux, there are multiple methods of producing a yield estimation of various targets. Ideally, the use of tabulated neutron cross-section data would provide the best estimation. The targets of interested are the stable V and Ti isotopes, ^{50}V, ^{51}V, ^{46}Ti, ^{47}Ti, ^{48}Ti, ^{49}Ti, and ^{50}Ti, as well as the elements in their natural abundances. For these reactions, the ENSDF and TALYS databases do not exceed energies of 25 MeV for most cross sections. As such, calculations using tabulated cross section data are expected to underestimate the yield produced. These calculations are still valuable as 93.3% of the neutron flux falls within the tabulated range.

3.2.1   Cinder90.

Cinder90 is used to estimate the inventory of residual nuclides in an irradiated material. It utilizes a self-contained nuclear data library to calculate the atom density (atoms per unit volume) and activity density (curies per unit volume) of all nuclides present at a specified time. It has many applications including burn-up, particle bombardment, and transmutation nuclide inventory.

Cinder is only validated up to 25 MeV, consistent with the readily available cross

section data. MCNPX and Cinder90 runs were conducted for 99.75% ^{51}V in its natural abundance, as well as each of the naturally occurring isotopes of Ti, listed in Section 3.2 above. When generating models for enriched isotopes of titanium, oxides were considered as that is the most readily available form of isotopically enriched titanium. These materials were considered to be 100% isotopically pure. The densities associated to each of the materials investigated are listed in Table 4. The TiO_2 densities were estimated by weighing the mass ratio of the isotopically enriched material to that of natural abundance and scaling the listed density accordingly.

Table 4. The listed values are the densities of the target materials. Values for enriched TiO_2 are derived by weighing the mass ratio of the isotopically enriched material to that of natural abundance and using it to scale the density. The listed density of natural abundance TiO_2 is 4.23 g cm^{-3}

Material	Density(g cm^{-3})
^{nat}V Foil	6.000
^{nat}Ti Foil	4.506
^{46}Ti Oxide	4.092
^{47}Ti Oxide	4.164
^{48}Ti Oxide	4.236
^{49}Ti Oxide	4.308
^{50}Ti Oxide	4.380

Cinder90 has specific requirements for the output files of MCNP, which alter the ideal use of MCNP described above. The first is that it is required to use MCNPX for the generation of this data, as Cinder90 has not yet been updated for compatibility with MCNP6. For the Cinder90 code to properly work with MCNPX, a Perl script exists that extracts data from the MCNPX output. For the data and modeling tools used in this experiment, the alteration in version is insignificant [20]. The aforementioned Perl script pulls material information for the cell of interest. As such, the neutron flux is regenerated for each new material. A comparison of the neutron flux is displayed in Figure 6.

24
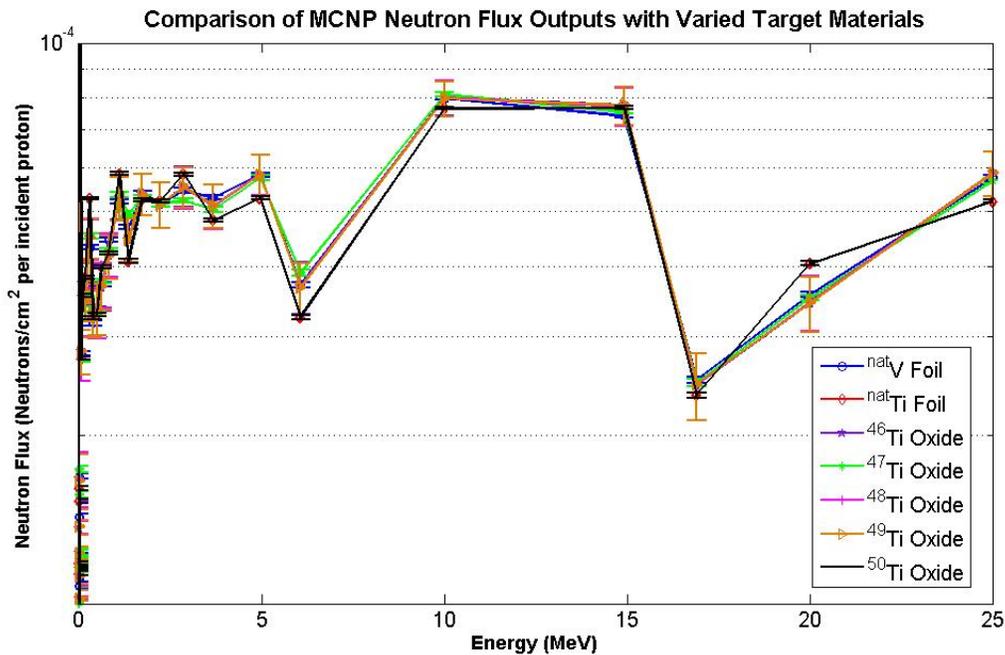
Figure 6. The results for neutron flux for each of the MCNP runs conducted in order to model production rate in varying materials in Cinder90.

The flux models in Figure 6 used a modified geometry that includes a 1 cm diameter and .1 cm thick target of each material placed in the center of cell 22 (see Figure 3). The targets are unlikely to have an impact on the shape of the neutron flux due to their thickness relative to the mean free path of the neutrons passing through. Any variations visible in the flux results due to varied materials are indistinguishable given the uncertainties.

The input decks for Cinder90 for each material can be found in Appendix B. They indicate that the MCNPX flux and cell with a specified material be run through an activation/burnout process to give activity of individual isotopes per unit volume of target material. Using the density relative to each material, and assuming an average proton beam current of 220 μAh, the results were modified to production rate in units of $\mu Cis^{-1}\mu Ah^{-1}$. Results of these calculations are displayed in Table 5.

25

Table 5. Reaction rates for several isotopes produced through the use of MCNPX and Cinder90. These values reflect models run using ENDF tabulated data up to 25 MeV only. Results given in $Cicm^{-3}$ have been adjusted to reflect a production rate in $\mu Cis^{-1}\mu Ah^{-1}$ assuming a proton beam running at 220 μAh. All values are rounded to the fourth decimal place. A complete list of isotopes generated, with unrounded values, can be found in Appendix C

Target Material	Product	Activity Density ($\mu Ci \ g^{-1}$)	Rate ($\mu Cis^{-1}\mu Ah^{-1}$)
^{nat}V Foil	^{47}Sc	0.0392	0.0002
	^{46}Sc	0.0000	0.0000
	^{48}Sc	4.1467	0.0002
	^{47}Ca	0.0202	0.0000
	^{44}Ti	0.0000	0.0000
^{nat}Ti Foil	^{47}Sc	8.4798	0.0386
	^{46}Sc	2.7297	0.0124
	^{48}Sc	15.322	0.0696
	^{47}Ca	0.4015	0.0018
	^{44}Ti	0.0000	0.0000
^{46}Ti Oxide	^{47}Sc	0.0000	0.0000
	^{46}Sc	1.5606	0.0071
	^{48}Sc	0.0000	0.0000
	^{47}Ca	0.0000	0.0000
	^{44}Ti	0.0000	0.0000
^{47}Ti Oxide	^{47}Sc	33.77	0.1535
	^{46}Sc	0.3923	0.0018
	^{48}Sc	0.4772	0.0022
	^{47}Ca	0.0100	0.0001
	^{44}Ti	0.0000	0.0000
^{48}Ti Oxide	^{47}Sc	70.30	0.3195
	^{46}Sc	95.40	0.4336
	^{48}Sc	230.9	1.0496
	^{47}Ca	3.5612	0.0162
	^{44}Ti	0.0000	0.0000
^{49}Ti Oxide	^{47}Sc	0.0121	0.0001
	^{46}Sc	0.0369	0.0002
	^{48}Sc	0.0665	0.0003
	^{47}Ca	0.0000	0.0000
	^{44}Ti	0.0000	0.0000
^{50}Ti Oxide	^{47}Sc	32.88	0.1494
	^{46}Sc	0.0319	0.0001
	^{48}Sc	60.41	0.2746
	^{47}Ca	1.515	0.0069
	^{44}Ti	0.0000	0.000

Based solely on the production rate of ^{47}Sc, ^{48}Ti oxide stands out as a target material with a production rate more than 2x any other target material at 0.3195 $\mu Cis^{-1}\mu Ah^{-1}$. Isotopic purity, however, is an exceptionally important factor for therapeutic pharmaceuticals. With the exception of ^{46}Ti, which shows negligible production rates for ^{47}Sc, an investigation of the isotopic purities was conducted.

3.2.1.1   Cinder90 Isotopic Purity Predictions.

The production rates may be used to estimate production for long periods of time. The mathematical relationship between the cross section and production rate assuming a thin target is,

$$A = Inx\sigma, \tag{3}$$

where A corresponds to activity in disintegrations per second, I is the number of particles incident on the target (particles/s), n is the number of target nuclei per unit volume, x is the thickness of the target in cm, and σ is the associated cross section [23]. The rate of production is then a time dependent extension of that, affected by the radioactive decay of the activated material. Therefore the production quantities of a radioisotope at the end of an irradiation time, t is,

$$R = Inx\sigma(1 - e^{-\lambda t}), \tag{4}$$

where λ is the radioactive decay constant for that isotope. In order to look at production over irradiation times, A was determined for a beam time of t equal to 1 hour, by setting R equal to the production rates given in Table 5 [23]. The MATLAB script developed to determine isotopic purity is given in Appendix D. This conversion can be seen for all isotopes considered in the calculation.

27

The isotopic purity of ^{47}Sc is calculated relative to ^{46}Sc, and ^{48}Sc. In the case of ^{nat}Ti and ^{50}Ti, for which appreciable amounts of ^{47}Ca are produced, additional decays are considered as ^{47}Ca $\beta-$ decays into ^{47}Sc, with a half-life of 4.536 days. The first step in determining purity is using the values for A to determine the production over a given length of time. The time length of interest is determined relative to the production of ^{47}Sc. Due to its half-life of 3.3492 d, an irradiation length of 10 hours was used. Production of all involved isotopes was calculated using Equation 4.

Decay from the produced value over time was calculated for each isotope produced. This decay process, for ^{46}Sc and ^{48}Sc is determined by the basic formula for radioactive decay,

$$A(t) = A_0 e^{-\lambda t}. \tag{5}$$

When ^{47}Ca is produced, the Bateman Equation must be used to account for the ingrowth of calcium into ^{47}Sc [26]. In this case the equation becomes,

$$N_2(t) = N_1(0)(\frac{\lambda_1}{\lambda_2 - \lambda_1})e^{-\lambda_1 t} - (N_2(0) - N_1(0)(\frac{\lambda 1}{\lambda 1 - \lambda 2})e^{-\lambda_2 t}). \tag{6}$$

Equation 6 is used in the calculations for ^{50}Ti oxide and ^{nat}Ti target materials. All other target materials use Equation 5 for decay calculations. The variable, 't', in both Equation 5 and Equation 6 refers to the time that has passed from the end of irradiation. The fractional isotopic purity of ^{47}Sc is then calculated as,

$$P_{fractional}(t) = \frac{A_{47Sc}(t)}{A_{47Sc}(t) + A_{48Sc}(t) + A_{46Sc}(t)}, \tag{7}$$

where $P_{fractional}$ is the fractional purity, and A_x corresponds to the abundance of each associated isotope, x. The resulting isotopic purities for each of the target materials of interest are listed in Table 6.

28

Table 6. The listed purities are the percent purity of ^{47}Sc relative to ^{46}Sc and ^{48}Sc in each potential target material. These values are derived from the production rates given by the Cinder90 modeling technique, listed in Table 5.

Material	^{47}Sc Purity (%)
^{nat}V Foil	90.3
^{nat}Ti Foil	44.3
^{47}Ti Oxide	96.6
^{48}Ti Oxide	10.8
^{49}Ti Oxide	8.1
^{50}Ti Oxide	84.3

Due to the relationships between the half-lives of the scandium isotopes, the purity of ^{47}Sc decreases relative to ^{46}Sc and increases relative to ^{48}Sc with time. There is, therefore, a point in the decay process that generates a maximum isotopic purity. Figure 7 through Figure 12 show this relationship, along with the production and decay of each isotope.

When considering a target material in light of Cinder90 results, it is important to consider the fact that many reactions that generally have low cross sections in the energy range of 0-25 MeV are not being considered.

In the case of Vanadium, (n,α) reactions have cross sections that are not tabulated, and are expected to be significant in the higher energies not included in this model, based on results of previous experiments with Vanadium [7]. It is anticipated that production rates exceed Cinder90 predictions slightly, due to the energy range of the flux ignored by the model. For ^{nat}V, the variance is expected to be particularly drastic, as the reactions of interest will primarily fall in the higher energy ranges. Due to the small percentage of neutron above 25 MeV the production rate may still be low, however Cinder shows promising values for isotopic purity of ^{47}Sc relative to ^{46}Sc and ^{48}Sc.

Based on these results, the most promising material appeared to be ^{47}Ti. ^{50}Ti showed promising potential as well. With the unknown results of the higher energies, both targets are selected. Based on previous successes and the expected inaccuracy of Cinder90 with ^{nat}V, this was also selected as a target. Due to its availability, and due to the
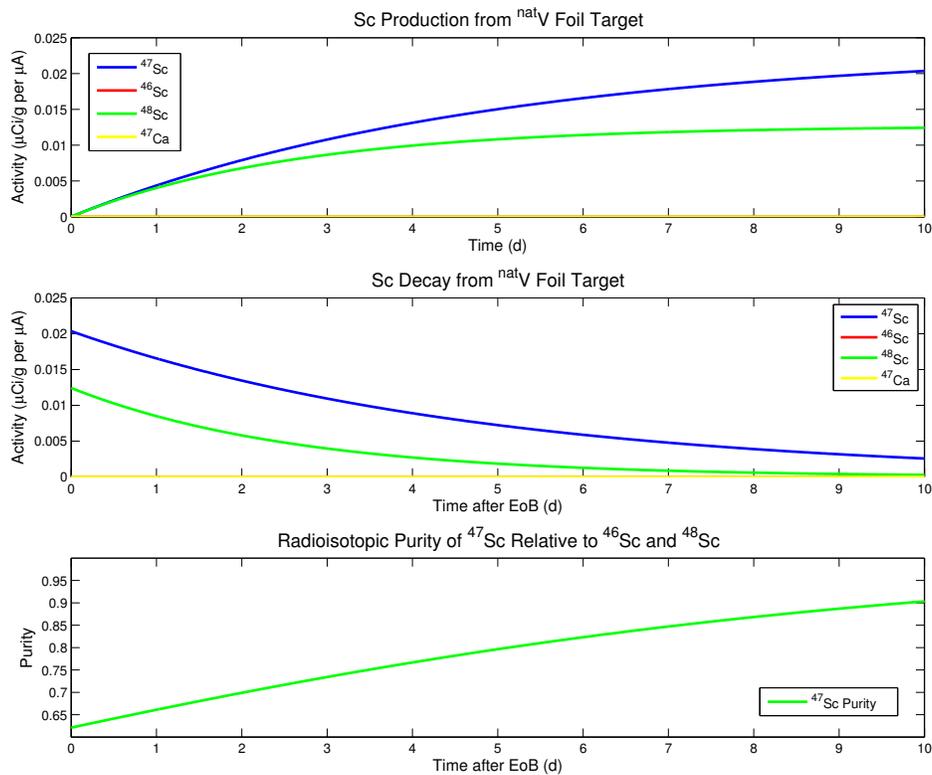
Figure 7. These plots were generated in the MATLAB script found in Appendix D. The calculations are based on production rates for a ^{nat}V target produced in Cinder90.The graph on the top shows the relative production of isotopes over the course of a 10 day irradiation. The middle graph shows relative decay rates as a function of time after the end of irradiation. The graph on the bottom shows the relative isotopic purity of ^{47}Sc.

30
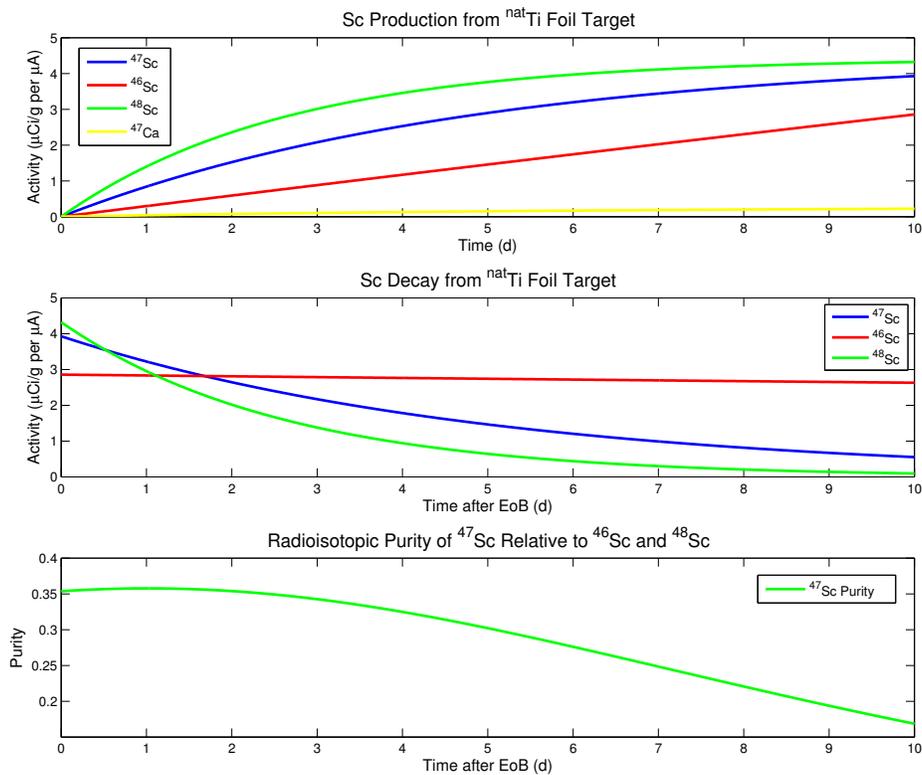
Figure 8. These plots were generated in the MATLAB script found in Appendix D. The calculations are based on production rates for a ^{nat}Ti target produced in Cinder90. The graph on the top shows the relative production of isotopes over the course of a 10-day irradiation. The middle graph shows relative decay rates as a function of time after the end of irradiation. The graph on the bottom shows the relative isotopic purity of ^{47}Sc.

31
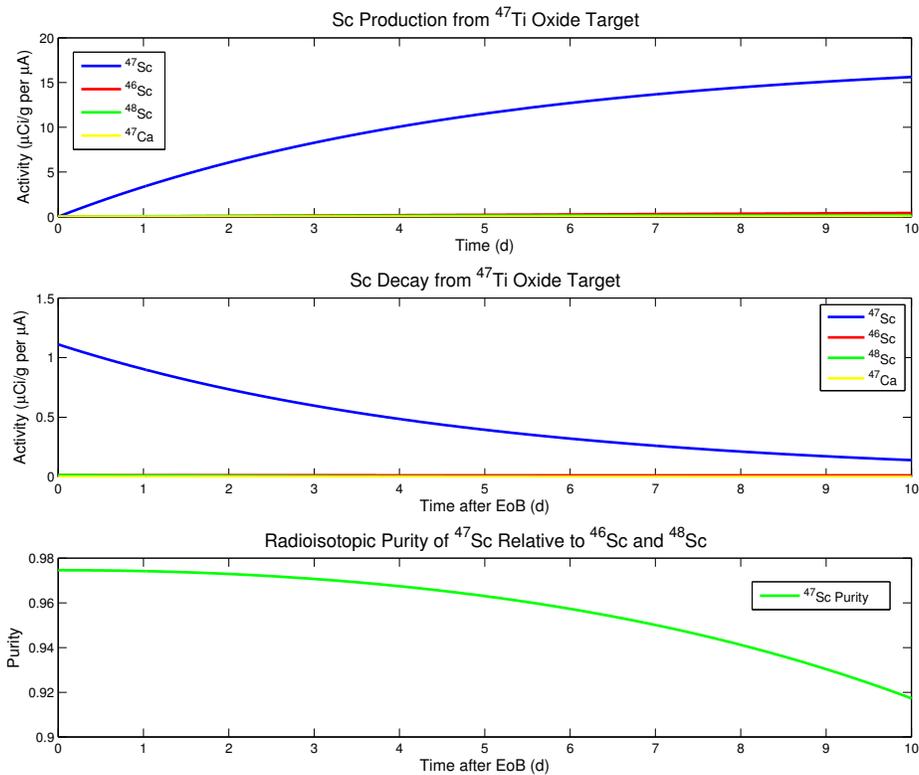
Figure 9. These plots were generated in the MATLAB script found in Appendix D. The calculations are based on production rates for a ^{47}Ti target produced in Cinder90. The graph on the top shows the relative production of isotopes over the course of a 10-day irradiation. The middle graph shows relative decay rates as a function of time after the end of irradiation. The graph on the bottom shows the relative isotopic purity of ^{47}Sc.

32
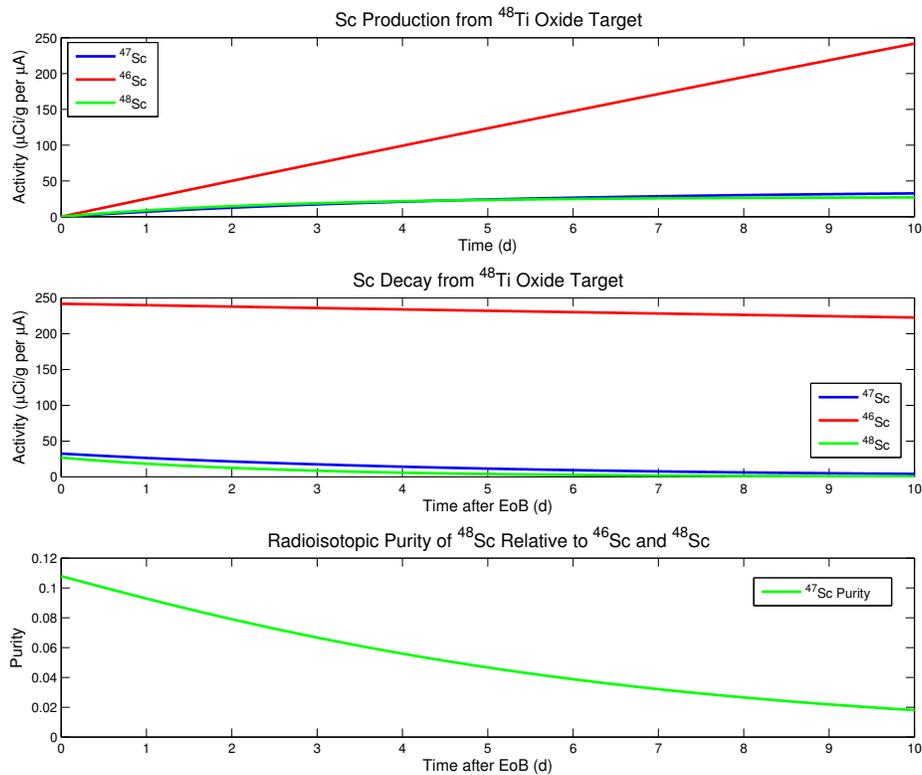
Figure 10. These plots were generated in the MATLAB script found in Appendix D. The calculations are based on production rates for a ^{48}Ti target produced in Cinder90. The graph on the top shows the relative production of isotopes over the course of a 10-day irradiation. The middle graph shows relative decay rates as a function of time after the end of irradiation. The graph on the bottom shows the relative isotopic purity of ^{47}Sc.

33
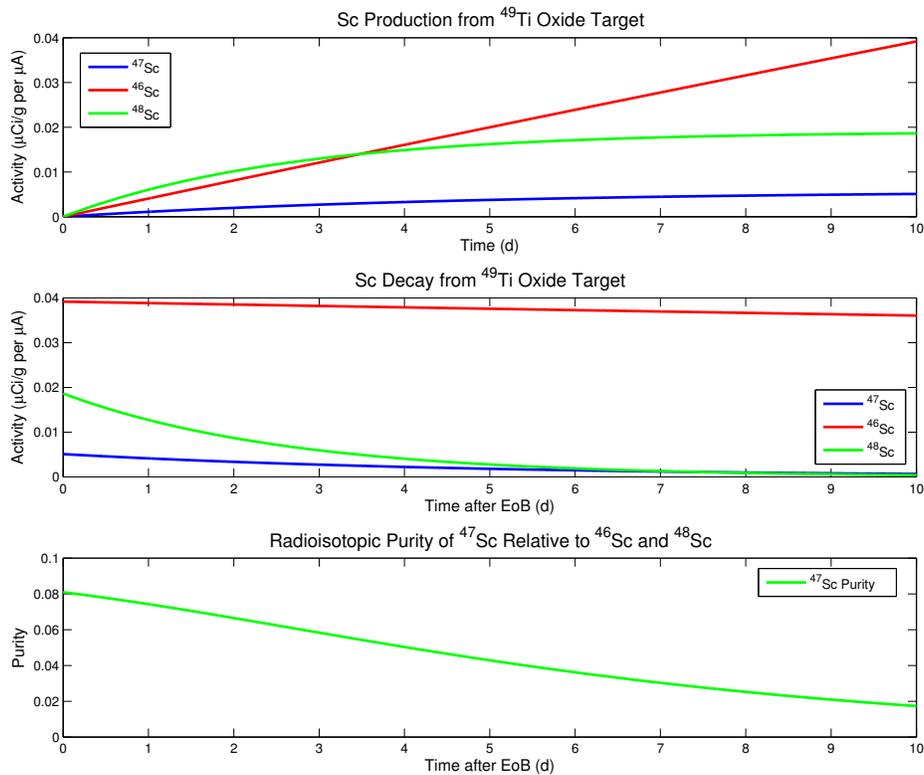
Figure 11. These plots were generated in the MATLAB script found in Appendix D. The calculations are based on production rates for a ^{49}Ti target produced in Cinder90. The graph on the top shows the relative production of isotopes over the course of a 10-day irradiation. The middle graph shows relative decay rates as a function of time after the end of irradiation. The graph on the bottom shows the relative isotopic purity of ^{47}Sc.

34
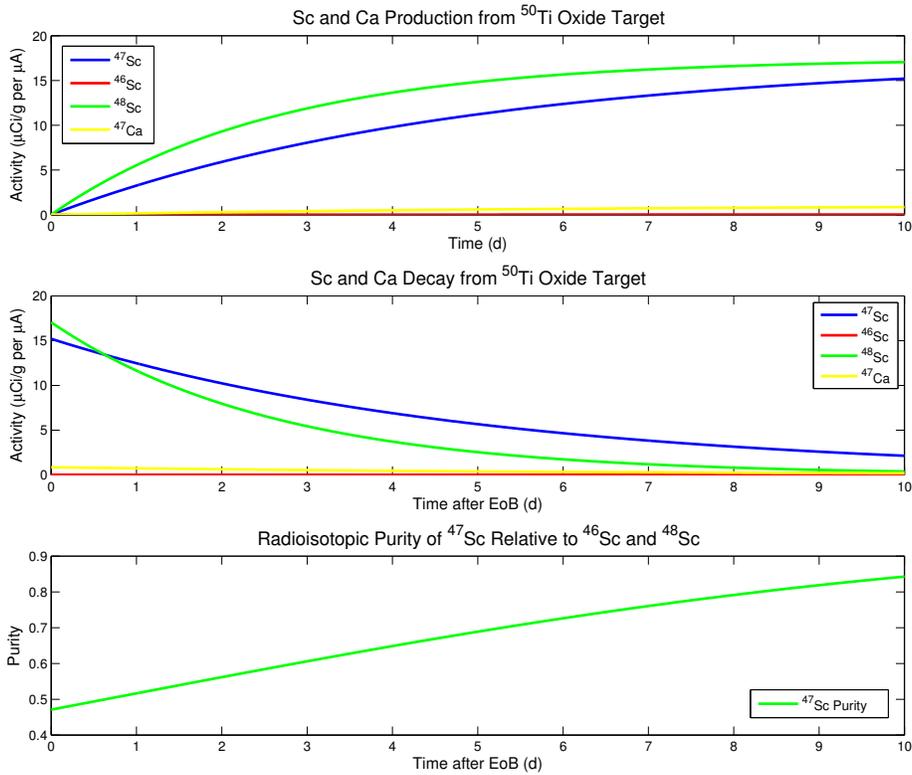
Figure 12. These plots were generated in the MATLAB script found in Appendix D. The calculations are based on production rates for a ^{50}Ti target produced in Cinder90. The graph on the top shows the relative production of isotopes over the course of a 10-day irradiation. The middle graph shows relative decay rates as a function of time after the end of irradiation. The graph on the bottom shows the relative isotopic purity of ^{47}Sc.

35

promise of various isotopes of titanium, ^{nat}Ti was selected as a target material as well.

Enriched ^{47}Ti(95.7%) and ^{50}Ti(83.1%) were procured in oxide form from Isoflex and Oak Ridge National Laboratory (ORNL) in oxide form. Natural abundance titanium and vanadium foils were obtained from Alfa Aesar.

3.2.2 MCNP Residual Nuclide Tally.

The output of Cinder90 is useful in that it is a robust and validated burn-up code. Its limitation is based on the lack of cross section data in the energy regions to be considered for this experiment. Another method in estimating yield is using the Ft8 tally in MCNP6 to determine cross sections at a given energy. The MCNP runs done in this section are independent of the flux geometry and rely on a simplistic geometry and set up to determine energy dependent cross sections for specified interactions. This method was used on the selected target materials of ^{nat}V, ^{nat}Ti, ^{47}Ti, and ^{50}Ti. These values were compared to the experimental results for the benefit of CEM and MCNP model improvement.

3.2.2.1 Ft8 RES Tally.

The residual nuclide tally (Ft8 RES) allows for the tallying of the residual nuclides in a specified tally energy range. A specific four digit ZAID may be entered for nuclide of interest (Z-number(XX), atomic number(XXX)). For a less specific tally, a range of Z numbers may be entered and user bins will be developed for each possible residual nucleus ZAID in that range. If no range is specified 2000+ possible residual bins will be listed [20].

This tally, in combination with the eighth entry on MCNPs LCA physics model card entry, NOACT, is very useful in extracting values that allow for the calculation of cross sections. The NOACT entry, when set to -2 forces MCNP to assume the source particle immediately collides with source material without the generation of secondary particles [20]. The residuals are then solely determined from the primary reactions, and not decay products [21].

An example input deck for residual nuclide tally is given in Figure 13. This example calls for the CEM3.03 model to be used with NOACT set to -2. The material was set

37

to match the isotopic abundance of the ^{47}Ti sample irradiated. The source was set with an energy of 100 MeV. A bash script was developed to run through all of the energy bin numbers used in estimating neutron flux. The Ft8 tally was set to calculate the residual neutrons for all residual nuclide ZAIDs with Z numbers from 19 to 23 (K, Ca, Sc, Ti, and V). For ease of flux calculation, a thin cylindrical target was specified.

For the case of this thesis, the value models are used beginning at zero. This allows two benefits. The first is a check for cross sections below 25 MeV which may be compared to empirical data. It also allows to draw a more complete comparison between the CEM3.30 physics model to the experimental outcome.

```
TestFile
1  1   -10.   -1 imp:n=1
2  0           1 imp:n=0

c Surface
1 rcc   0 0 0   0 0.0133 0   0.01

c Material Cards
m1    22000      1
mode n p
PHYS:P 110 0 0 0 1 0 0
PHYS:N 110 0 1 0
c Physics Models
LCA    7j -2 1
c Source Information
SDEF POS 0 0 0 DIR=-1 VEC=0 0 1 PAR=1 erg 100
NPS 10000000
c Tally
f8:n 1
ft8 res 19 23
PRDMP   2j -1
```

Figure 13. This is an example of the MCNP input deck that produces a tally of all residual nuclides with Z numbers between 19 and 23 (K, Ca, Sc, Ti, and V) resulting from direct neutron reactions. The 8th LCA entry of NOACT=-2 forces the model to assume all particles react instantaneously in the target with no secondary particles forming. The CEM3.03 physics model is used for this calculation. This deck is modified to run for energy levels ranging from 0 to 100 MeV. Each energy value is run for each of the target materials: ^{nat}V, ^{nat}Ti, ^{47}Ti-oxide, and ^{50}Ti-oxide.

3.2.3 Cross Section Derivation.

Corresponding cross sections are derived in MATLAB using MCNP results. Cross sections are calculated using the residual tallies, as well as the number of nucleons in the target, and the number of neutrons specified by the NPS card on the input deck (in this case 10^7 neutrons). Because of the nature of simulation, the reactions occur instantaneously, and the time element of the reaction rate and neutron flux is excluded. Cross sections were determined by,

$$\sigma = \frac{N_R}{\Phi \rho_A}, \tag{8}$$

where σ is the microscopic cross section, N_R is the number of residual nuclei per unit volume, Φ is the number of neutrons per unit area, and ρ_A is the atom density per unit volume. The residual tallies extracted from MCNP are given with a statistical error. This error was propagated through the calculation as well, giving a cross section error. Once all MCNP6 outputs have been converted into cross sections, these values can be extracted and organized by nuclide.

To guage the validity of the cross section calculation, a comparison is drawn from the data calculated in the lower energy regions where empirical data exists, to the tabulated data. In this study the ENDF6 nuclear database was used as ENDF is the default library utilized by MCNP when data is available. Figure 14 shows a comparison the MCNPs excitation function for the production of ^{47}Sc from ^{47}Ti using neutrons to the ^{47}Ti(n,p)^{47}Sc cross section up to 20 MeV tabulated in the ENDF6 library.

As is evident in this plot, there are variances in the modeled excitation functions and the results, indicating inaccuracy with estimating yield. This exercise in comparing the instantaneous production rates estimated by MCNP to those determined experimentally will be useful in increasing accuracy of future model development.

39
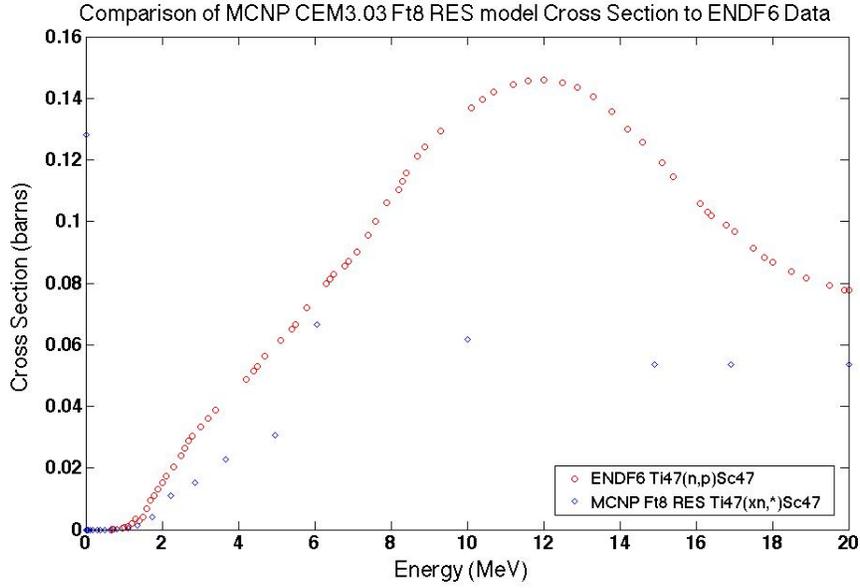
Figure 14. This plot shows a comparison of the modeled cross section obtained for ^{47}Ti neutron reactions generating ^{47}Ti to the ^{47}Ti(n,p)^{47}Sc cross section tabulated in ENDF6. The plot only shows a comparison up to 20 MeV, which is where the tabulated data ceases to exist.

3.2.4 MCNP Yield Estimation.

With an estimation for neutron flux and cross section data derived from the CEM3.03 physics model in MCNP, a yield estimation was made. The neutron flux calculation used, described in Section 3.1, was given per area per source proton. For this calculation, both neutron flux and cross section were contained in arrays based on energy bins. Through linear interpolation, they can be treated as functions of energy. The derived reaction rate becomes,

$$r(E) = \frac{\sigma(E)}{\Phi(E)N_p\rho_A}, \tag{9}$$

where r(E) is the reaction rate, resulting in the expected number of residual nuclei as a function of energy generated per unit volume. In this equation, the number of source protons specified on the input deck appear as N_p. In summing the energy bins in r(E), an estimated number or residual nuclei, R, generated through irradiation may

40

be obtained per source proton per gram of target material. This value was converted to μCuries and modified to account for the source intensity of 220 μA, which is equivalent to $1.375x10^{15}$ protons/s, giving rates in μCis^{-1} per gram of target material. From these values, as described in Section 3.2.1, predictions for isotopic purity were made. The estimated reaction rates and isotopic purity for the isotopes of interest in each of the selected target materials are given in Table 7.

Table 7. Reaction rates for isotopes of interest produced through the use of the Ft8 RES tally in MCNP in unites of μCi s^{-1} μAh^{-1}. These are compared to the results from the Cinder90 model, which are presented in the same unites of μCi s^{-1} μAh^{-1}. Isotopic purity associated to a 10-day irradiation is also listed. Plots showing the growth and decay for a ten day irradiation for each of the samples listed can be found in Figures 15 to 18. The values representing purity in the figure represent the isotopic purity corresponding to the MCNP calculation

Target Material	Isotope	MCNP6 Rate	Cinder90 Rate
^{nat}**V Foil**	^{47}Sc	0.00005 *13*	0.0002
(2.3% MCNP6 Purity)	^{46}Sc	0.0 *0*	0.0000
	^{48}Sc	0.0194 *11*	0.0002
	^{47}Ca	0.0 *0*	0.0000
	^{44}Ti	0.0 *0*	0.0000
^{nat}**Ti Foil**	^{47}Sc	0.0516 *12*	0.0386
(35.4% MCNP6 Purity)	^{46}Sc	0.0195 *12*	0.0124
	^{48}Sc	0.0820 *12*	0.0696
	^{47}Ca	0.0 *12*	0.0018
	^{44}Ti	0.0089 *12*	0.0000
^{47}**Ti Oxide**	^{47}Sc	0.2094 *11*	0.1535
(29.6% MCNP6 Purity)	^{46}Sc	0.3037 *12*	0.0018
	^{48}Sc	0.0045 *11*	0.0022
	^{47}Ca	0.0 *0*	0.0001
	^{44}Ti	0.1118 *12*	0.0000
^{50}**Ti Oxide**	^{47}Sc	0.0262 *11*	0.1494
(44.0% MCNP6 Purity)	^{46}Sc	0.0121 *12*	0.0001
	^{48}Sc	0.0098 *12*	0.2746
	^{47}Ca	0.0 *0*	0.0069
	^{44}Ti	0.0035 *12*	0.0000

The error listed in the chart is the result propagated from the statistical error out-

puts from both measurements in MCNP. The isotopic purity percentages predicted by MCNP are comparable to those predicted by the Cinder output. They are entirely the product of the MCNP CEM3.03 physics model. The purity values, in both cases, are the maximum purity that would result from a 10-day irradiation. The case for the 10 day exposure and cooling period are shown in Figures 15 through 18. The purity values are significantly lower based on the MCNP6 model generated in this experiment.
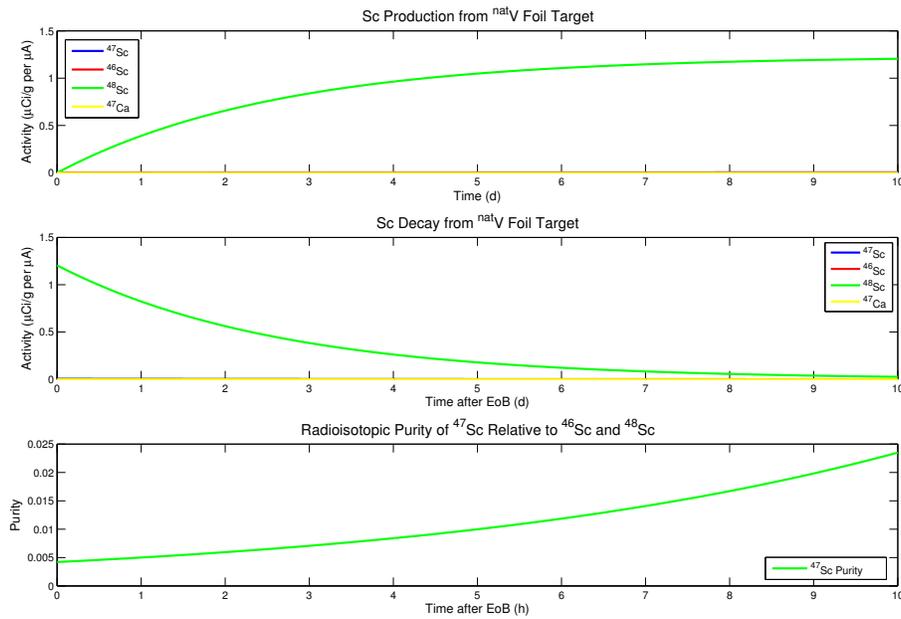
Figure 15. These plots were generated in the MATLAB script found in Appendix D. The calculations are based on production rates for a ^{nat}V target produced in MCNP6. The graph on the top shows the relative production of isotopes over the course of a 10-day irradiation. The middle graph shows relative decay rates as a function of time after the end of irradiation. The graph on the bottom shows the relative isotopic purity of ^{47}Sc.
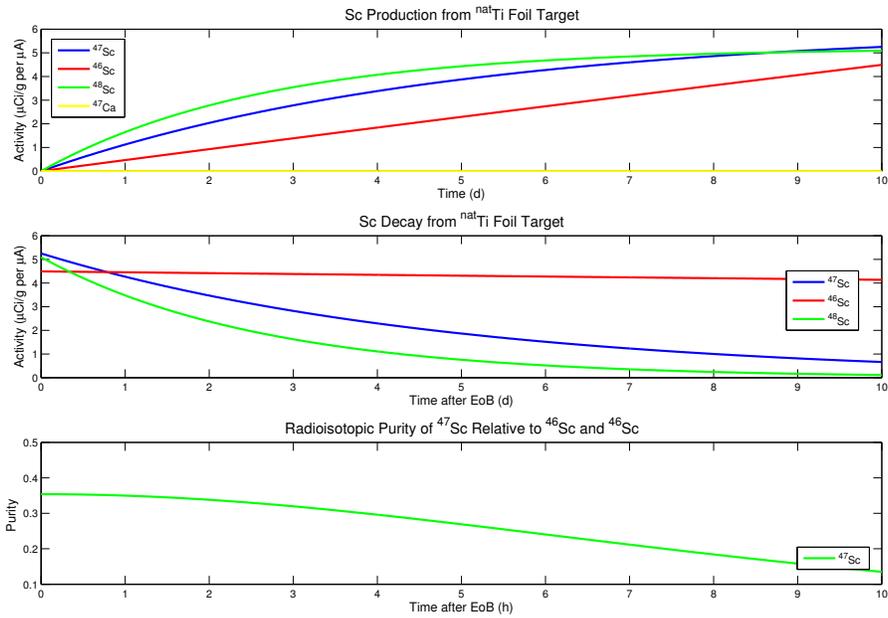
Figure 16. These plots were generated in the MATLAB script found in Appendix D. The calculations are based on production rates for a ^{nat}Ti target produced in MCNP6. The graph on the top shows the relative production of isotopes over the course of a 10-day irradiation. The middle graph shows relative decay rates as a function of time after the end of irradiation. The graph on the bottom shows the relative isotopic purity of ^{47}Sc.
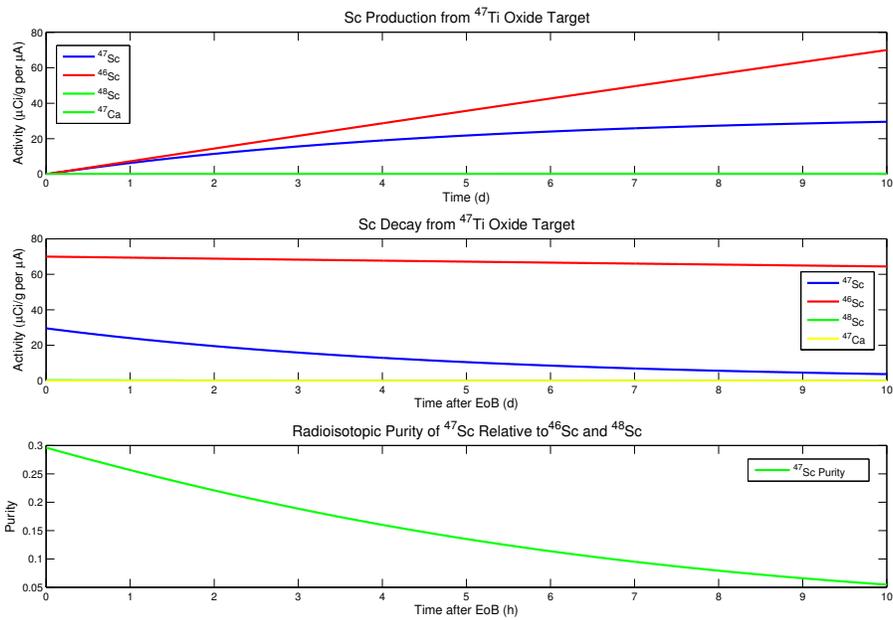
Figure 17. These plots were generated in the MATLAB script found in Appendix D. The calculations are based on production rates for a ^{47}Ti target produced in MCNP6. The graph on the top shows the relative production of isotopes over the course of a 10-day irradiation. The middle graph shows relative decay rates as a function of time after the end of irradiation. The graph on the bottom shows the relative isotopic purity of ^{47}Sc.

44

Figure 18. These plots were generated in the MATLAB script found in Appendix D. The calculations are based on production rates for a ^{50}Ti target produced in MCNP6. The graph on the top shows the relative production of isotopes over the course of a 10-day irradiation. The middle graph shows relative decay rates as a function of time after the end of irradiation. The graph on the bottom shows the relative isotopic purity of ^{47}Sc.

The time was used to draw a comparison between the modeled efforts and the experimental data, and does not reflect the ideal irradiation length to yield maximum purity. Irradiation length for best achievable isotopic purity was drawn in considering the experimental production rates, and is discussed in Chapter 5.

A surprising outcome of the MCNP6 output in comparison to the Cinder90 results was the values for Ti-44 production. It appeared that ^{44}Ti may be produced from the titanium targets due to predicted cross sections in the higher energy range. This is interesting because, if this method was discovered to produced ^{47}Sc with a high enough isotopic purity, and ^{44}Ti was also produced in usable quantities, then a theragnostic pair could be coproduced, allowing for the direct production of ^{47}Sc and the production of a ^{44}Sc with an unprecedented 60 year half-life.

4. Experimental Technique

The physical experimental preparation began 13 September 2013. The irradiation was carried out on 22 September 2013 with a beginning of beam (BOB) Julian time of 266.0285 and an end of beam (EOB) time of 266.0703. The irradiation lasted for one hour. Details of each step in the experiment, including methods and measurements, are presented in this section.

4.1   Target Preparation

The RbCl and Ga target stacks irradiated by IPF are shown in Figure 19. This effort is performed nearly continuously for 6 months. This experiment used the current IPF configuration with a slight modification made to the target stack holder that did not affect the primary operations of IPF.
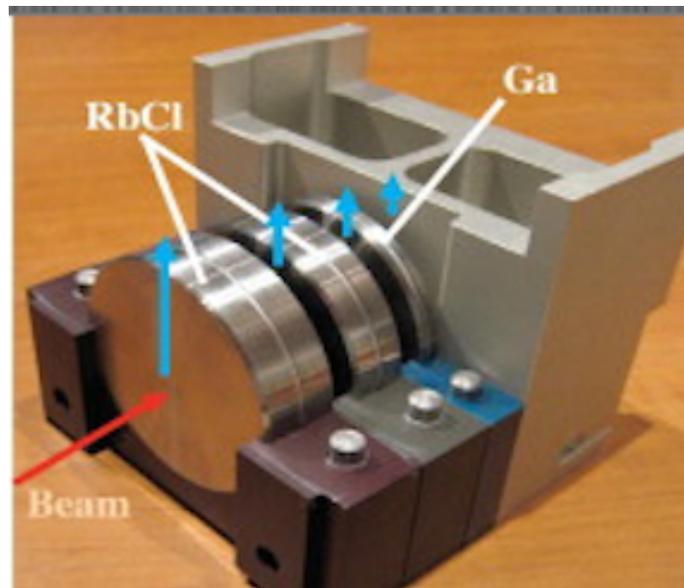
Figure 19. Target stack used for the production of Sr and Ge at IPF. For this experiment, the aluminum block behind the targets is removed and replaced with a spacer designed to seal and hold target materials for spallation neutron bombardment [8].
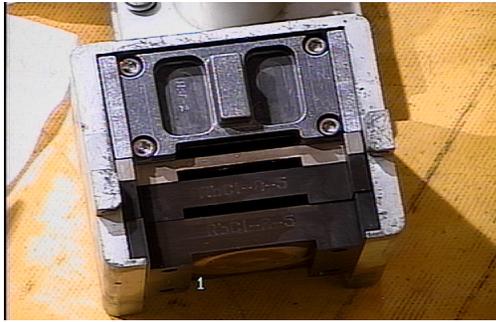
(a) Assembled Spallation Neutron Target Holder

(b) Spallation Neutron Target Holder Interior

Figure 20. (a) The neutron target holder replaces the aluminum spacer in the rear of the target stack. This is the assembled form of the target holder behind the Ga and RbCl targets. (b) The interior of the target holder, with space for up to five vials (ideal for powder or liquid samples) and two spaces for thin targets.

In the rear of the stack is an aluminum spacer. For the purpose of neutron irradiations, a new spacer was developed that fits in this space. The spallation neutron target holder (SNTH) has space for several samples with the maximum dimensions of 8.658 x 6.73 x 1.67cm. Figure 20 shows the SNTH. There are two slots, one in the front and the back, available for foil targets, and 5 locations suited for targets sealed in ampoules. This target stack has a sealable lid that holds the targets securely within their space.

For the experiment conducted, the target stack held both oxide targets and one of each of the ^{nat}Ti and ^{nat}V foils. The foil targets were sealed with Kapton tape and contained in the front most slot of the SNTH, closest to the proton targets. The ^{47}Ti and ^{50}Ti oxide targets were sealed in quartz ampoules and placed in the small cylindrical slots to the right and left of center.

4.1.1 Oxide Powder Preparation.

The oxide powders were prepared on 17 September 2013. The ampoules were created using high purity quartz glass to minimize activation of the ampule, and due to its ability to withstand high temperatures. The ampoules were sealed on one end, and filled with powder. Measurements were made using a digital scale.

48

Vial Label	T-47 (Vial1)	Error	T-50 (Vial2)	Error
Tare (g)	4.8639	0.0005	0.0000	0.0005
Filled (g)	4.9043	0.0005	0.0407	0.0010
Oxide (g)	0.0404	0.0005	0.0407	0.0010

Table 8. Oxides were measured and encapsulated in vacuum-sealed quartz ampules on 17 Sept 2013. The quartz tube used for this sample was made in the lab using Luc's quartz - it was 6 inches in length. A glass funnel was used to add oxide powder to the tube - some powder may have stuck to the funnel, leading to the increased error. Other sources of error, present in both measurements, include changes in condensation and on spring pressure in scale.

Approximately 40 mg of each oxide sample was selected due to availability. With 100 mg of ^{47}Ti oxide and 83 mg of ^{50}Ti oxide, the selected sample size allowed for a back-up sample of each in the event of a mishap during the experiment or for future investigation based on the results of this experiment. Once filled, ampules were connected to a vacuum tube. This created a pressure gradient between the inside and outside of the vial causing the walls of the ampule to collapse inward with the introduction of heat. A seal was then generated by applying heat using a focused flame. The oxide targets and their position within the SNTH are shown in Figure 21, with the ^{47}Ti sample on the left and ^{50}Ti sample shown on the right.
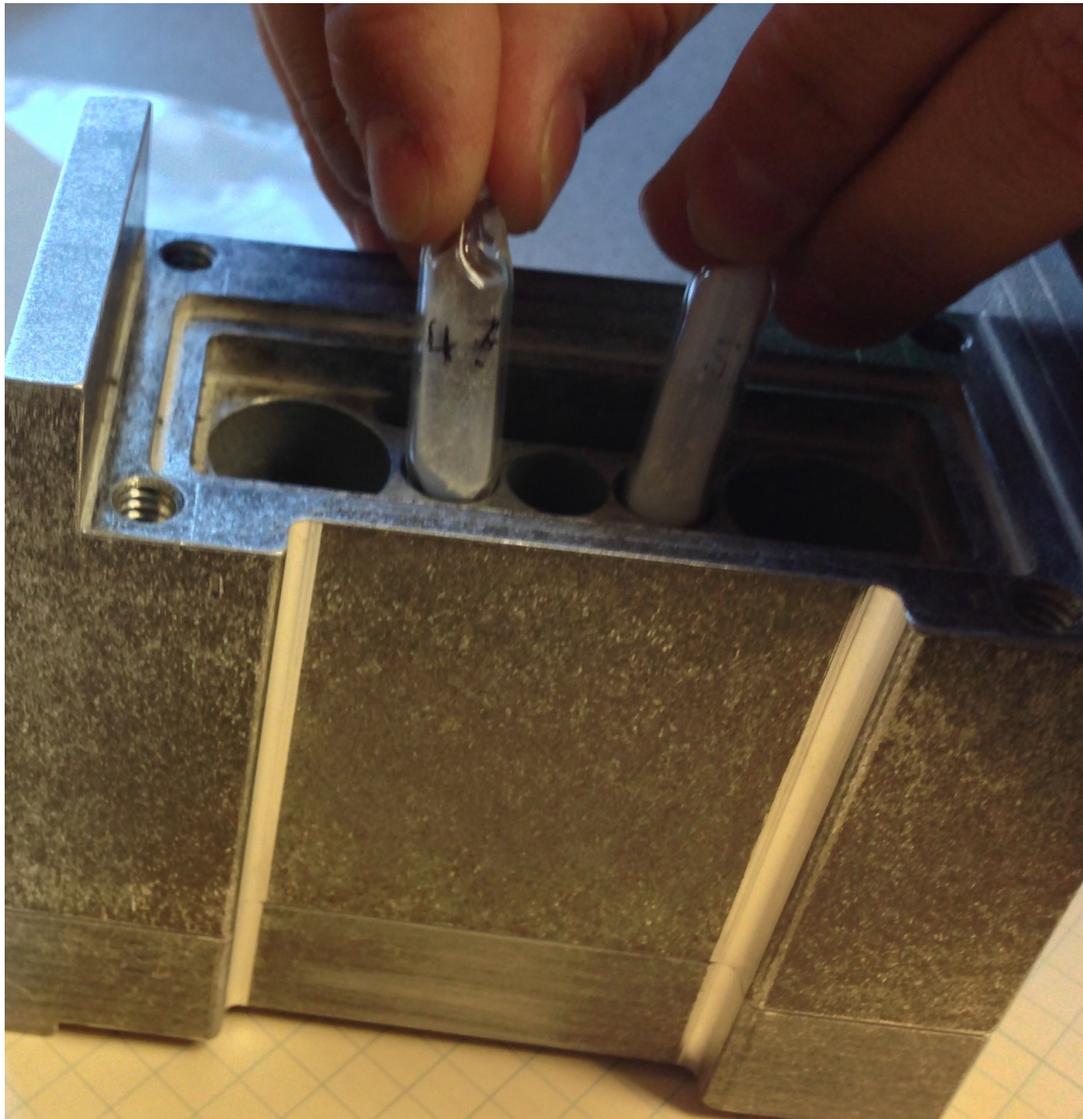
Figure 21. The ^{47}Ti and ^{50}Ti samples in sealed quartz ampoules, shown in reference to their locations within the SNTH during the irradiation. The ^{47}Ti sample is on the left in this image, and the ^{50}Ti sample on the right.

4.1.2 Foil Target Preparation.

Vanadium and titanium foils were ordered with a thickness of 0.127 mm. A handheld punch was used to punch out foils with a diameter of about 1 cm. These dimensions matched the specifications of the HPGe detectors used for spectroscopy. Each of these foils were carefully cleaned, measured and weighed. Three diameter and thickness mea-

surements, as well as five weight measurements were taken for each sample to ensure accuracy and to characterize error in the measurement. For both ^{nat}Ti and ^{nat}V, Sample 1 was selected for irradiation. Measurements for these foil samples are found in Table 22. The measurements for all samples prepared of each target material are listed in Appendix G

^{nat}V Foil Measurements			
Sample 1			
	Dia. (mm)	Thick. (mm)	Mass (g)
	10.34	0.140	0.0694
	10.33	0.137	0.0694
	10.31	0.135	0.0693
			0.0695
			0.0695
Average	10.32667	0.13733	0.06942
Std Dev	0.01528	0.00252	0.00008
Error	0.00882	0.00145	0.00004
^{nat}Ti Foil Measurements			
Sample 1			
	Dia. (mm)	Thick. (mm)	Mass (g)
	10.37	0.138	0.0509
	10.36	0.136	0.0508
	10.37	0.136	0.051
		0.139	0.0509
			0.0511
Average	10.367	0.137	0.05094
Std Dev	0.006	0.001	0.0001
Error	0.003	0.0007	0.00005

Table 9. Foil measurements and associated error. These measurements were taken on 18 Sept 13.

Error in the measurements of the foils was determined using measurement statistics [27]. The final value for each measurement was taken as:

$$x = \overline{x} \pm \sigma_{\overline{x}}, \tag{10}$$

51

where $\overline{x}$ is the average value of x, and $\sigma_{\overline{x}}$ is the the standard error, determined by,

$$\sigma_{\overline{x}} = \frac{\sigma_x}{\sqrt{N}}. \tag{11}$$

Once the foils have been properly measured, they were sealed using Kapton tape. Kapton tape was ideal due to its chemical stability at high temperatures. It contains low Z elements and can withstand very high radiation doses and intensities without breaking down [23]. Once properly sealed, tabs were added to each sample to ensure ease of removal from the SNTH. These tabs and the location in the SNTH in which the foils were placed for irradiation are visible in Figure 22.

(a) Vanadium Foil Sample 1   (b) Titanium Foil Sample 1

Figure 22. Four samples of both the Ti-nat and V-nat foils were measured and produced. Samples V1 and Ti1 were those actually irradiated. Others were prepared for the case of mishaps during irradiation or for follow-on irradiations. The irradiated samples ((a) ^{nat}V; (b) ^{nat}Ti) are shown in reference to the location within the SNTH in which they were held.

4.2   Irradiation

The irradiation took place on 22 Sept 13. At 1825 the beam was shut off and the target stack was lifted. The SNTH with ^{nat}V Foil Sample 1, ^{nat}Ti Foil Sample 1, and the ^{47}Ti and ^{50}Ti oxide ampoules were put in place of the standard aluminum spacer. Manipulation of the target stack and target samples was done using remote handling

equipment on the upper level of IPF. This level includes an equipment room and hot cell, allowing easier loading and retrieval of materials [8]. Figure 23(a) shows the hot cell and remote handling equipment in IPF's upper level. Figure 23(b) shows the system that allows targets to be lowered into the beam without entrance into the beam tunnel [8].
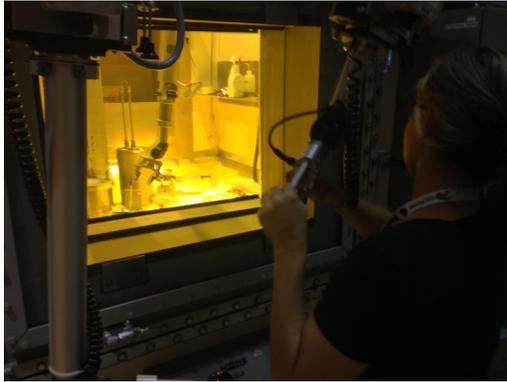
(a) Hot Cell at IPF

(b) IPF Hot Cell Beam Lift

Figure 23. (a) IPF hot cell and remote handling system. This photograph, taken after the experiment irradiation on 22 September 2013, shows the hot cell inside of IPF and use of the remote handling system for manipulation of materials inside the hot cell (b) A photograph of the lift-system used to lower targets into the proton beam without entering the beam tunnel and interrupting accelerator operations.

The targets were lowered into place and the irradiation was started at 1841. The documented beginning of beam (BOB) time was 266.0285. The beam ran for an hour and was shut off with an end of beam (EOB) time of 1941, documented as 266.0703. Investigation of the post-irradiated aluminum target holder revealed scorch marks, indicating that the proton beam current may be penetrating into the SNTH. Similarly, scorching was evident at the top of the quartz ampules. Both are visible in Figure 24.

(a) SNTH Post-Irradiation

(b) Post Irradiation Quartz Ampoules

Figure 24. Scorch mark visible on both the SNTH and the quartz ampoules after irradiation. Photographs taken after removal of the target from beam on 22 Sept 2013.

Once the samples were removed from the beam, the SNTH was removed from the target stack and replaced with the aluminum spacer. This was placed immediately back into the beam to minimize impact on IPF production. The samples were then removed and placed in bags in preparation for transport.

4.3 Sample Transport

On Monday, 23 Sept 13, the samples were loaded into a cask and transported to TA-48. The samples were prepared to be removed from the cask. Upon removal they were checked to ensure dose safety for transport into a hood for preparation. The following measurements were obtained at 30 cm: 18 mRem (Ti-47 Sample), 15 mRem (Ti-50 Sample), 2.5 mRem (Ti-nat Sample) and 1.5 mRem (V-nat Sample). The truck and cask used for transport can be seen in Figure 25(a). Figure 25(b) shows the samples at the time the above measurements were taken.

54

(a) Transport Vehicle and Cask

(b) Targets After Transport

Figure 25. (a) Four samples of both the Ti-nat and V-nat foils were carefully transported in the cask shown in the foreground of this image. The cask was transported from IPF to TA-48 via the truck visible in the background. (b) The foils were removed from the cask carefully with many measurements in accordance to radiation safety procedures. The following measurements were obtained at 30 cm: 18 mRem (^{47}Ti Sample), 15 mRem (^{50}Ti Sample), 2.5 mRem (^{nat}Ti Sample) and 1.5 mRem (^{47}V Sample).

Once cleared by the responsible radiation safety members at IPF, the samples were moved to a cold cell and were prepared for counting.

4.4 Counting Preparation of Foil Samples

Preparation of foil samples for counting required centering samples on counting disks, which were specifically designed for the gamma detectors to be used in the count room at Los Alamos. Prior to mounting the foils to the disks, however, the Kapton enclosed foils required surface cleaning.

The surface of the Kapton tape was highly radioactive. The primary source of this radioactivity was ^{24}Na with a characteristic gamma peak at 1392.5 keV. This peak was visible when placing the samples in the gamma counter at the hot cell facility (Counter

77). ^{23}Na is a common element, and may come from various places in the environment, including from physical handling prior to irradiation.

With the use of Fantastik brand all purpose cleaner and Kimwipes, the samples were cleaned to a level deemed acceptable for transport to the count room. Background in the hot cell facility was measured at 1.75×10^3 dpm. The activity of the exterior was determined by wiping the sample and measuring the activity of the wipe. The Ti-foil sample wipe measured at 4.5813×10^3 dpm after the first cleaning attempt, and measured at background levels after the second. The V-foil sample was cleaned twice with readings of 3.75×10^3 dpm on the first Kimwipe used.

Once cleaned, the foil samples were taped to the counting disks using a layer of 25 μm thick Kapton tape covering both foils. Figure 26 shows the foils fully prepared for counting, prior to being moved to the count room.
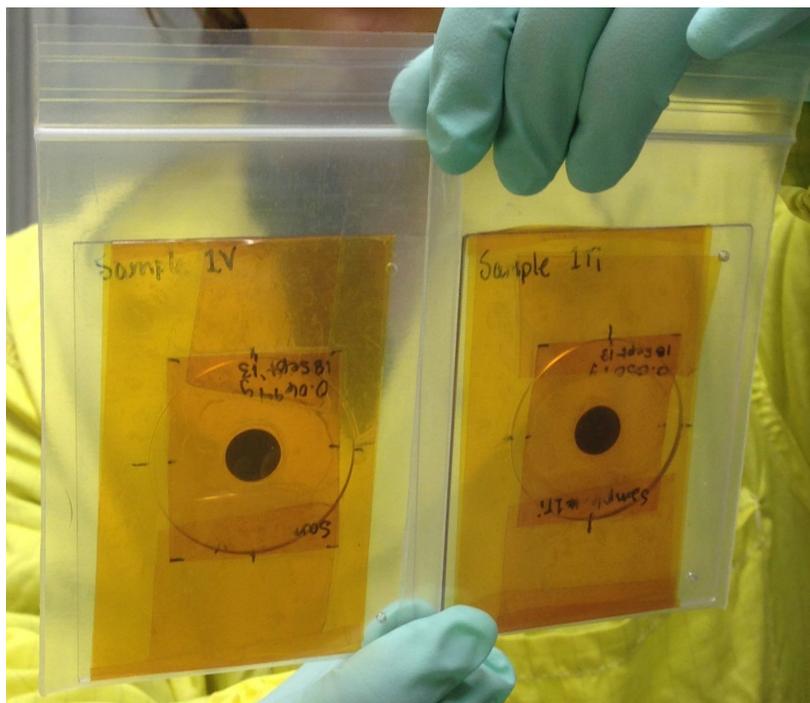
Figure 26. ^{nat}**V and** ^{nat}**Ti foils cleaned and prepared on counting disks for the count room, where they were placed in Counter 43 with respective identification numbers of** $2023-01-047$ **and** $2022-01-047$**.**

The samples were cleared and moved to Counter #43 in the count room. Samples in the count room are identified by a shot-jug-mass identification number. The ^{nat}V foil, placed in counter position 7, was given the identification number 2023-01-047. The ^{nat}Ti foil, placed in counter position 4, was given the identification number 2022-01-047.

4.5   Counting Preparation of Oxide Samples

The oxide samples were set to be counted in Counter 55, which was calibrated for 5 mL of liquid in the polypropylene vials shown in Figure 27. The vials used for counting were selected, labeled and weighed on 24 Sept 13 for the 47Ti and 50Ti oxide samples. The respective weights were 8.4260 g and 8.3869 g.
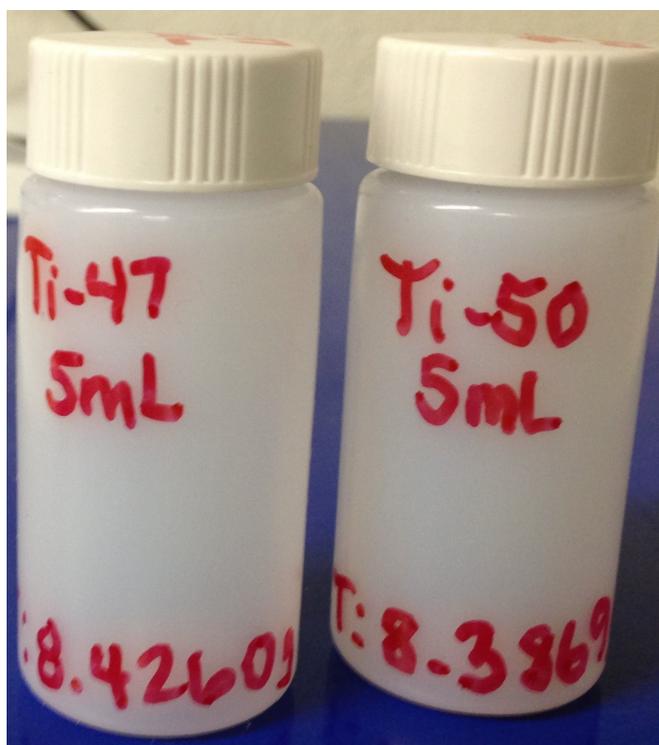
Figure 27. Polypropylene vials prepared for 5 mL of the dissolved ^{47}V and ^{50}Ti oxide solutions to be introduced to Counter 55.

Due to this calibration, and for the sake of a homogeneous sample distribution, the

57

oxide samples were diluted into a solution of water, ammonium sulfate ($(NH_4)_2SO_4$) and sulfuric acid (H_2SO_4) [28]. Several methods of dissolution were considered in dealing with TiO_2. These methods were tested on cold samples. The following method was selected. 5 mL water was added to a 150 mL sample of TiO_2 and shaken until a milky, homogeneous solution formed. Next, 30 mL of H_2SO_4 and 12 g of $(NH_4)_2SO_4$ was added. This solution was then heated gently to begin, then strongly in order to completely dissolve the sample.

The cold cell example began with 49.7 mg of TiO_2 to which 2 mL of H_2O was added. 10 mL of H_2SO_4, and 2 mL of $(NH_4)_2SO_4$ were added, and the solution was placed over heat. This dissolution process took 48 m in the cold cell sample until completely clear.

Before beginning this process with the hot oxide samples, they were removed from the quartz ampoules. This process proved to be more difficult than planned, as scoring and emptying the quartz left a large amount of oxide behind, stuck to the interior of the ampoule. To avoid these losses, the quartz ampoule was smashed in large polypropylene vials where the initial solution was formed. The polypropylene Vial was then emptied into a quartz vial where the dissolution process took place. Once completed, 5 mL of each sample were transferred to the polypropylene vials shown in Figure 27.

[50]Ti oxide was the first to be prepared. A large metal rod was used to break open the quartz ampoule. There was powder on the end of the rod after the ampoule was broken. To return the powder to the Vial with the rest of the sample, 14.2936 mL of water was used to rinse. This solution was moved to a quartz vial. The large polypropylene Vial was rinsed with 5 mL of H_2SO_4, now added to the solution. Another 5 mL of H_2SO_4 was added to the quartz Vial along with 4.0136 g of $(NH_4)_2SO_4$. For the [50]Ti solution, a second Vial was added in which 13 mL of solution was placed over heat.

To prepare [47]Ti same method of breaking the quartz ampoule was used. Rather than using an excessive amount of water to clean off the rod, 2 mL of H_2O and 8 mL of H_2SO_4

were used. This solution was transferred by pipet to a quartz ampoule. Another 5 mL of H_2SO_4 was used to rinse out the large polypropylene Vial. The result was a reaction with the iron in the rod, leading to a brown-orange color, visible in Figure 28. Next, 4.0305 g of $(NH_4)_2SO_4$ was added. Rather than transferring this solution to another Vial, as was done with ^{50}Ti, this entire solution was moved onto heat for dissolution.

After 74 min over heat, ^{47}Ti and ^{50}Ti samples had fully dissolved. In order to separate the solutions from the quartz shards, they were pipetted into transfer polypropylene vials. From these vials, 5 mL of each solution was transferred into the final vials. Several stages of the vials used in this project are pictured in Figure 28.
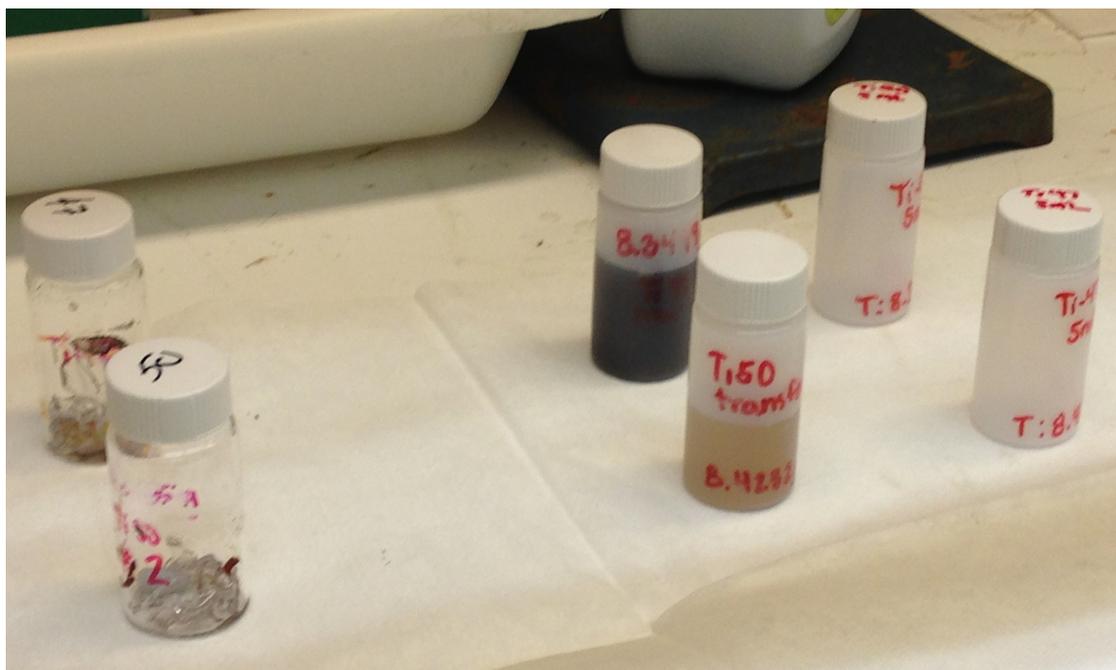
Figure 28. The vials in this photograph are from various stages of vials used in the dissolution process of ^{47}Ti and ^{50}Ti. The quartz vials on the far left are the vials that were heated to dissolution. The quartz still remains in the vials as the solutions were removed and transferred to polypropylene transfer vials. Finally, 5 mL of each solution were transferred to the vials on the far right to be placed in Counter 55.

TiO_2 is typically completely translucent when dissolved into solution, which is what occurred in the cold sample. The murky colors seen here are the result of the tool used to

break the quartz ampoules. At 1504 MST on 23 September 2013, the vials were transferred to the count room. The identification numbers for ^{47}Ti and ^{50}Ti, respectively, were 2022-02-047 and 2022-03-047. Figure 29 shows the respective samples placed in Counter 55. The ^{47}Ti sample was placed in position 8, and ^{50}Ti was placed in position 10.
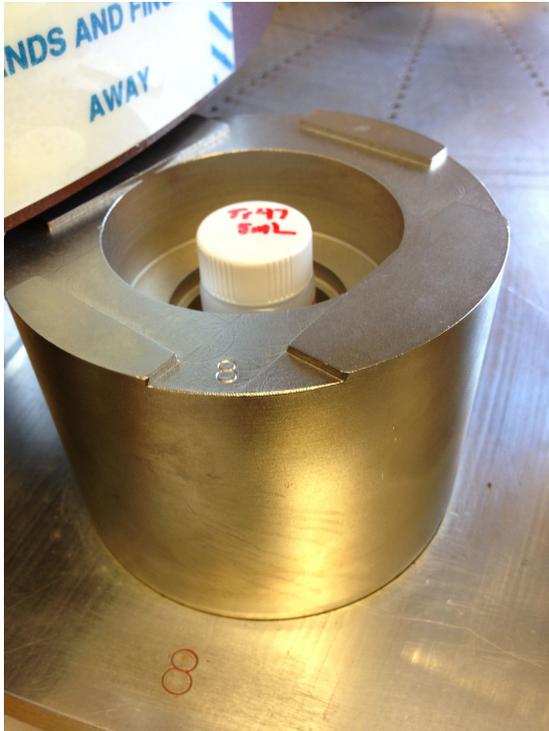
(a) ^{47}Ti Oxide Solution in Counter 55   (b) ^{50}Ti Oxide Solution in Counter 55
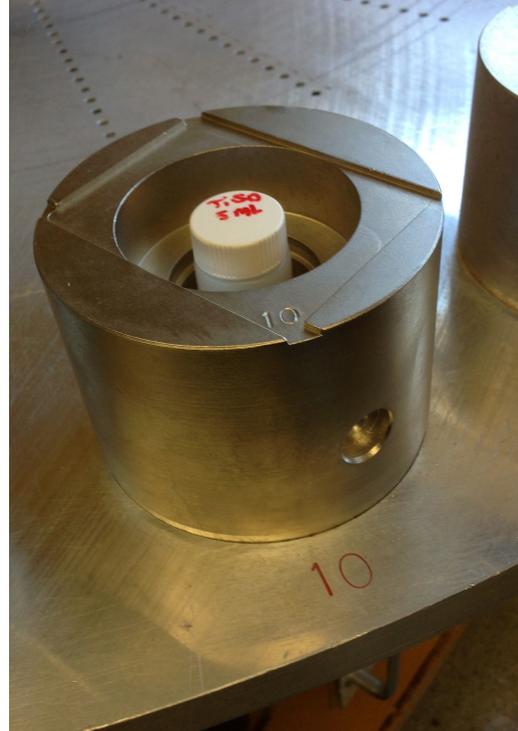
Figure 29. The ^{47}Ti sample in position 8, and ^{50}Ti in position 10 of Counter 55 in the count room at TA-48.

4.6   Gamma Counting

After dissolution, HPGe detectors (Counters 43 and 55 in the count room and Counter 77 in the hot cells) were used to allow for gamma spectroscopy. With all isotopes easily distinguishable, three sets of count data are likely sufficient for the analysis.

It is ideal, however, to take more in the event that something unexpected is produced that does interfere with this peak, as is possible in this energy regime. Should this occur, three data points are insufficient in performing peak decay analysis [9]. Tables 10 and 11 list the expected production results from the vanadium and titanium targets respectively.

Table 10. Projected products from neutron irradiation of V-nat foils. The gamma energies, half-lives, modes of decay and decay products are listed for each of the potential irradiation products.

Isotope	Gamma(s) [keV]	Half-Life	Decay Mode	Decay Product
52V	1434.1	3.76 m	β -	Cr-52
51Ti	320.1	5.76 m	β -	V-51
50V	N/A	N/A	N/A	N/A
50Ti	N/A	N/A	N/A	N/A
49Ti	N/A	N/A	N/A	N/A
49Sc	1762; 1623	57.3 m	β -	Ti-49
48Sc	983.5; 1312.1; 1037.5	43.7 h	β -	Ti-48
47Sc	159.4	3.349 d	β -	Ti-47
46Sc	1120.5; 889.3	83.81 d	β -	Ti-46

Based on these lists, there was little cause for concern. Still, 8 counts were taken for both of the foil targets and 7 counts for each of the oxide targets. Multiple counts were taken in order to improve statistics of the weighted fits. Spectroscopy methods and results are given in Section 5.1 of Chapter 5.

Table 11. Projected products from neutron irradiation of Ti-nat foils, Ti-50 and Ti-47 oxides. The gamma energies, half-lives, modes of decay and decay products are listed for each of the potential irradiation products. Abundance of products will differ between foils and oxide targets, however expected products remain the same. Note: For the oxides, products resulting from O(n,*) reactions are omitted due to negligible half-lives.

Isotope	Gamma(s) [keV]	Half-Life	Decay Mode	Decay Product
Ti45	161; 165; 166	184 m	ϵ	45Sc
Ti44	146; 78; 67	59.1 y	ϵ	44Sc
K43	617; 593; 396; 372; 220	22.3 h	β -	43Sc
K42	1524	12.36 h	β -	42Ca
51Ti	320.1	5.76 m	$\beta-$	51V
50Ti	N/A	N/A	N/A	N/A
50Sc	1553.8; 1121.1; 523.8	1.71 m	β -	50Ti
49Ti	N/A	N/A	N/A	N/A
49Sc	1762; 1623	57.3 m	β -	49Ti
48Ti	N/A	N/A	N/A	N/A
48Sc	983.5; 1312.1; 1037.5; 175.4	43.7 h	β -	48Ti
48Ca	N/A	N/A	N/A	N/A
47Ti	N/A	N/A	N/A	N/A
47Sc	159.4	3.349 d	$\beta-$	47Ti
47Ca	1297.1	4.536 d	$\beta-$	47Sc
46Sc	1120.5; 889.3	83.81 d	$\beta-$	46Ti
46Ca	N/A	N/A	N/A	N/A
45Sc	N/A	N/A	N/A	N/A
45Ca	12.47	162.7 d	β -	45Sc
44Sc	1157; 511	3.97 h	$\beta+$	44Ca
44Ca	N/A	N/A	N/A	N/A
43Sc	511; 372; 220	3.891 h	$\beta+$	43Ca
43Ca	N/A	N/A	N/A	N/A

5. Results and Analysis

The primary peaks of interest for analysis are listed in Table 12 along with their prominent gamma energies and associated intensities.

Table 12. The isotopes under investigation with gamma energies and intensities. These values were taken from Brookhaven National Laboratory's National Nuclear Database, Nuclear Database (NuDat) 2.6.

Isotope	Peak Energy (keV)	Intensity(%)
^{47}Sc	159.381	68.3
^{48}Sc	983.526	100.1
	1312.120	100.1
^{46}Sc	889.227	99.98
	1120.545	99.98
^{47}Ca	1297.09	67
^{44}Ti	67.87	93.0
	78.32	96.4

The scandium isotopes are listed due to their hindrance to the use of ^{47}Sc as a therapeutic pharmaceutical, disused in Chapter 2. ^{47}Ca is of interest because it will β-decay into ^{47} as discussed in Section 3.2.1.1. Finally, ^{44}Ti is of interest in this experiment as it has potential as a generator for ^{44}Sc which forms a theragonistic pair with ^{47}Sc. While the modeled experiment did not predict useful quantities of ^{44}Sc being produced, there was a potential that in the higher energies, higher cross sections for production exist. Investigation of all production results were done using tools made available by the count room, as well as data processing scripts written in MATLAB.

5.1 Count room Spectroscopy

The spectral data taken by the count room was available in multiple formats. Both raw and processed data were available allowing for by hand investigations or robust

peak analysis. Investigation of raw data was useful in determining the overall state of the sample, and in determining potential interference of Compton electron contributions to low energy peaks. For individual peak analysis, LANL runs all spectra through three well-validated peak fitting models, RAYGUN, SPECANL, and UNISAMPO. To ensure uniform analysis, all models were considered and one was selected based on modeling strengths and documented validation.

5.1.0.1 UNISAMPO.

After a review of the available peak fitting options, UNISAMPO was selected as the primary analysis tool used. UNISAMPO is the Unix platform integration of SAMPO, which engages a cubic spline fitting method to isolate energy peaks from raw spectral data. This method works by modeling the background and noise continuum of a spectrum with a continuous curve comprised of optimized cubic splines [29]. UNISAMPO identifies peaks through a weighted difference method. It is also generally paired with SHAMAN, a tool that utilizes a gamma library of over 2600 nuclides to perform automated identification of radionuclides [29].

The output of UNISAMP is collected and compiled for each peak in a given sample over time. The output data given includes the date and time of the count made, the shot, jug and mass numbers of the sample, the position within the detector for which the count was made, the start and end times of the count made and the EOB time for that sample (all in Julian time), the time since EOB that the count was made given in days, the count length, the energy of the peak under investigation, the FWHM of the peak, the raw area under the peak, the number of peak gammas and associated error determined based on shelf number and efficiency, and the peak efficiency of the detector.

The data for each peak and sample was pulled into a text file. The calculated peak gamma values, elapsed time, count length, error and efficiency were extracted for each

64

to use for analysis. An example of the data is shown in Table 13 for the ^{47}Sc 159.4 keV peak in the ^{Nat}Ti sample.

Table 13. The data in this chart is extracted from the UNISMAPO output for analysis of the 159.4 keV peak of ^{47}Sc extracted from spectra for the ^{nat}Ti sample.

PeakGammas (particles x 10^6)	Time Elapsed (d)	Count Length (min)	Percent Error	Efficiency
7.934	0.7896	20	0.1	0.004564
6.842	1.599	20	0.1	0.004461
5.091	3.093	20	0.2	0.004393
4.162	4.097	20	0.2	0.004367
3.699	4.699	20	0.2	0.004355
1.816	8.203	20	0.3	0.004319
0.8815	11.71	20	0.4	0.004306
0.4345	15.22	60	0.3	0.004301

5.2 Decay Analysis Method

In order to determine activity at EOB, analysis of the decay of energy peaks was conducted. The peak analysis tools provided a total number of counts within the peak and the intrinsic peak efficiency. Using the UNISAMPO data a nonlinear least squares model was developed to generate an estimate for the activity present for each isotope at the time the proton beam was shut off.

The peak gamma data was calculated by the count room analysis tools. The peak gamma count corresponds to the number of radiation quanta emitted by the source at the peak energy being investigated,

$$S = N \frac{4\pi}{\epsilon_{ip}\Omega}, \tag{12}$$

where S is the number of quanta emitted by the source over the period of measurement,

N is the number of events detected within the peak, ϵ_{ip} is the intrinsic peak efficiency, and Ω is the solid angle determined by the position of the source within the detector [26]. Plotting this peak gamma count value allows for a fit for the decay scheme of that particular energy.

A least square fit of the basic decay for each peak was investigated as a starting point. The basic equation used to fit the data can be written as,

$$N(t) = N_0 e^{-\lambda t}, \tag{13}$$

where N(t) is the count value in time, N_0 is the number of quanta emitted for the peak energy investigated at EOB, and t is the time elapsed since EOB [26]. It should be noted that the count lengths determining N(t) have varying count lengths. This was adjusted by dividing the total number of counts by the count length, thus giving a count rate, N(t).

For the ^{nat}Ti and the ^{50}Ti samples, it was expected that ^{47}Ca be produced, and thus the Bateman Equation (Equation 6) must be engaged in order to properly fit the data. As well, it is possible that other isotopes in the same decay chain may be produced, emitting gammas at the same energies as the isotopes of interest. In the ^{nat}V sample, the presence of ^{48}V isotope was expected to be present within the 983.5 keV and 1312.12 keV gamma lines of ^{48}Sc.

5.2.1   Weighted Linear Least Squares Fit.

The peak data was characterized by a statistical error associated with the total number of counts. For a number of counts, N, this is determined as $\sigma = \sqrt{N}$ [26]. This uncertainty value was used as a weight in a least squares fit of the data. This ensured that more statistically accurate data points are given stronger consideration in the fitting of the data.

66

In fitting the exponential function characterizing nuclear decay, it is best to first linearize the equation. Rather than fitting N(t), the fit was conducted to the parameter z, such that

$$z = ln(N(t)) = ln(N_0) + \lambda t. \tag{14}$$

Once linearized, a weighted linear least squares fit was applied. The weights corresponding to a basic linear equation, $y = A + Bx$, for y_i values with different uncertainties, σ_i, are $w_i = 1/\sigma_i^2$. For the linearized exponential, $z_i = ln(y_i)$, the uncertainty of z_i became $1/\sqrt{y_i}$, therefore making the weight of z_i, simply y_i [27]. It should be noted that the uncertainty in the counts was associated to the total number of counts taken, not the counts/minute (N(t)) being used to generate the fit. This ensured that the fit is based on the statistical accuracy of a given point. The best estimate for N_0 using this fit was,

$$N_0 = e^{(\Sigma wt^2 \Sigma wN(t) - \Sigma wt \Sigma wN(t))/\Delta}, \tag{15}$$

where Δ is characterized as,

$$\Delta = \Sigma w \Sigma wt^2 - (\Sigma wN(t))^2. \tag{16}$$

The uncertainty in this value is then determined by,

$$\sigma_{N_0} = N_0 \sqrt{\frac{\Sigma wt^2}{\Delta}} \tag{17}$$

The MATLAB script developed to execute this least squares fit and estimate the activity at EoB is located in Appendix H.

5.3 Peak Fit Results

The results of the weighted nonlinear fit model for the 159.4 keV ^{47}Sc peak are given in Figures 30 to 33. This process proved very useful in determining the various isotopes contributing to each peak. For the ^{47}Sc peaks, it was found that all samples but the ^{nat}V had appreciable contributions due to co-production of ^{47}Ca. While contributions were not abundant in the ^{nat}V sample, they were detectable. As such, fits for all ^{47}Sc peaks included ingrowth of calcium. This required first finding initial values for the 1297.1 keV peak of ^{47}Ca. The associated figures are included in Appendix I.
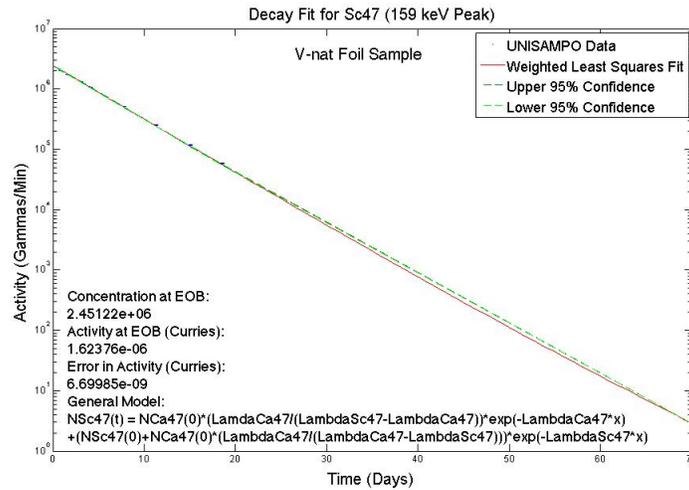
Figure 30. This figure, generated in MATLAB from the peak fitting data extracted by the UNISAMPO data analysis tool shows a weighted nonlinear model fit of the 159.4 keV peak of ^{47}Sc within the ^{nat}V sample. It is plotted with 95% confidence bounds determined by error propagated throughout the fitting process. NOTE: The confidence bounds and error bars are difficult to see in this fit due to the low statistical error within the peak. The activity at EoB calculated for this sample is 1.624$\pm$.007 μCi.
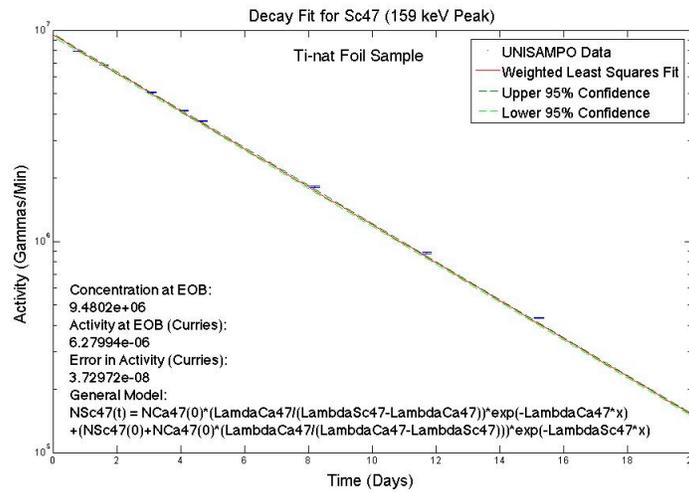
Figure 31. This figure, generated in MATLAB from the peak fitting data extracted by the UNISAMPO data analysis tool shows a weighted nonlinear model fit of the 159.4 keV peak of ^{47}Sc within the ^{nat}Ti sample. It is plotted with 95% confidence bounds determined by error propagated throughout the fitting process. NOTE: The confidence bounds and error bars are difficult to see in this fit due to the low statistical error within the peak. The activity at EoB calculated for this sample is **6.26±.03 μCi.**
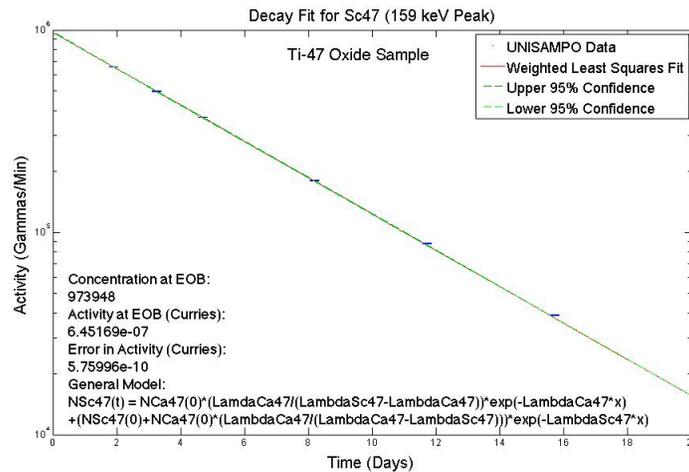
Figure 32. This figure, generated in MATLAB from the peak fitting data extracted by the UNISAMPO data analysis tool shows a weighted nonlinear model fit of the 159.4 keV peak of ^{47}Sc within the ^{47}Ti sample. It is plotted with 95% confidence bounds determined by error propagated throughout the fitting process. NOTE: The confidence bounds and error bars are difficult to see in this fit due to the low statistical error within the peak. The activity at EoB calculated for this sample is **0.6451±.0006 μCi.**
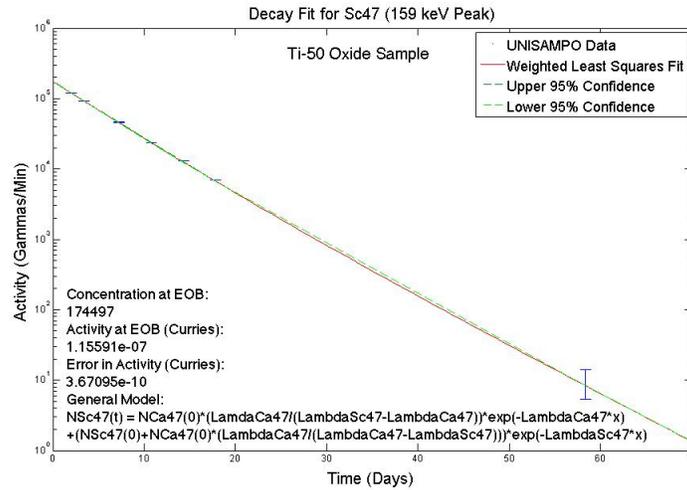
Figure 33. This figure, generated in MATLAB from the peak fitting data extracted by the UNISAMPO data analysis tool shows a weighted nonlinear model fit of the 159.4 keV peak of ^{47}Sc within the ^{50}Ti sample. It is plotted with 95% confidence bounds determined by error propagated throughout the fitting process. NOTE: The confidence bounds and error bars are difficult to see in this fit due to the low statistical error within the peak. The activity at EoB calculated for this sample is 0.1156±.0004 μCi.

5.3.0.1 ^{48}Sc Peak Analysis.

The ^{48}Sc peaks for both ^{50}Ti and ^{nat}Ti targets follow basic decay fit as expected. The fits for the 1312 peak of ^{48}Sc are shown in Figures 34 and 35. The expected trend for the ^{nat}V target was seen as well, in that both the 983 and 1312 keV peaks included influence from ^{48}V, decaying with a half-life of 15.97 days. The fit for the 1312 keV peak in ^{nat}V including the ingrowth of ^{48}V is displayed in Figure 36.

The decay formula to which this fit is modeled is,

$$N(t) = N_1(0)e^{-\lambda_1 t} + N_2(0)e^{-\lambda_2 t} \tag{18}$$

70
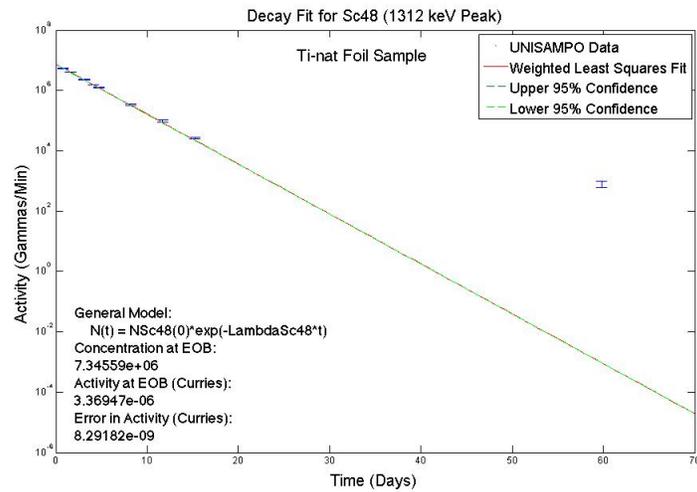
Figure 34. This figure, generated in MATLAB from the peak fitting data extracted by the UNISAMPO data analysis tool shows a weighted nonlinear model fit of the 1312 keV peak of ^{48}Sc within the ^{nat}Ti sample. It is plotted with 95% confidence bounds determined by error propagated throughout the fitting process.
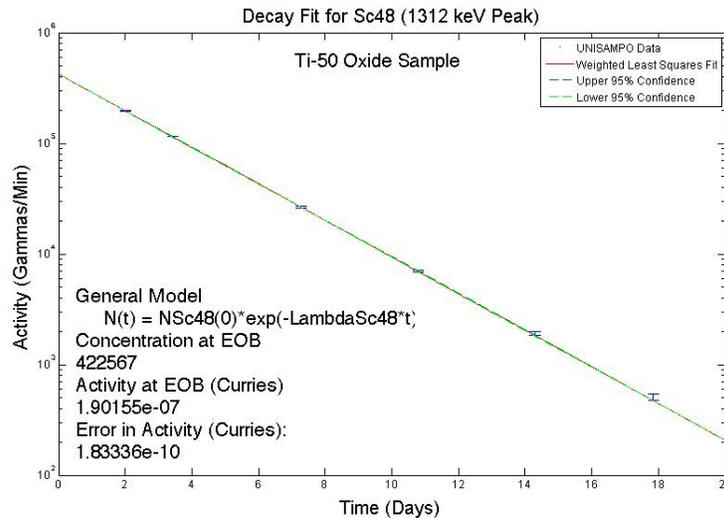
Figure 35. This figure, generated in MATLAB from the peak fitting data extracted by the UNISAMPO data analysis tool shows a weighted nonlinear model fit of the 1312 keV peak of ^{48}Sc within the ^{50}Ti sample. It is plotted with 95% confidence bounds determined by error propagated throughout the fitting process.

71
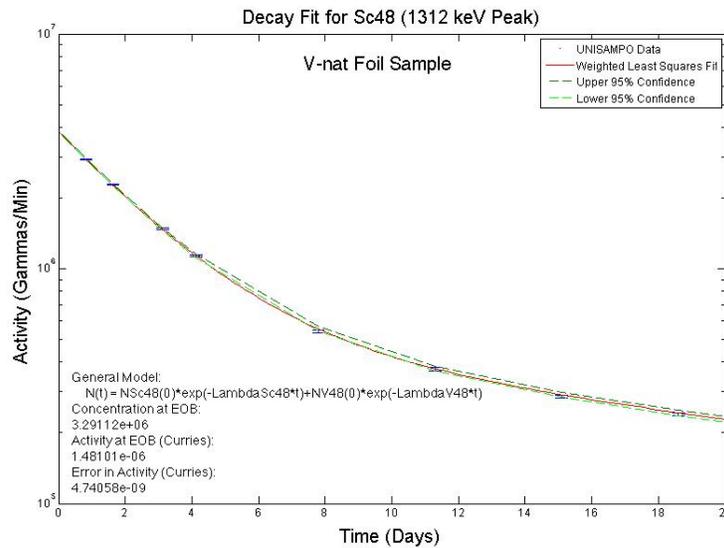
Figure 36. This figure, generated in MATLAB from the peak fitting data extracted by the UNISAMPO data analysis tool shows a weighted nonlinear model fit of the 1312 keV peak of ^{48}Sc within the ^{nat}V sample. It is plotted with 95% confidence bounds determined by error propagated throughout the fitting process.

An unexpected observation was evidence of ^{48}V present in the ^{47}Ti Sample. The fit matches well, however the increased uncertainty in the data points causes flair in the confidence bounds towards the end of the fit. In fitting both the 983 keV peak and the 1312 keV peak (Figure 37), the activity at EoB for each falls well within margin of error.

For the 983 keV peak, the activity calculated is $0.1254 \pm .00007 \mu$Ci, and for 1312 keV the value was $0.125 \pm .0001$, bringing confidence to the fit. It appears that proton reactions are therefore occurring within the ^{47}Ti Sample. It is very unlikely that protons are entering from the proton beam. It is possible that, because the sample is not thin, like the foil, protons are being produced and secondary particle reactions are being observed. Further investigation is required to verify the source of protons.

72
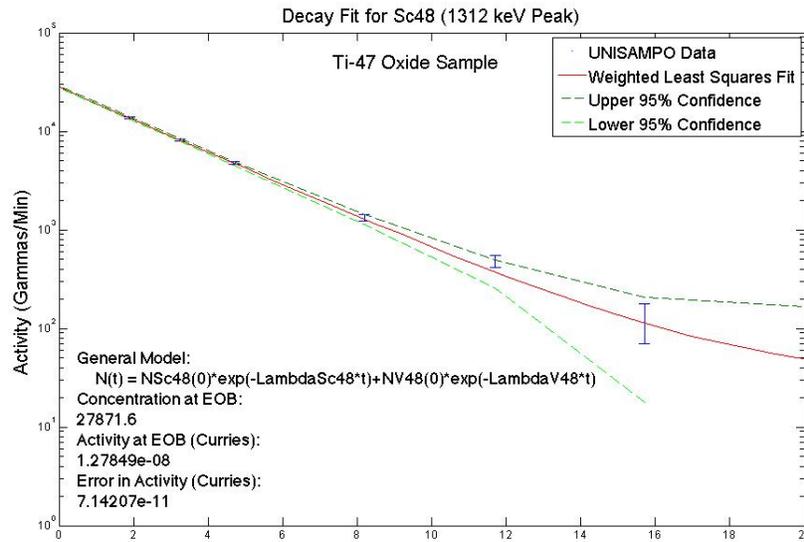
Figure 37. This figure, generated in MATLAB from the peak fitting data extracted by the UNISAMPO data analysis tool shows a weighted nonlinear model fit of the 1312 keV peak of ^{48}Sc within the ^{47}Ti sample. It is plotted with 95% confidence bounds determined by error propagated throughout the fitting process.

An indicator of well-fit data for all samples is given by the agreement between the two different peaks emitted by the same isotope. Table 14 shows the results for the 983 keV and 1312 keV energy peaks for all samples.

Table 14. The results for activity at EoB based on a weighted nonlinear model for ^{48}Sc energy peaks. The values include error propagated from the 1σ statistical error in counting.

Target Sample	Activity at EoB from 983 keV Peak (μCi)	Activity at EoB from 1312 keV (μCi)
^{nat}V Foil	1.48±.005	1.48±.009
^{nat}Ti Foil	3.28±.01	3.27±.01
^{47}Ti Oxide	0.0125±.0001	0.0125±0.0001
^{50}Ti Oxide	0.188±.0001	0.190±0.0001

The activities determined from the 983 keV and 1312 keV peak are in very good agreement for all samples. Figures showing the results for the 983 keV peak for all

73

samples are located in Appendix J.

5.3.0.2 ^{46}Sc Peak Analysis.

^{46}Sc has a half-life of 83.79 days, which significantly increased the statistical error in measurements. Even so, fits with propagated error gave results that fell in relatively close agreement, as shown in Table 15.

Table 15. The results for activity at EoB based on a weighted nonlinear model for ^{46}Sc energy peaks. The values include error propagated from the 1σ statistical error in counting.

Target Sample	Activity at EoB from 889 keV Peak (μCi)	Activity at EoB from 1120 keV (μCi)
^{nat}V Foil	0.0493±.0003	0.0486±.0005
^{nat}Ti Foil	0.203±.001	0.202±.002
^{47}Ti Oxide	0.0346±.0001	0.0350±0.0001
^{50}Ti Oxide	0.0025±.00001	0.0025±0.00001

Upon initial investigation, it appeared that there might be ingrowth of another isotope in both peaks for all three titanium targets. An investigation of potential contaminants showed no logical answer. The other potential explanation was error in the peak fitting method for the first few counts, as the half-life and low abundances of ^{46}Sc in early counts resulted in a small peaks. To check this, fits of the data from both the RAYGUN and SPECANL fitting tools were made. An example of this comparison is shown in Figure 38.

74
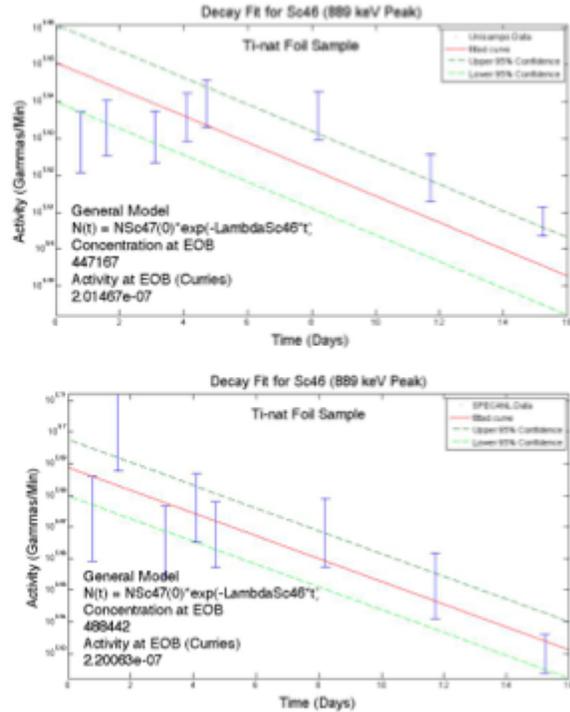
Figure 38. A comparison of analysis tool results for 889 keV ^{46} Peak in ^{nat}Ti shows that there is no specific trend for the data leading to the conclusion that the variances in the data are a product of poor statistics.

All comparison plots showed no specific trend in the data, and came in reasonable agreement to a derived initial activity. Consideration of this investigation led to the conclusion that variations in the data are a result of statistical error associated with early counts of a relatively long-lived isotope. In order to decrease error in the fit models after analyzing the results, another count was taken for a longer duration. With more time having passed, better statistics were obtained for the ^{46}Sc fits. Fits for both the 889 keV and 1120 keV peaks of ^{46}Sc in all samples are located in Appendix K.

5.3.0.3 ^{44}Ti Peak Analysis.

^{46}Ti has peaks at 67 keV and 76 keV. Very small peaks were evident at 67 keV and were investigated. With a 59.1 year half-life, it is unlikely that ^{44}Ti would be detectable in early counts. This was confirmed by attempted fitting of the 67 keV peak data, an

75

example of which is displayed in Figure 39.
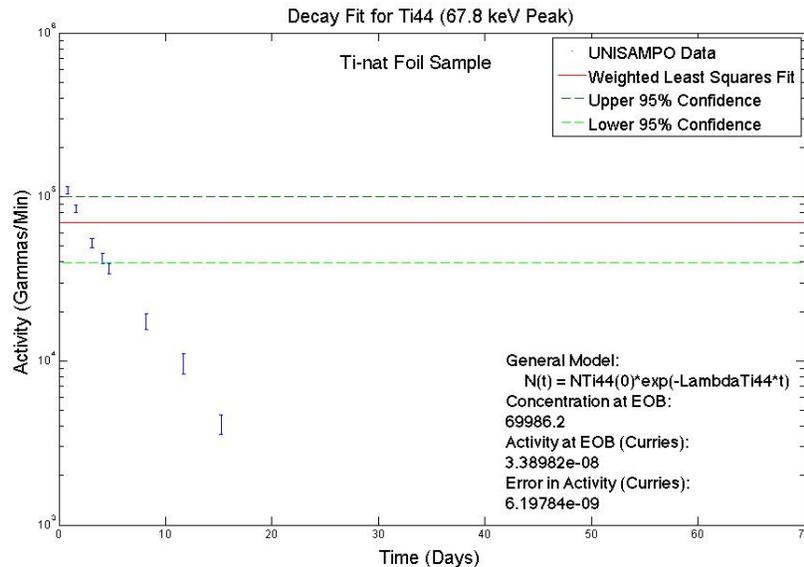
Figure 39. Failed fitting attempt of a 67 keV peak to the decay model of ^{44}Ti.

It is still possible that detectable levels of ^{44}Ti are in the data, but much longer counts are required after the decay of the shorter-lived isotopes.

5.4   Radiochemical Loss in Oxide Dilution

The activity values for the ^{47}Ti and ^{50}Ti oxide samples must be adjusted to account for the loss of activity resulting from the dilution of the radioactive oxide powders, described in Section 4.5. The samples sent to Counter 55 in the count room of TA-48 comprised of 5mL of the diluted solution. There were 5 separate vials used in this process for the ^{50}Ti sample and 4 vials used in the ^{47}Ti sample, each described in Table 16. Only ^{47}Ti Vial #4 and ^{50}Ti Vial #5 were sent to Counter 55. A separate count for all nine vials were made in the counter in the hot cells facility (Counter 77) in order to determine the relative loss of radioactive material.

76

Table 16. Descriptions of vials used in each step of the oxide dilution process. Included is the start time of each sample when counted in counter 77 in Julian time, the live time value of the count length in minutes, and the shelf number from which it was counted.

Specimen	Description	Start Time	Live Time (min)	Shelf
^{47}Ti Vial #1	Large Polypropylene Vial in which quartz ampule was opened	267.8581	5	6
^{47}Ti Vial #2	Quartz Vial with full solution	267.9030	3	6
^{47}Ti vial #3	Quartz Vial with 5 mL removed	267.9381	5	5
^{47}Ti Vial #4	Polypropylene Vial sent to count room	267.9274	5	6
^{50}Ti Vial #1	Large Polypropylene Vial in which quartz ampule was opened	267.6758	5	6
^{50}Ti Vial #2	Vial in which dilution of sulfuric acid was made	267.8721	5	6
^{50}Ti Vial #3	Quartz Vial with full solution	267.8967	3	6
^{50}Ti Vial #4	Quartz Vial with 5 mL removed	267.9284	5	5
^{50}Ti Vial #5	Polypropylene Vial sent to count room	267.9202	5	6

5.4.1 Peak Analysis of Counter 77 Data.

In order to determine the radioactive losses peak analysis was performed on each of the spectral plots. Each peak is fitted by performing a least squares fit of a single Gaussian to the peak. The MATLAB script performing this function uses a peak fit function, peakfit4.2.1, which provides a fit and residual plot of each peak as it runs through, and allows the operator to accept or reject it based on goodness of fit. An example of a peak residual plot is shown in Figure 40.
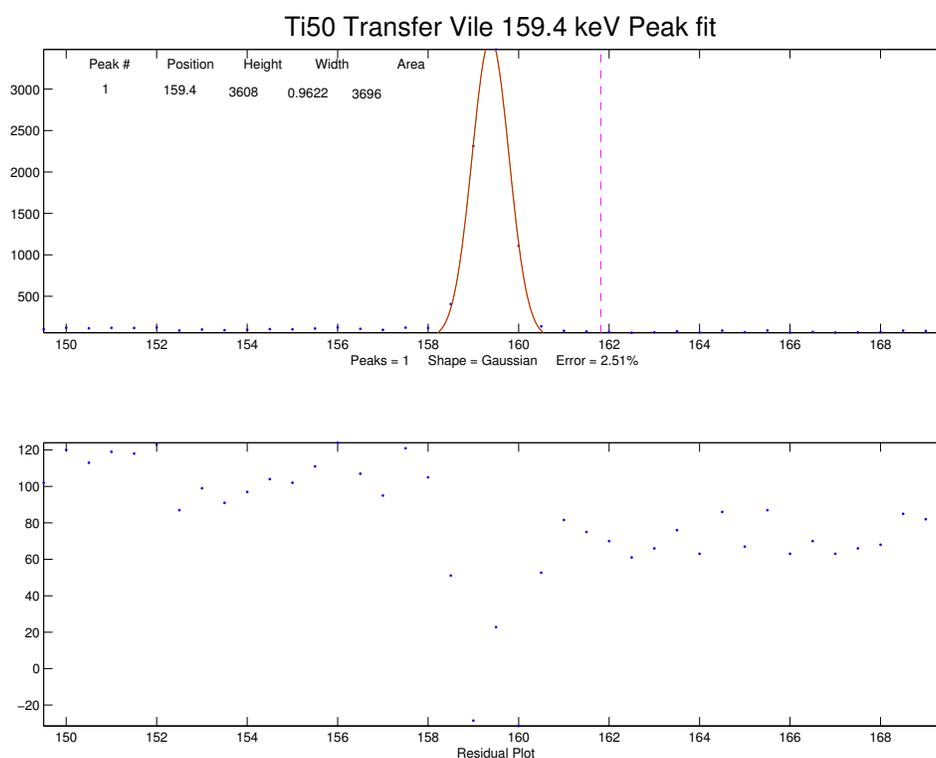
Figure 40. Sample fit and residual plot generated using peakfit4.2.1 for the 159.4 keV peak with in the ^{50}Ti Transfer Vial spectrum.

Once the peaks were isolated and a sum of the counts under the peak was determined, the values were adjusted based on both the intensity of the individual peak and the peak

78

efficiency of the detector.

The detector efficiencies were taken from an efficiency calibration done in 2010 for each individual shelf. The intrinsic peak efficiency can be determined by,

$$\epsilon_{ip} = \frac{N4\pi}{S\Omega}, \tag{19}$$

where N is the number of counts detected, S is the number of gammas emitted by the source, and Ω is the solid angle from the source position to the detector. The efficiency calibration data includes consideration for the solid angle and distance of the shelf from the detector in its determination. The decay rate per peak can therefore be calculated by,

$$R_\gamma = \frac{N}{I_{pk}\epsilon_{ip}\tau}, \tag{20}$$

where N is the number of counts beneath the peak, I_{pk} is the peak intensity, ϵ_{ip} is the intrinsic efficiency and τ is the count length. The results for each individual peak were then treated by their best-fit decay model determined by fits performed on the counts taken in the count room, discussed in Section 5.1. A MATLAB script, located in Appendix L, was written to perform all of the above tasks. An example of the final output from this script is shown in Table 17,

Table 17. This sample of the Counter 77 analysis script output shows the activity at EoB determined for ^{50}Ti Vial #1.

Isotope	Activity (μCi)	Activity Error (μCi)
^{47}Sc	0.0471	0.0011
^{46}Sc (889keV)	0.0096	0.0009
^{46}Sc (1120keV)	0.0093	0.0010
^{48}Sc (983keV)	0.0828	0.0039
^{48}Sc (1312keV)	0.0861	0.0045
^{47}Ca	0.0078	0.0014

79

A direct comparison of activity at EoB was then made for those calculated from the Counter 77 and Counter 55 by determining the ratio of the activity at EoB from each counter for ^{47}Ti Vial #4 and ^{50}Ti Vial #5. The resulting ratios from Counter 55 to Counter 77 for these vials are listed in Table 18.

Table 18. Ratios between the activity determined at EoB for ^{47}Ti Vial #4 and ^{50}Ti Vial #5 from Counter 77 and Counter 55.

Isotope	^{47}Ti Vial #4	^{50}Ti Vial #5
^{47}Sc		1.07
^{46}Sc (889keV)	1.92	0.95
^{46}Sc (1120keV)	1.99	0.70
^{48}Sc (983keV)	2.05	0.96
^{48}Sc (1312keV)	1.98	1.02
^{47}Ca	1.99	0.90

The ratio values were then used to determine losses for each isotope in each Vial used in the dilution process, listed in μCi in Table 19. The lost activities were added to the activity calculated for the oxide targets, and considered in determining production rates.

Table 19. Activity lost per isotope in each Vial used during the oxide dilution process.

^{47}**Ti**		
Vial #1		
Isotope	**Peak Energy (keV)**	**Activity Loss (μCi)**
^{47}Sc	159.4	0.4377±.005
^{46}Sc	889	0.118±.005
	1120	0.102±.007
^{48}Sc	983	0.103±.006
	1312	0.085±.007
^{47}Ca	1297	0.057±0.005
Vial #3		
Isotope	**Peak Energy**	**Activity Loss (μCi)**
^{47}Sc	159.4	1.513±.007
^{46}Sc	889	0.102±.003
	1120	0.102±.003
^{48}Sc	983	0.111±.003
	1312	0.075±.003
^{47}Ca	1297	0.0026±0.0006
^{50}**Ti Vial #5**		
Vial #1		
Isotope	**Peak Energy (keV)**	**Activity Loss (μCi)**
^{47}Sc	159.4	0.050±.001
^{46}Sc	889	0.007±.001
	1120	0.007±.001
^{48}Sc	983	0.080±.004
	1312	0.088±.004
^{47}Ca	1297	0.007±0.001
Vial #2		
Isotope	**Peak Energy (keV)**	**Activity Loss (μCi)**
^{47}Sc	159.4	0.9714±.005
^{46}Sc	889	0.048±.002
	1120	0.041±.003
^{48}Sc	983	1.60±.02
	1312	1.60±.02
^{47}Ca	1297	0.057±0.006
Vial #4		
Isotope	**Peak Energy**	**Activity Loss (μCi)**
^{47}Sc	159.4	0.116±.001
^{46}Sc	889	0.0053±.0004
	1120	0.0058±.0004
^{48}Sc	983	0.1915±.004
	1312 81	0.1997±.004
^{47}Ca	1297	0.0128±0.001

5.5 Experimental Production Rates

The production rate of each isotope relative to each target material was calculated based on the beam current at IPF during the irradiation. Beam logs for the event are shown in Figure 41.
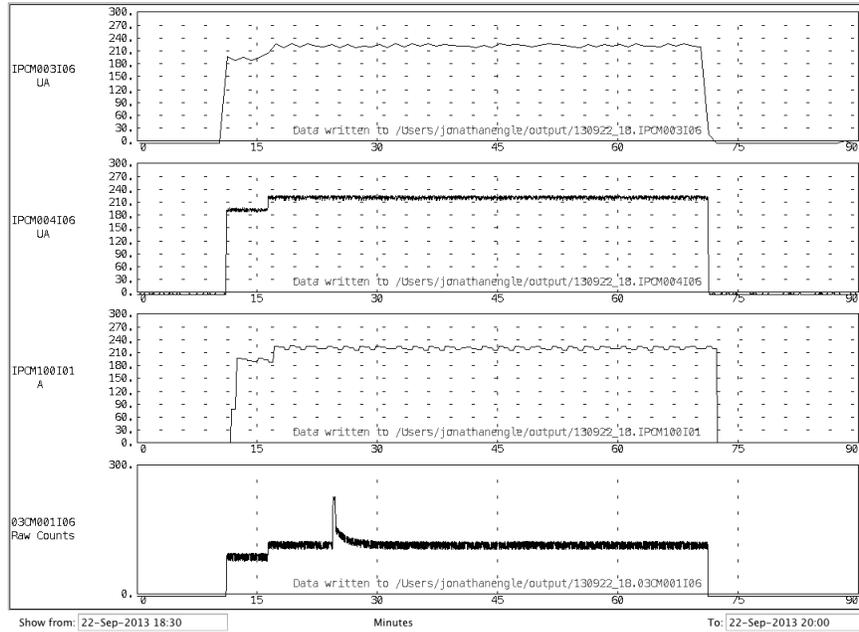
Figure 41. IPF Beam Log for 22 Sept 2013 from 1820 to 1955 MST.

For the first 5 minutes after the beam was turned on the beam was running at an average of 191.22 μAh, after which it rose to an average of 221.48 μAh. The average beam energy was 218.0 μAh. This was the value used in determining production rate in units of μCi g^{-1} μAh^{-1}. The masses for each material used are listed in Chapter 4 in Tables 8 and 22. The resulting production rates for ^{47}Sc, ^{47}Ca, ^{46}Sc, and ^{48}Sc are provided in Table 20.

Comparison of the Experimental and Cinder90 productions rates reveal that Cinder90 did underestimate the production in most cases. As suspected, the vanadium target showed production rates three orders of magnitude higher than Cinder90s esti-

82

Table 20. Production rates determined from experimental results.

Target Material	Isotope	Rate($\mu Ci\ s^{-1}\ \mu Ah^{-1}$)
^{nat}V Foil	^{47}Sc	0.1462±0.0052
	^{46}Sc	0.0035±0.0035
	^{48}Sc	0.1333±0.0046
	^{47}Ca	0.0002±0.0000
^{nat}Ti Foil	^{47}Sc	0.4430±0.0133
	^{46}Sc	0.0003±0.0003
	^{48}Sc	0.2319±0.0069
	^{47}Ca	0.0026±0.0001
^{47}Ti Oxide	^{47}Sc	0.2958±0.0333
	^{46}Sc	0.0264±0.0032
	^{48}Sc	0.0163±0.0021
	^{47}Ca	0.0010±0.0002
^{50}Ti Oxide	^{47}Sc	0.1352±0.0213
	^{46}Sc	0.0063±0.0011
	^{48}Sc	0.2325±0.0370
	^{47}Ca	0.0154±0.0026

mation, as the reactions for production of ^{47}Sc fall in the energy regime not populated with cross sections. Unfortunately, the MCNP6 prediction of a problematic amount of ^{48}Sc coming into the production scheme proved true, lowering the isotopic purity from the values given in the Cinder90 model. The ^{50}Ti target is the one for which all production rates except for ^{47}Ca were lower than predicted.

5.6 Experimental Isotopic Purities

Using experimental productions rates, use of the method used for the modeled rates in Section 3.2.1 may be employed in order to determine the isotopic purities of the experimental results. Table 21 shows the maximum achievable isotopic purity of ^{47}Sc relative to ^{46}Sc and ^{48}Sc after a 10 minute irradiation.

The ^{nat}V foil target did have much higher production rates than predicted, however the increase in production rates for ^{47}Sc extended to ^{48}Sc as well. Figure 42 displays the

83

Table 21. The listed purities are the percent purity of ^{47}Sc relative to ^{46}Sc and ^{48}Sc in each potential target material. These values are derived from the production rates determined from the experimental results listed in Table 20.

Material	^{47}Sc Purity (%)
^{nat}V Foil	71.7
^{nat}Ti Foil	93.8
^{47}Ti Oxide	80.9
^{50}Ti Oxide	61.7

isotopic purity as a function of time after EOB, as well as relative production and decay of isotopes within the target.
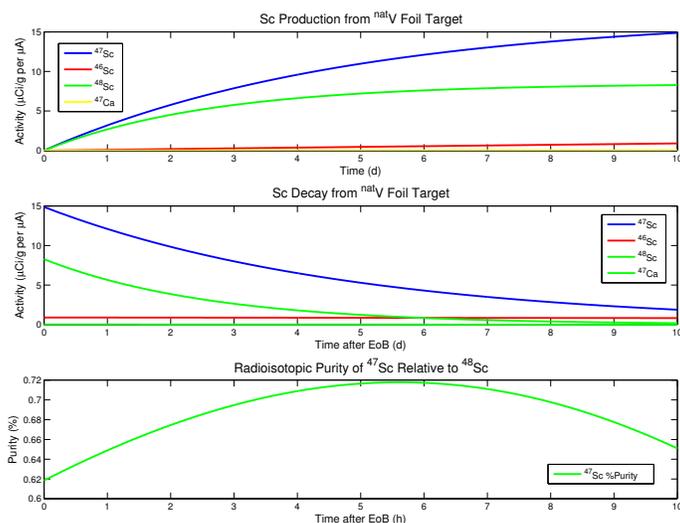
Figure 42. These plots were generated in the MATLAB script found in Appendix D. The calculations are based on production rates determined from experimental results. The graph on the top shows the relative production of isotopes over the course of a 10-day irradiation. The middle graph shows relative decay rates as a function of time after the end of irradiation. The graph on the bottom shows the relative isotopic purity of ^{47}Sc.

Due to a high production rate of ^{48}Sc, the highest achievable isotopic purity of ^{47}Sc for this irradiation was only 71.8%, as opposed to the 90.3% prediction by Cinder90. For the same reason, the ^{47}Ti and ^{50}Ti Oxide targets, pictured in Figures 43 and 44 gave similar results.

84
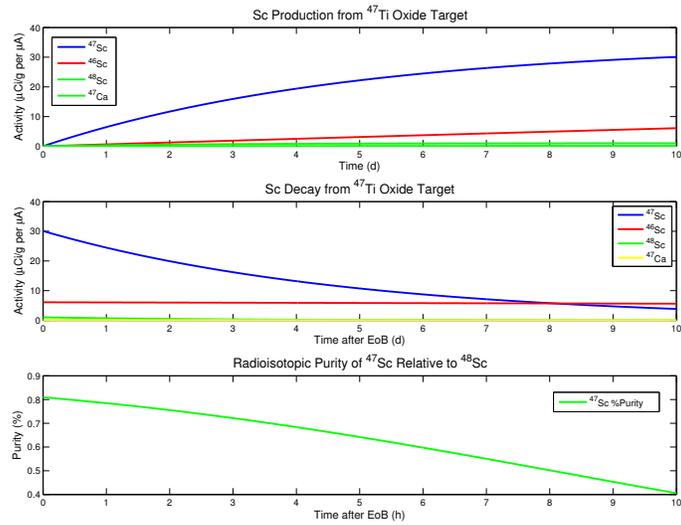
Figure 43. These plots were generated in the MATLAB script found in Appendix D. The calculations are based on production rates determined from experimental results. The graph on the top shows the relative production of isotopes over the course of a 10-day irradiation. The middle graph shows relative decay rates as a function of time after the end of irradiation. The graph on the bottom shows the relative isotopic purity of ^{47}Sc.
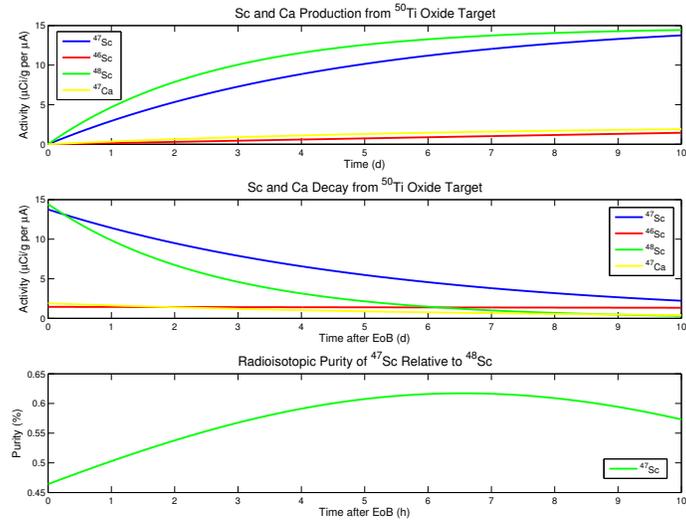
Figure 44. These plots were generated in the MATLAB script found in Appendix D. The calculations are based on production rates determined from experimental results. The graph on the top shows the relative production of isotopes over the course of a 10-day irradiation. The middle graph shows relative decay rates as a function of time after the end of irradiation. The graph on the bottom shows the relative isotopic purity of ^{47}Sc.

^{50}Ti analysis resulted in a 61.7% maximum purity, as opposed to the predicted 84.3%.

^{47}Ti was expected to produce purities above 95
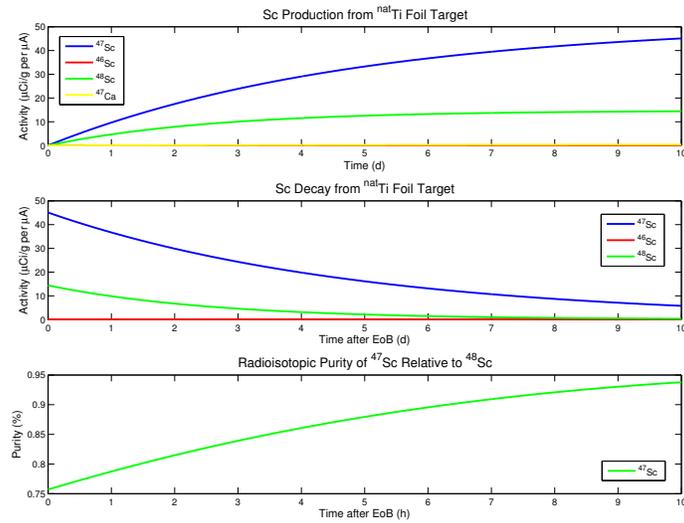
Figure 45. These plots were generated in the MATLAB script found in Appendix D. The calculations are based on production rates determined from experimental results. The graph on the top shows the relative production of isotopes over the course of a 10-day irradiation. The middle graph shows relative decay rates as a function of time after the end of irradiation. The graph on the bottom shows the relative isotopic purity of ^{47}Sc.

Contrary to predicted values, ^{nat}Ti gave the highest potential isotopic purity at 93.8%.

6. Conclusions

Scandium-47 ($T_{1/2} = 3.41d$) has potential as a pharmaceutical for imaging and therapeutic applications. It has beta emissions at 441.1 keV ($E_{\beta-,max}$, $I_{\beta-} = 68\%$) and 600.5 keV$_{max}$ ($E_{\beta-,max}$, $I_{\beta-} = 32\%$) that are well suited for internal radiation therapy, as well as an imageable 159.4 keV gamma to permit in vivo-tracking of compound biodistribution. Scandium has shown to form stable complexes with aminopolycarboxylic acids, such as folate conjugates, which are useful as tumor biomarkers or antigens. Additionally, ^{47}Sc has a theragnostic pair in ^{44}Sc (94.27% $\beta+$; $T_{1/2} = 3.97h$), a positron-emitting isotope successfully developed in recent years.

An investigation was conducted in exploiting ^{47}Ti(n,np) ^{47}Sc, ^{50}Ti(n,3p) ^{47}Sc, ^{nat}V(n,x)^{47}Sc, and ^{nat}Ti(n,x)^{47}Sc reactions as potential routes to therapeutically relevant quantities of ^{47}Sc. Targets of ^{nat}V, ^{nat}Ti, and enriched ^{47}Ti (95.7% isotopic abundance) and ^{50}Ti (83.1%) oxide targets were exposed to the spallation neutrons resulting from the proton-irradiation of RbCl and Ga targets at the Los Alamos National Laboratory (LANL) Isotope Production Facility (IPF). A 1 hr activation experiment at an average beam current of 218±14 μAh incident on IPF targets was conducted.

The resulting production rates for ^{47}Sc, expressed as activity created per gram of target material and per Ah of incident proton beam are 0.146±.005 μCi g^{-1} μAh^{-1} in the ^{nat}V foil, 0.44±0.01 μCi g^{-1} μAh^{-1} in the ^{nat}Ti foil, and 0.29±0.03 μCi g^{-1} μAh^{-1} and 0.14±0.02 μCi g^{-1} μAh^{-1} in the ^{47}Ti and ^{50}Ti-oxide samples, respectively.

Radioisotopic purities of ^{47}Sc in excess of 90% were expected by activation of ^{47}Ti targets. Experimental results yielded a maximum isotopic purity of 93.8% in the ^{nat}Ti foil target. ^{50}Ti produced small yields of ^{47}Ca with 100% radioisotopic purity, which decays into ^{47}Sc. Isotopic purity of ^{47}Sc with the ingrowth of calcium in ^{50}Ti was only 61.7%. Experiments using bremsstrahlung irradiation and high flux reactor irradiation resulted in isotopic purities in excess of 99%. Further manipulation of production is

required to produce ^{47}Sc with purity levels acceptable for pharmaceutical use.

6.1 Future Work

Future work in the production of ^{47}Sc would require a different production method that may yield higher isotopic purities. A consideration of potential proton experiments at IPF may produce more ideal results. The most promising published work has been done using bremsstrahlung-radiation as was seen in previous efforts performed at the Laboratory of Nuclear Science in Japan. Further experimentation with a bremsstrahlung beam irradiation of ^{47}Ti targets is likely the best method for ^{47}Sc production based on published isotopic purities [15].

In the same regard, the only document which published production quantities was Brookhaven National Laboratory, when considering the ^{47}Ti(n,p)^{47}Sc in their High Flux Beam Reactor [7].

For the future of work with the IPF spallation neutron flux, there are several radioisotopes for which this production is ideal. Working to better characterizes the neutron flux or investigating the production potential of other pharmaceuticals are both useful. There is a great deal of potential for future work in modeling. Revisiting the neutron flux characterization, as well as the MCNP6 cross sections models may lead to better methods or additions to the physics model code to allow models to more accurately represent empirically derived data.

Appendices

PRODUCTION POTENTIAL OF ^{47}Sc USING SPALLATION NEUTRON FLUX AT THE LOS ALAMOS ISOTOPE PRODUCTION FACILITY

A. MCNP Neutron Flux Model

Attached is the MCNP6 and X input deck used for the characterization of the neutron flux across the neutron irradiation sample holder. Modifications are made to both the maximum energy tallied based on the neutron tally bins, the type of tally (F4 or F5), the importance values, and the LCA line. The LCA line is altered to indicate which physics model to use, and was modified for an investigation of Bertini, Isabel, INCL4 and CEM3.03, as described in Chapter 3.

```
c              JWE12Feb25 Inconel capsules
c                         Modified (corrected) Geometry
c              JWE12Mar22 Cleaned up Materials
c                         Cleaned up cell specs
c              KAD13JUN   Modified Geometry to include foil Target
c                         Weight windows and Importances Modified
c ++++++++++++++++++++++++++++++++++++++++++++++++++++
c
c              CELLS
c
c ++++++++++++++++++++++++++++++++++++++++++++++++++++++
c
c
c              IPF Dispersable Items
c
c
c ++++++++++++++++++++++++++++++++++++++++++++++++++++++
c         UPDATES:
c Inconel Window
   1    10    -8.3 -1
c Rb Target A (front)
   3     9    -1.46 -3
c Capsule Rb A (front)
  29    10    -8.44 -29 3
c Al holder Rb A (front)
   9     5    -2.7 (-9 29 ):-51 :-52
c Rb Target B
   5     9    -1.46 -5
c Capsule Rb B
   8    10    -8.44 -4 5
c Al holder Rb B
  10     5    -2.7 (-10 4 ):-53 :-54
c Ga Target
   7    16   -8.908 -7
c Ga Capsule
   6     6     -8.6 -6 7
c Al holder Ga
  11     5    -2.7 (-11 6 ):-55 :-56
c Al Spacer (rear)
  22     4      -1 -21
  221    25       -1 -221
c Al holder Spacer
  23     5    -2.7 (-23 21 ):-57 :-58
c   water volume
  12     4      -1 -13 9 23 10 11 1 52 51 53 54 55 56 57 58
c Aluminum Carrier
  13     5    -2.7 13 -14
c ++++++++++++++++++++++++++++++++++++++++++++++++++++++
c
c
```

```
c                   IPF NON-Dispersable Items
c
c
c ++++++++++++++++++++++++++++++++++++++++++++++++++++++
c Targetry Air Box
    15      3 -0.000958 -15 14 17
c Steel Cube Shielding
    18      2    -7.5 -18 15 33
c Dirt Box Shielding
    24      1    -1.6 -24 18
c Vault Air Volume
    25      3 -0.000958 -25 20 24 26 39 40
c Concrete layer
    26     11   -2.25 -26 19
c PE Layer thru concrete wall
    19     13   -0.92 -19 35
c PE Layer thru Air
    40     13   -0.92 -40 42
c Pb Layer
    20     14  -11.34 -20 37
c Beam line tubing at Target/ thru Air
    16      2    -7.5 -17 16
c Beam line vacuum at Target/ thru Air
    17      0         -16
c Beam line tubing thru Steel
    32      2    -7.5 -33 32
c Beam line vacuum thru Steel
    33      0         -32
c Beam line tubing 1 thru PE
    34      2    -7.5 -35 34
c Beam line vacuum 1 thru PE
    35      0         -34
c Beam line tubing 2 thru PE
    42      2    -7.5 -42 41
c Beam line vacuum 2 thru PE
    43      0         -41
c Beam line tubing thru Pb
    36      2    -7.5 -37 36
c Beam line vacuum thru Pb
    37      0         -36
c Beam line tubing thru Air
    38      2    -7.5 -39 38
c Beam line vacuum thru Air
    39      0         -38
c Outside World
    41      0          25


c ++++++++++++++++++++++++++++++++++++++++++++++++++++++
c
c                   SURFACES
```

```
c
c ++++++++++++++++++++++++++++++++++++++++++++++++++++++
c
c
c                  IPF Dispersable Items
c                       jweEds12Mar22a
c
c                       mod: kad13Jun
c ++++++++++++++++++++++++++++++++++++++++++++++++++++++
c Inconel Window
    1        rcc 0 0 -0.064 0 0 0.064 5.08
c Rb A (HE, Inner Cyl)
    3        rcc 0 0 -2.814 0 0 2.2 2.54
c Inconel A OD (Outer Cyl)
   29        rcc 0 0 -2.864 0 0 2.3 2.74
c Al Holder for RbA (box)
    9        rpp -5.08 5.08 -3.81 3.81 -2.864 -0.564
   51        rpp -5.08 -2.4 -3.81 3.81 -0.564 -0.064
   52        rpp 2.4 5.08 -3.81 3.81 -0.564 -0.064
c Rb B (Inner Cyl)
    5        rcc 0 0 -5.264 0 0 1.85 2.54
c Inconel B OD (Outer Cyl)
    4        rcc 0 0 -5.314 0 0 1.95 2.74
c Al Holder RbB
   10        rpp -5.08 5.08 -3.81 3.81 -5.314 -3.364
   53        rpp -5.08 -2.4 -3.81 3.81 -3.364 -2.864
   54        rpp 2.4 5.08 -3.81 3.81 -3.364 -2.864
c Ga Target (Inner Cyl)
    7        rcc 0 0 -6.353 0 0 0.508 2.54
c Ga capsule (Outer Cyl, Nb)
    6        rcc 0 0 -6.384 0 0 0.569 2.74
c Al Holder Ga
   11        rpp -5.08 5.08 -3.81 3.81 -6.384 -5.814
   55        rpp -5.08 -2.4 -3.81 3.81 -5.814 -5.314
   56        rpp 2.4 5.08 -3.81 3.81 -5.814 -5.314
c Al Spacer Interior
   21        rpp -4.379 4.279 -2.92 3.81 -8.67 -7
  221        rpp -0.5   0.5   -0.5  0.5  -8.0  -7.995
c Al Spacer Exterior
   23        rpp -5.08 5.08 -3.81 3.81 -9.55 -6.884
   57        rpp -5.08 -2.4 -3.81 3.81 -6.884 -6.384
   58        rpp 2.4 5.08 -3.81 3.81 -6.884 -6.384
c ++++++++++++++++++++++++++++++++++++++++++++++++++++++
c
c
c                  IPF NON-Dispersable Items
c
c
c ++++++++++++++++++++++++++++++++++++++++++++++++++++++
c inner box aluminum frame
```

```
      13        rpp −5.09 5.09 −8.255 7.62 −9.715 0
c outer box aluminum frame
      14        rpp −6.35 6.35 −8.255 8.255 −10.215 0
c Target Box Air Volume
      15        rpp −24.13 24.13 −38.1 38.1 −33.02 17.78
c Beam Line at Target Inner Surface
      16        rcc 0 0 0 0 0 17.78 5.715
c Beam Line at Target Outer Surface
      17        rcc 0 0 0 0 0 17.78 5.88011
c Steel Box
      18        rpp −152.4 152.4 −152.4 152.4 −167.64 137.16
c PE Layer thru concrete
      19        rpp −24.13 24.13 −38.1 38.1 137.16 152.4
c PE Layer thru Air
      40        rpp −24.13 24.13 −38.1 38.1 152.4 162.56
c Pb Layer
      20        rpp −24.13 24.13 −38.1 38.1 162.56 167.64
c Dirt Box
      24        rpp −368.3 303.53 −259.08 350.52 −401.32 137.16
c Vault Air Volume Outer Surface
      25        rpp −492.761 579.12 −259.08 350.52 −401.32 574.039
c Concrete Layer
      26        rpp −368.3 303.53 −259.08 350.52 137.16 152.4
c Beam Line thru Steel Inner Surface
      32        rcc 0 0 17.78 0 0 119.38 5.715
c Beam Line thru Steel Outer Surface
      33        rcc 0 0 17.78 0 0 119.38 5.88011
c Beam Line 1 thru PE Layer Inner Surface
      34        rcc 0 0 137.16 0 0 15.24 5.715
c Beam Line 1 thru PE Layer Outer Surface
      35        rcc 0 0 137.16 0 0 15.24 5.88011
c Beam Line 2 thru PE Layer Inner Surface
      41        rcc 0 0 152.4 0 0 10.16 5.715
c Beam Line 2 thru PE Layer Outer Surface
      42        rcc 0 0 152.4 0 0 10.16 5.88011
c Beam Line thru Pb Layer Inner Surface
      36        rcc 0 0 162.56 0 0 5.08 5.715
c Beam Line thru Pb Layer Outer Surface
      37        rcc 0 0 162.56 0 0 5.08 5.88011
c Beam Line thru vault space Inner Surface
      38        rcc 0 0 167.64 0 0 406.396 5.715
c Beam Line thru vault space Outer Surface
      39        rcc 0 0 167.64 0 0 406.396 5.88011

c +++++++++++++++++++++++++++++++++++++++++++++++++++
c Make sure particle selections are correct
c +++++++++++++++++++++++++++++++++++++++++++++++++++
mode  n h
c +++++++++++++++++++++++++++++++++++++++++++++++++++
c
```

```
c                   DATA
c
c ++++++++++++++++++++++++++++++++++++++++++++++++++++++++
c TA53 Tuff Density = 1.6 (gm/cm^3)
m1    1001.60c         -0.00665
      8016.60c           -0.518 11023.60c        -0.0028 13027.60c
-0.0594
      14000.60c          -0.344 20000.60c         -0.083 26000.55c
-0.01
      19000.60c         -0.0337
c SEG Steel Density = 7.50 (gm/cm^3)
m2    26000.55c         -0.953
      24000.50c          -0.015 28000.50c          -0.01 25055.60c
-0.0044
c Nickel 625 Density = 8.44 (gm/cm^3) (RbCl capsule B)
m12   24000.50c          -0.22
      28000.50c           -0.6 41093.24c          -0.04 42000.60c
-0.09
c Air-Los Alamos Density=0.958E-03 gm/cm^3
m3    8016.60c            -0.2
      7014.60c            -0.8
c water
m4    1001.60c              2
      8016.60c              1
c Aluminum (carrier)
m5    13027.60c             1
c Niobium
m6    41093.24c             1
c Gallium
m7    31000.60c             1
c RbCl (rear)
m8    37085.70c        0.7217
      37087.70c        0.2783 17000.60c             1
c Rb Metal (density is 1.46 g/cm3)
m9    37085.70c        0.7217
      37087.70c        0.2783
c Inconel window
m10   26000.55c         -0.189
      24000.50c          -0.19 28000.50c         -0.525 41093.24c
-0.0512
      42000.60c        -0.0305
c Concrete
m11   1001.60c         -0.00248
      8016.60c           -0.35 11023.60c        -0.0041 13027.60c
-0.0081
      14000.60c        -0.00358 20000.60c       -0.00311 26000.55c
-0.556
c Polyethylene
m13   1001.60c         -0.1437
c Lead
```

```
m14    82000.50c            1
c natural Nickel (density = 8.908 g/cm3)
m15    28000.60c            1
c enriched Ni-58 using Isoflex COA from 3/12/13
c       28064         0.00005
m16    28058.          0.9948
       28060.          0.00505 28061.         5e-005 28062.
5e-005
       30000.          7.42e-006 27000.       2.85e-006 26000.
5.71e-006
       29000.          2.85e-006 13000.       3.116e-005
c 316 SS Density = 7.92 (gm/cm^3) (RbCl capsule B)
m24    26000.55c        -0.655
       24000.50c         -0.17 28000.50c        -0.12 25055.60c
-0.02
       42000.60c         -0.025 14000.60c        -0.01
c Vanadium Foil
m25    23000.              1
c Titanium Foil
m205   22000               1
c Thorium metal
m29    90232.1
[NOTE: tr Lines omitted for Appendix Submission]
c ++++++++++++++++++++++++++++++++++++++++++++++++++++
c Importances
c ++++++++++++++++++++++++++++++++++++++++++++++++++++
imp:n   1 18r 2 3 4 5 1 11r          0 $ 1, 41
imp:h   1 34r          0               $ 1, 41
c
c ++++++++++++++++++++++++++++++++++++++++++++++++++++
c Physcis Model CEM303 Enabled
c ++++++++++++++++++++++++++++++++++++++++++++++++++++
LCA 8j 1
c define X and Y Gaussian beam spot
sp1     -41 1.27 0
sp2     -41 1.27 0
c define probability of each transformation
si3 l 1 998i 1000
sp3 1 999r
c
c
c
c ++++++++++++++++++++++++++++++++++++++++++++++++++++
c Check beam current specification
c ++++++++++++++++++++++++++++++++++++++++++++++++++++
sdef erg=100 dir=-1 vec=0 0 1 x=d1 y=d2 z=0.00254 par=9 tr=d3
c         wgt 1.2484e+015 $ 220 uA
c ++++++++++++++++++++++++++++++++++++++++++++++++++++
c Check nps and PRDMP frequencies
c ++++++++++++++++++++++++++++++++++++++++++++++++++++
```

```
nps   2+7
c control writing to MCTAL and RUNTPE files with PRDMP
prdmp 1+6 1+6 -1
phys:n 101 $ 3j 25
c note: phys:h emax analogElimit tabl(def=-1)
c          for tabl=0, use physics models fall E
c          for tabl=-1, use tables when available
phys:h 100 j 0
c histp card lists cells for which history is desired
histp 221
c
c ++++++++++++++++++++++++++++++++++++++++++++++++++++
c Add tally below
c ++++++++++++++++++++++++++++++++++++++++++++++++++++
F5:N 0 0 -7.995 0.15
c CINDER90 activation cross sections provided in
c 63 group LaBauve neutron energy group structure
c energies added & included up to 100 MeV (kad _ Jul 13)
e5     1.000e-11 5.000e-09 1.000e-08 1.500e-08 2.000e-08 2.500e-
08
       3.000e-08 3.500e-08 4.200e-08 5.000e-08 5.800e-08 6.700e-
08
       8.000e-08 1.000e-07 1.520e-07 2.510e-07 4.140e-07 6.830e-
07
       1.125e-06 1.855e-06 3.059e-06 5.043e-06 8.315e-06 1.371e-
05
       2.260e-05 3.727e-05 6.144e-05 1.013e-04 1.670e-04 2.754e-
04
       4.540e-04 7.485e-04 1.234e-03 2.035e-03 2.404e-03 2.840e-
03
       4.087e-02 6.738e-02 1.111e-01 1.832e-01 3.020e-01 3.887e-
01
       4.979e-01 0.639279  0.82085   1.10803   1.35335   1.73774
       2.2313    2.86505   3.67879   4.96585   6.065     10.00
       14.9182   16.9046   20.0      22.0      24.0      26.0
       28.0      30.0      32.0      34.0      36.0      38.0
       40.0      42.0      44.0      46.0      48.0      50.0
       52.0      54.0      56.0      58.0      60.0      62.0
       64.0      66.0      68.0      70.0      72.0      74.0
       76.0      78.0      80.0      82.0      84.0      86.0
       88.0      90.0      92.0      94.0      96.0      98.0
       100.0
c ++++++++++++++++++++++++++++++++++++++++++++++++++++
c Weight Window Generator
c ++++++++++++++++++++++++++++++++++++++++++++++++++++
WWG 5 29 0 J J J J 0
c Weight windows
wwe:n  1.0100E+02
wwn1:n  4.5710E-01  1.0506E-01  1.0763E-01  1.8980E-01  4.8317E-
02
```

```
        4.9446E-02  1.0979E-01  2.0569E-02  2.2949E-02  3.3503E-
02
        2.2275E-02  0.0000E+00  2.7193E-02  6.9016E-02  2.4683E-
01
        4.6479E-01  4.7006E-01  7.8447E+29  0.0000E+00
1.4804E+18
        0.0000E+00  0.0000E+00  0.0000E+00  1.1757E+00
1.3459E+00
        1.4637E+00  2.3970E+00  0.0000E+00  0.0000E+00
0.0000E+00
        0.0000E+00  0.0000E+00  0.0000E+00  0.0000E+00
0.0000E+00
        -1.0000E+00
```

B. Cinder90 Script

This is the PERL script written to extract data (neutron flux and cell information) from the outputs of an MCNP from which to run the production and burnout models. This code was modified for each different target material by modification of the out and histp files requested. Further discussion of this data may be found in Chapter 3.

```
# input when stripped by comment lines
title_lines
 Activation Test

codes
cinder /apps/enp/LANL/cinder-1.05/bin/cinder
tabcode /apps/enp/LANL/cinder-1.05/bin/tabcode
htape3x /apps/enp/LANL/MCNP_CODE/MCNPX/bin/linux/htape3x

# specify mcnp6 rather than x
files
mcnpx_outp Ti46MCNPforCinder
mcnpx_histp histpy
bigza_file /apps/enp/LANL/cinder-1.05/data/bigza

# name the directory
run_options
dname
/home/ENP/gap14m/kdelorme/InputFiles/Test/CellRun3/CinderTi46Thesis
dcounter 1

# CINDER90 used for activation with defaults
cinder_options
library /apps/enp/LANL/cinder-1.05/data/c90lib0742

# normalization is number of particles
normalization
snorm 6.25E12

# time steps
history
3 220 1.0 h 1.0 h 1.0 h
4 0.0 1.0 h 1.0 h 1.0 h 1.0 h

# cell list info
cell_list
  Titanium Cell
  221
```

C. Cinder90 Activity and Rate Data

The following data is the output of the Cinder90 code for all predicted results of each of the samples investigated. Further discussion of this data may be found in Chapter 3.

Target:	Vanadium			
Density:	6	g/cc		
Isotope	**A**	**Activity(Ci/cc)**	**Activity(uCi/g)**	**ProdRate (uCi/g per uA h)**
H	3	1.02E-10	1.7017E-05	7.7348E-08
Si	33	1.08E-26	1.8000E-21	8.1818E-24
P	33	6.14E-30	1.0225E-24	4.6477E-27
S	37	2.01E-19	3.3500E-14	1.5227E-16
S	38	4.01E-27	6.6767E-22	3.0348E-24
S	39	6.12E-28	1.0198E-22	4.6356E-25
S	40	1.87E-27	3.1233E-22	1.4197E-24
Cl	38	2.94E-23	4.8917E-18	2.2235E-20
Cl	38*	1.80E-26	2.9967E-21	1.3621E-23
Cl	39	7.59E-20	1.2645E-14	5.7477E-17
Cl	40	9.33E-19	1.5550E-13	7.0682E-16
Cl	41	5.38E-26	8.9600E-21	4.0727E-23
Cl	42	3.93E-29	6.5500E-24	2.9773E-26
Ar	39	2.16E-23	3.5983E-18	1.6356E-20
Ar	41	2.36E-15	3.9250E-10	1.7841E-12
Ar	42	5.16E-23	8.6000E-18	3.9091E-20
Ar	43	1.03E-17	1.7217E-12	7.8258E-15
Ar	44	6.43E-28	1.0723E-22	4.8742E-25
Ar	45	2.26E-30	3.7650E-25	1.7114E-27
Ar	46	1.58E-30	2.6300E-25	1.1955E-27
K	40	1.61E-40	2.6767E-35	1.2167E-37
K	42	4.54E-17	7.5717E-12	3.4417E-14
K	43	3.99E-16	6.6467E-11	3.0212E-13
K	44	1.09E-14	1.8167E-09	8.2576E-12
K	45	7.67E-17	1.2777E-11	5.8076E-14
K	46	1.54E-17	2.5633E-12	1.1652E-14
K	47	7.66E-18	1.2762E-12	5.8008E-15
Ca	45	1.41E-17	2.3567E-12	1.0712E-14
Ca	47	2.61E-18	4.3533E-13	1.9788E-15
Ca	49	1.42E-19	2.3600E-14	1.0727E-16
Sc	43	5.10E-30	8.5050E-25	3.8659E-27
Sc	44	8.54E-20	1.4228E-14	6.4674E-17
Sc	44*	5.97E-21	9.9417E-16	4.5189E-18
Sc	45*	2.43E-16	4.0550E-11	1.8432E-13
Sc	46	2.74E-12	4.5600E-07	2.0727E-09
Sc	46*	2.47E-09	4.1117E-04	1.8689E-06
Sc	47	2.04E-07	3.3917E-02	1.5417E-04
Sc	48	3.21E-07	5.3567E-02	2.4348E-04
Sc	49	1.85E-08	3.0817E-03	1.4008E-05
Sc	50	1.18E-06	1.9700E-01	8.9545E-04
Sc	50*	6.94E-07	1.1572E-01	5.2598E-04
Ti	45	1.16E-21	1.9250E-16	8.7500E-19
Ti	51	3.80E-05	6.3333E+00	2.8788E-02
V	47	2.98E-17	4.9650E-12	2.2568E-14
V	48	7.30E-11	1.2162E-05	5.5280E-08

V	49	2.62E-09	4.3683E-04	1.9856E-06
V	50	1.68E-18	2.7983E-13	1.2720E-15
V	52	2.40E-03	3.9983E+02	1.8174E+00

Target:	Titanium			
Density:	4.506	g/cc		
Isotope	A	Activity(Ci/cc)	Activity(uCi/g)	ProdRate (uCi/g per uA h)
H	3	2.79E-09	6.1806E-04	2.8094E-06
Al	30	7.05E-24	1.5644E-18	7.1107E-21
Si	32	2.41E-30	5.3462E-25	2.4301E-27
Si	33	3.63E-21	8.0448E-16	3.6567E-18
P	33	1.40E-18	3.1003E-13	1.4092E-15
P	34	4.50E-15	9.9889E-10	4.5404E-12
P	35	3.40E-23	7.5477E-18	3.4308E-20
S	35	7.11E-20	1.5788E-14	7.1763E-17
S	37	2.05E-15	4.5473E-10	2.0669E-12
S	38	7.16E-25	1.5888E-19	7.2217E-22
S	39	1.06E-25	2.3435E-20	1.0652E-22
S	40	3.23E-25	7.1771E-20	3.2623E-22
Cl	36	1.26E-23	2.7896E-18	1.2680E-20
Cl	38	4.41E-13	9.7847E-08	4.4476E-10
Cl	38*	4.88E-13	1.0832E-07	4.9237E-10
Cl	39	6.82E-16	1.5126E-10	6.8757E-13
Cl	40	8.08E-16	1.7941E-10	8.1548E-13
Cl	41	9.48E-24	2.1039E-18	9.5630E-21
Cl	42	7.16E-26	1.5885E-20	7.2207E-23
Ar	39	1.14E-19	2.5255E-14	1.1480E-16
Ar	41	4.07E-13	9.0280E-08	4.1036E-10
Ar	42	1.05E-21	2.3258E-16	1.0572E-18
Ar	43	3.08E-15	6.8353E-10	3.1070E-12
Ar	44	2.43E-15	5.4017E-10	2.4553E-12
Ar	45	1.60E-18	3.5508E-13	1.6140E-15
Ar	46	1.08E-17	2.3857E-12	1.0844E-14
K	40	3.23E-25	7.1704E-20	3.2593E-22
K	42	6.98E-13	1.5482E-07	7.0371E-10
K	43	1.42E-14	3.1514E-09	1.4324E-11
K	44	1.34E-13	2.9827E-08	1.3558E-10
K	45	1.23E-13	2.7341E-08	1.2428E-10
K	46	8.06E-15	1.7883E-09	8.1286E-12
K	47	2.50E-15	5.5415E-10	2.5189E-12
Ca	41	2.12E-25	4.7048E-20	2.1386E-22
Ca	45	7.10E-07	1.5766E-01	7.1662E-04
Ca	47	1.81E-06	4.0146E-01	1.8248E-03
Ca	49	1.23E-06	2.7230E-01	1.2377E-03
Sc	41	1.68E-20	3.7284E-15	1.6947E-17
Sc	42	2.65E-15	5.8899E-10	2.6772E-12
Sc	42*	1.74E-19	3.8571E-14	1.7532E-16
Sc	43	6.58E-07	1.4603E-01	6.6376E-04
Sc	44	1.01E-06	2.2304E-01	1.0138E-03
Sc	44*	5.41E-07	1.2013E-01	5.4604E-04
Sc	45*	6.15E-03	1.3651E+03	6.2049E+00
Sc	46	1.23E-05	2.7297E+00	1.2408E-02

Sc	46*	3.36E-02	7.4478E+03	3.3854E+01
Sc	47	3.82E-05	8.4798E+00	3.8545E-02
Sc	48	6.90E-05	1.5322E+01	6.9645E-02
Sc	49	8.49E-05	1.8830E+01	8.5593E-02
Sc	50	6.17E-05	1.3686E+01	6.2210E-02
Sc	50*	2.90E-05	6.4314E+00	2.9234E-02
Ti	43	5.16E-14	1.1454E-08	5.2062E-11
Ti	44	1.32E-12	2.9250E-07	1.3295E-09
Ti	45	1.86E-04	4.1300E+01	1.8773E-01
Ti	51	3.89E-04	8.6307E+01	3.9231E-01
V	52	5.72E-13	1.2683E-07	5.7650E-10

Target:	Ti46			
Density:	4.09	g/cc		
Isotope	**A**	**Activity(Ci/cc)**	**Activity(uCi/g)**	**ProdRate (uCi/g per uA h)**
H	3	2.11E-07	5.1467E-02	2.3394E-04
H	4	8.57E-17	2.0941E-11	9.5188E-14
He	5	5.04E-14	1.2323E-08	5.6012E-11
He	6	7.79E-17	1.9034E-11	8.6519E-14
He	7	7.79E-17	1.9039E-11	8.6541E-14
Li	8	7.23E-13	1.7685E-07	8.0385E-10
Be	8	4.79E-04	1.1719E+02	5.3267E-01
Be	10	1.92E-23	4.6944E-18	2.1338E-20
Be	11	1.02E-13	2.4914E-08	1.1325E-10
B	9	2.64E-17	6.4597E-12	2.9362E-14
B	12	6.95E-07	1.7002E-01	7.7284E-04
C	14	1.42E-13	3.4719E-08	1.5781E-10
C	15	3.43E-08	8.3888E-03	3.8131E-05
N	16	3.24E-03	7.9218E+02	3.6008E+00
O	15	1.27E-04	3.1149E+01	1.4159E-01
Mg	27	2.00E-30	4.8973E-25	2.2261E-27
Mg	28	4.01E-32	9.7971E-27	4.4532E-29
Mg	29	5.91E-33	1.4447E-27	6.5670E-30
Al	29	1.31E-30	3.1932E-25	1.4514E-27
Al	30	1.15E-30	2.8166E-25	1.2803E-27
Al	31	3.40E-30	8.3203E-25	3.7820E-27
Si	31	5.15E-20	1.2579E-14	5.7179E-17
Si	32	2.62E-36	6.4132E-31	2.9151E-33
Si	33	1.58E-24	3.8655E-19	1.7571E-21
P	33	3.69E-27	9.0147E-22	4.0976E-24
P	34	5.86E-19	1.4337E-13	6.5170E-16
S	35	4.46E-18	1.0910E-12	4.9589E-15
S	37	2.93E-17	7.1687E-12	3.2585E-14
S	38	5.81E-25	1.4215E-19	6.4614E-22
S	39	8.88E-26	2.1699E-20	9.8633E-23
S	40	2.72E-25	6.6455E-20	3.0207E-22
Cl	36	2.60E-27	6.3667E-22	2.8940E-24
Cl	38	1.26E-14	3.0709E-09	1.3959E-11
Cl	38*	7.86E-24	1.9227E-18	8.7397E-21
Cl	39	1.10E-17	2.6846E-12	1.2203E-14
Cl	40	1.37E-16	3.3374E-11	1.5170E-13
Cl	41	8.69E-24	2.1252E-18	9.6599E-21
Cl	42	6.80E-28	1.6621E-22	7.5550E-25
Ar	37	1.16E-17	2.8460E-12	1.2936E-14
Ar	39	2.54E-19	6.2152E-14	2.8251E-16
Ar	41	3.51E-13	8.5819E-08	3.9009E-10
Ar	42	1.44E-20	3.5208E-15	1.6004E-17
Ar	43	1.60E-15	3.8998E-10	1.7726E-12
Ar	44	2.86E-16	6.9829E-11	3.1740E-13
K	40	4.08E-27	9.9756E-22	4.5343E-24

K	42	1.68E-13	4.1002E-08	1.8637E-10
K	43	6.33E-14	1.5474E-08	7.0338E-11
K	44	1.61E-12	3.9340E-07	1.7882E-09
K	45	3.90E-14	9.5428E-09	4.3376E-11
K	46	4.94E-24	1.2083E-18	5.4923E-21
Ca	41	9.37E-22	2.2907E-16	1.0412E-18
Ca	45	1.06E-07	2.5966E-02	1.1803E-04
Sc	42	2.06E-14	5.0367E-09	2.2894E-11
Sc	43	5.15E-06	1.2594E+00	5.7246E-03
Sc	44	5.28E-03	1.2897E+03	5.8624E+00
Sc	44*	4.24E-06	1.0355E+00	4.7066E-03
Sc	45*	8.04E-02	1.9648E+04	8.9309E+01
Sc	46	6.38E-06	1.5606E+00	7.0938E-03
Sc	46*	5.76E-03	1.4071E+03	6.3959E+00
Sc	47	2.57E-13	6.2714E-08	2.8506E-10
Sc	48	5.43E-23	1.3279E-17	6.0358E-20
Ti	43	4.01E-13	9.7995E-08	4.4543E-10
Ti	44	1.03E-11	2.5232E-06	1.1469E-08
Ti	45	1.44E-03	3.5257E+02	1.6026E+00

Isotope	A	Activity(Ci/cc)	Activity(uCi/g)	ProdRate (uCi/g per uA h)
Target:	Ti47			
Density:	4.16	g/cc		
Isotope	**A**	**Activity(Ci/cc)**	**Activity(uCi/g)**	**ProdRate (uCi/g per uA h)**
H	3	2.12E-07	0.050865385	0.000231206
H	4	8.54E-17	2.05168E-11	9.32583E-14
He	5	5.03E-14	1.20865E-08	5.49388E-11
He	6	7.76E-17	1.86466E-11	8.47574E-14
He	7	7.76E-17	1.86538E-11	8.47902E-14
Li	8	7.23E-13	1.73798E-07	7.89991E-10
Be	8	4.78E-04	114.8076923	0.521853147
Be	10	1.92E-23	4.60577E-18	2.09353E-20
Be	11	1.02E-13	2.44712E-08	1.11233E-10
B	9	2.63E-17	6.32933E-12	2.87697E-14
B	12	6.93E-07	0.1665625	0.000757102
C	14	1.42E-13	3.40144E-08	1.54611E-10
C	15	3.42E-08	0.008216346	3.7347E-05
N	16	3.24E-03	778.3653846	3.538024476
O	15	1.27E-04	30.55288462	0.138876748
Si	33	7.56E-25	1.81755E-19	8.26158E-22
P	33	4.30E-28	1.03269E-22	4.69406E-25
S	37	1.41E-17	3.38462E-12	1.53846E-14
S	38	2.81E-25	6.76442E-20	3.07474E-22
S	39	4.29E-26	1.03101E-20	4.68641E-23
S	40	1.31E-25	3.15865E-20	1.43575E-22
Cl	38	2.06E-21	4.95673E-16	2.25306E-18
Cl	38*	1.41E-23	3.37981E-18	1.53628E-20
Cl	39	5.31E-18	1.2774E-12	5.80638E-15
Cl	40	6.54E-17	1.57115E-11	7.14161E-14
Cl	41	5.52E-24	1.32788E-18	6.03584E-21
Cl	42	2.75E-26	6.61779E-21	3.00809E-23
Ar	39	1.51E-21	3.63462E-16	1.6521E-18
Ar	41	1.66E-13	3.97837E-08	1.80835E-10
Ar	42	4.96E-21	1.19183E-15	5.4174E-18
Ar	43	7.96E-16	1.91394E-10	8.69974E-13
Ar	44	6.80E-17	1.63365E-11	7.4257E-14
Ar	45	3.67E-20	8.8125E-15	4.00568E-17
Ar	46	2.46E-19	5.91827E-14	2.69012E-16
K	40	1.12E-38	2.69712E-33	1.22596E-35
K	42	7.82E-14	1.87885E-08	8.54021E-11
K	43	3.40E-14	8.18029E-09	3.71831E-11
K	44	1.00E-12	2.40625E-07	1.09375E-09
K	45	1.32E-14	3.16106E-09	1.43684E-11
K	46	9.33E-15	2.24375E-09	1.01989E-11
K	47	6.68E-17	1.60577E-11	7.29895E-14
Ca	45	2.08E-08	0.005009615	2.2771E-05
Ca	47	4.15E-08	0.009971154	4.53234E-05
Ca	49	1.83E-08	0.004387019	1.9941E-05
Sc	42	2.63E-16	6.32452E-11	2.87478E-13

Sc	43	2.11E-08	0.005060096	2.30004E-05
Sc	44	7.59E-06	1.825240385	0.008296547
Sc	44*	1.73E-08	0.004161058	1.89139E-05
Sc	45*	6.57E-02	15788.46154	71.76573427
Sc	46	1.63E-06	0.392307692	0.001783217
Sc	46*	1.47E-03	353.125	1.605113636
Sc	47	1.41E-04	33.77403846	0.153518357
Sc	48	1.99E-06	0.477163462	0.002168925
Sc	49	1.55E-06	0.371634615	0.001689248
Sc	50	9.21E-07	0.221394231	0.001006337
Sc	50*	4.33E-07	0.104038462	0.000472902
Ti	43	5.12E-15	1.23029E-09	5.59222E-12
Ti	44	4.21E-14	1.01298E-08	4.60446E-11
Ti	45	1.85E-05	4.442307692	0.020192308
Ti	51	5.82E-06	1.397836538	0.006353802

Target:	Ti48			
Density:	4.24	g/cc		
Isotope	**A**	**Activity(Ci/cc)**	**Activity(uCi/g)**	**ProdRate (uCi/g per uA h)**
H	3	2.126E-07	9.0142E-01	4.0974E-03
H	4	8.56E-17	3.6286E-10	1.6494E-12
He	5	5.04E-14	2.1365E-07	9.7115E-10
He	6	7.78E-17	3.2979E-10	1.4990E-12
He	7	7.78E-17	3.2991E-10	1.4996E-12
Li	8	7.22E-13	3.0609E-06	1.3913E-08
Be	8	4.79E-04	2.0305E+03	9.2297E+00
Be	10	1.92E-23	8.1408E-17	3.7004E-19
Be	11	1.02E-13	4.3163E-07	1.9620E-09
B	9	2.64E-17	1.1194E-10	5.0880E-13
B	12	6.95E-07	2.9460E+00	1.3391E-02
C	14	1.42E-13	6.0166E-07	2.7348E-09
C	15	3.43E-08	1.4535E-01	6.6067E-04
N	16	3.23E-03	1.3712E+04	6.2328E+01
O	15	1.27E-04	5.4018E+02	2.4553E+00
Al	30	7.06E-24	2.9943E-17	1.3610E-19
Si	32	2.41E-30	1.0231E-23	4.6505E-26
Si	33	3.63E-21	1.5400E-14	6.9999E-17
P	33	1.40E-18	5.9318E-12	2.6963E-14
P	34	4.51E-15	1.9114E-08	8.6881E-11
S	35	7.13E-20	3.0218E-13	1.3736E-15
S	37	2.05E-15	8.6962E-09	3.9528E-11
S	38	6.90E-25	2.9239E-18	1.3290E-20
S	39	1.05E-25	4.4690E-19	2.0313E-21
S	40	3.23E-25	1.3687E-18	6.2212E-21
Cl	36	1.26E-23	5.3382E-17	2.4264E-19
Cl	38	4.42E-13	1.8724E-06	8.5108E-09
Cl	38*	4.89E-13	2.0729E-06	9.4224E-09
Cl	39	6.76E-16	2.8667E-09	1.3030E-11
Cl	40	8.10E-16	3.4340E-09	1.5609E-11
Cl	41	1.06E-23	4.5071E-17	2.0487E-19
Cl	42	1.33E-25	5.6434E-19	2.5652E-21
Ar	39	1.14E-19	4.8336E-13	2.1971E-15
Ar	41	4.06E-13	1.7197E-06	7.8170E-09
Ar	42	3.68E-20	1.5586E-13	7.0847E-16
Ar	43	1.55E-15	6.5550E-09	2.9796E-11
Ar	44	1.76E-15	7.4624E-09	3.3920E-11
Ar	45	7.44E-19	3.1554E-12	1.4343E-14
Ar	46	5.00E-18	2.1196E-11	9.6344E-14
K	40	3.23E-25	1.3712E-18	6.2328E-21
K	42	7.30E-13	3.0944E-06	1.4065E-08
K	43	2.40E-14	1.0163E-07	4.6197E-10
K	44	1.43E-13	6.0802E-07	2.7637E-09
K	45	1.61E-13	6.8264E-07	3.1029E-09
K	46	3.34E-15	1.4179E-08	6.4448E-11

K	47	1.70E-15	7.1868E-09	3.2667E-11
Ca	45	5.64E-07	2.3905E+00	1.0866E-02
Ca	47	8.40E-07	3.5612E+00	1.6187E-02
Sc	42	5.51E-26	2.3362E-19	1.0619E-21
Sc	43	1.50E-14	6.3642E-08	2.8928E-10
Sc	44	4.92E-13	2.0848E-06	9.4764E-09
Sc	44*	2.89E-14	1.2245E-07	5.5660E-10
Sc	45*	3.26E-02	1.3822E+05	6.2829E+02
Sc	46	2.25E-05	9.5400E+01	4.3364E-01
Sc	46*	3.26E-02	1.3839E+05	6.2906E+02
Sc	47	1.66E-05	7.0299E+01	3.1954E-01
Sc	48	5.45E-05	2.3091E+02	1.0496E+00
Sc	49	1.78E-12	7.5472E-06	3.4305E-08
Ti	43	1.07E-24	4.5453E-18	2.0660E-20
Ti	44	3.44E-31	1.4594E-24	6.6337E-27
Ti	45	3.86E-15	1.6366E-08	7.4393E-11

Target:	Ti49		
Density:	4.31	g/cc	
Isotope	**A**	**Activity(Ci/cc)**	**Activity(uCi/g)**	**ProdRate (uCi/g per uA h)**

Isotope	A	Activity(Ci/cc)	Activity(uCi/g)	ProdRate (uCi/g per uA h)
H	3	3.00E-09	6.9698E-04	3.1681E-06
Be	8	6.81E-06	1.5805E+00	7.1841E-03
B	12	9.88E-09	2.2928E-03	1.0422E-05
C	14	2.02E-15	4.6821E-10	2.1282E-12
C	15	4.88E-10	1.1313E-04	5.1424E-07
N	16	4.62E-05	1.0712E+01	4.8692E-02
O	15	1.81E-06	4.2042E-01	1.9110E-03
Al	29	4.15E-33	9.6195E-28	4.3725E-30
Si	31	1.04E-37	2.4176E-32	1.0989E-34
Si	32	9.73E-38	2.2571E-32	1.0259E-34
P	32	5.96E-32	1.3831E-26	6.2866E-29
P	33	1.03E-30	2.3828E-25	1.0831E-27
P	35	4.24E-32	9.8469E-27	4.4758E-29
S	35	6.21E-30	1.4408E-24	6.5493E-27
S	37	7.21E-27	1.6729E-21	7.6039E-24
S	38	8.67E-27	2.0123E-21	9.1468E-24
S	39	3.64E-26	8.4501E-21	3.8410E-23
S	40	7.08E-28	1.6436E-22	7.4710E-25
S	41	3.31E-28	7.6729E-23	3.4877E-25
Cl	36	7.43E-37	1.7237E-31	7.8348E-34
Cl	38	2.87E-15	6.6613E-10	3.0278E-12
Cl	38*	4.44E-15	1.0302E-09	4.6826E-12
Cl	39	2.92E-15	6.7726E-10	3.0785E-12
Cl	40	2.41E-16	5.5870E-11	2.5395E-13
Cl	41	5.89E-16	1.3675E-10	6.2160E-13
Cl	42	6.12E-26	1.4206E-20	6.4575E-23
Ar	37	6.22E-30	1.4432E-24	6.5598E-27
Ar	39	6.81E-22	1.5798E-16	7.1810E-19
Ar	41	6.20E-16	1.4392E-10	6.5419E-13
Ar	42	2.95E-20	6.8538E-15	3.1154E-17
Ar	43	4.85E-19	1.1246E-13	5.1118E-16
Ar	44	1.05E-18	2.4408E-13	1.1095E-15
Ar	45	1.17E-22	2.7239E-17	1.2381E-19
Ar	46	7.89E-22	1.8295E-16	8.3158E-19
K	38	5.32E-28	1.2353E-22	5.6148E-25
K	40	1.35E-28	3.1253E-23	1.4206E-25
K	42	2.53E-05	5.8770E+00	2.6714E-02
K	43	4.23E-15	9.8167E-10	4.4621E-12
K	44	2.52E-16	5.8469E-11	2.6577E-13
K	45	9.04E-16	2.0972E-10	9.5328E-13
K	46	5.53E-18	1.2835E-12	5.8342E-15
K	47	6.88E-18	1.5965E-12	7.2569E-15
Ca	45	3.77E-10	8.7541E-05	3.9791E-07
Ca	47	1.33E-10	3.0789E-05	1.3995E-07
Sc	42	8.38E-26	1.9450E-20	8.8410E-23

Sc	43	2.08E-17	4.8329E-12	2.1968E-14
Sc	44	3.86E-19	8.9559E-14	4.0709E-16
Sc	44*	1.67E-17	3.8677E-12	1.7581E-14
Sc	45*	4.95E-13	1.1473E-07	5.2151E-10
Sc	46	1.59E-07	3.6914E-02	1.6779E-04
Sc	46*	4.65E-04	1.0777E+02	4.8988E-01
Sc	47	5.20E-08	1.2070E-02	5.4862E-05
Sc	48	2.87E-07	6.6520E-02	3.0236E-04
Sc	49	9.89E-06	2.2954E+00	1.0433E-02
Ti	43	1.63E-24	3.7842E-19	1.7201E-21
Ti	44	4.05E-23	9.3991E-18	4.2723E-20
Ti	45	5.89E-15	1.3654E-09	6.2065E-12

Target:	Ti50			
Density:	4.38	g/cc		
Isotope	**A**	**Activity(Ci/cc)**	**Activity(uCi/g)**	**ProdRate (uCi/g per uA h)**
H	3 3	1.06E-07	0.024223744	0.000110108
H	4	3.76E-17	8.58676E-12	3.90307E-14
He	5	2.36E-14	5.379E-09	2.445E-11
He	6	3.41E-17	7.77397E-12	3.53362E-14
He	7	3.41E-17	7.77626E-12	3.53466E-14
Li	8	3.56E-13	8.13242E-08	3.69655E-10
Be	8	4.23E-04	96.62100457	0.439186384
Be	10	9.15E-24	2.08813E-18	9.49149E-21
Be	11	4.99E-14	1.13858E-08	5.17538E-11
B	9	1.16E-17	2.63927E-12	1.19967E-14
B	12	6.08E-07	0.138881279	0.000631279
C	14	1.24E-13	2.83562E-08	1.28892E-10
C	15	3.00E-08	0.006851598	3.11436E-05
N	16	3.18E-03	725.5707763	3.298048983
O	15	1.20E-04	27.44292237	0.124740556
Al	30	3.09E-24	7.05708E-19	3.20776E-21
Si	32	1.06E-30	2.41324E-25	1.09693E-27
Si	33	1.59E-21	3.63014E-16	1.65006E-18
P	33	6.14E-19	1.40205E-13	6.37298E-16
P	34	2.04E-15	4.64612E-10	2.11187E-12
P	35	2.34E-23	5.3379E-18	2.42632E-20
S	35	3.12E-20	7.12329E-15	3.23786E-17
S	37	9.31E-16	2.12648E-10	9.66584E-13
S	38	3.17E-25	7.22831E-20	3.2856E-22
S	39	4.61E-26	1.05183E-20	4.78103E-23
S	40	1.42E-25	3.23516E-20	1.47053E-22
Cl	36	5.52E-24	1.25982E-18	5.72644E-21
Cl	38	2.16E-13	4.92922E-08	2.24056E-10
Cl	38*	2.39E-13	5.46347E-08	2.4834E-10
Cl	39	2.96E-16	6.75799E-11	3.07181E-13
Cl	40	3.57E-16	8.15297E-11	3.70589E-13
Cl	41	1.15E-23	2.63242E-18	1.19655E-20
Cl	42	2.38E-26	5.42694E-21	2.46679E-23
Ar	39	5.11E-20	1.16667E-14	5.30303E-17
Ar	41	1.90E-13	4.34703E-08	1.97592E-10
Ar	42	4.53E-21	1.03516E-15	4.70527E-18
Ar	43	8.00E-15	1.82648E-09	8.3022E-12
Ar	44	2.08E-15	4.75799E-10	2.16272E-12
Ar	45	5.17E-18	1.17922E-12	5.36011E-15
Ar	46	3.51E-17	8.00685E-12	3.63948E-14
K	40	1.59E-25	3.63699E-20	1.65318E-22
K	42	3.33E-13	7.59132E-08	3.4506E-10
K	43	5.03E-15	1.14749E-09	5.21586E-12
K	44	2.84E-13	6.48858E-08	2.94936E-10
K	45	6.70E-14	1.53014E-08	6.95517E-11

K	46	2.50E-14	5.71461E-09	2.59755E-11
K	47	9.12E-15	2.08311E-09	9.46866E-12
Ca	45	7.07E-08	0.016148402	7.34018E-05
Ca	47	6.63E-06	1.514611872	0.006884599
Ca	49	1.03E-05	2.351598174	0.010689083
Sc	41	1.71E-21	3.89269E-16	1.76941E-18
Sc	42	2.99E-16	6.81735E-11	3.0988E-13
Sc	42*	1.78E-20	4.07306E-15	1.85139E-17
Sc	43	7.62E-08	0.017385845	7.90266E-05
Sc	44	9.67E-08	0.022075342	0.000100342
Sc	44*	6.43E-08	0.014671233	6.66874E-05
Sc	45*	7.93E-04	181.0045662	0.822748028
Sc	46	1.40E-07	0.031872146	0.000144873
Sc	46*	1.18E-04	27.00913242	0.122768784
Sc	47	1.44E-04	32.87671233	0.149439601
Sc	48	2.65E-04	60.4109589	0.274595268
Sc	49	8.60E-03	1963.926941	8.926940639
Sc	50	5.38E-04	122.8082192	0.558219178
Sc	50*	2.53E-04	57.69406393	0.262245745
Ti	43	5.81E-15	1.32626E-09	6.02844E-12
Ti	44	1.53E-13	3.48174E-08	1.58261E-10
Ti	45	2.39E-05	5.452054795	0.024782067
Ti	51	3.43E-03	782.6484018	3.557492736

D. MATLAB Script: Production Rate Calculation

The following script was developed to show the relationships between relative production rates over time, and to determine and plot the maximum isotopic purity. Further discussion of this script may be found in Chapter 3.

```matlab
% % Scandium 47 Production and Purities
% K. Austin DeLorme
clear
clc
hold off

%%% Select for Cinder or Experimental results
n = 1;
%# ask for inputs
tmp = input(sprintf('select n=1 (Experimental) or n=2 (Cinder90): ',n));
%# if the user hits 'return' without writing anything, tmp is empty and the default is
used
if ~isempty(tmp)
n = tmp;
end

if n==1;
% Production Rates (uCi/g per uAh)
VNat_Sc47_R=0.1462;
TiNat_Sc47_R=0.4430;
Ti47_Sc47_R=0.2108;
Ti50_Sc47_R=0.3479;
VNat_Sc48_R=0.1335;
TiNat_Sc48_R=0.2324;
Ti47_Sc48_R=0.0065;
Ti50_Sc48_R=0.5539;
VNat_Sc46_R=0.0035;
TiNat_Sc46_R=0.0230;
Ti47_Sc46_R=0.0110;
Ti50_Sc46_R=0.0061;
Ti50_Ca47_R=.0307;
TiNat_Ca47_R=0.0026;
VNat_Ca47_R=0.0002;
Ti47_Ca47_R= 0.0006;
else
VNat_Sc47_R=0.0002;
TiNat_Sc47_R=0.0386;
Ti47_Sc47_R=0.1535;
Ti48_Sc47_R=0.3195;
Ti49_Sc47_R=0.00005;
Ti50_Sc47_R=0.1494;
VNat_Sc48_R=0.0002;
TiNat_Sc48_R=0.0696;
Ti47_Sc48_R=0.0022;
Ti48_Sc48_R=0.4337;
Ti49_Sc48_R=0.0003;
```

```
Ti50_Sc48_R=0.2746;
VNat_Sc46_R=0.0000;
TiNat_Sc46_R=0.0124;
Ti47_Sc46_R=0.0018;
Ti48_Sc46_R=1.0496;
Ti49_Sc46_R=0.00017;
Ti50_Sc46_R=0.0001;
VNat_Ca47_R=0.0000;
TiNat_Ca47_R=0.0018;
Ti47_Ca47_R=0.0001;
Ti48_Ca47_R=1.0496;
Ti49_Ca47_R=0.0000;
Ti50_Ca47_R=.0069;
end


% Constant Values
Half47 = 3.3492;
Half48 = 1.8196;
HalfCa = 4.536;
Half46 = 83.79;
Lam47 = log(2)/Half47;
Lam48 = log(2)/Half48;
Lam46 = log(2)/Half46;
LamCa = log(2)/HalfCa;

% A sat (uCi/g)
VNat_Sc47_A=VNat_Sc47_R*(1/(1-exp(-Lam47*(1/24))));
TiNat_Sc47_A=TiNat_Sc47_R*(1/(1-exp(-Lam47*(1/24))));
Ti47_Sc47_A=Ti47_Sc47_R*(1/(1-exp(-Lam47*(1/24))));
Ti50_Sc47_A=Ti50_Sc47_R*(1/(1-exp(-Lam47*(1/24))));
VNat_Sc48_A=VNat_Sc48_R*(1/(1-exp(-Lam48*(1/24))));
TiNat_Sc48_A=TiNat_Sc48_R*(1/(1-exp(-Lam48*(1/24))));
Ti47_Sc48_A=Ti47_Sc48_R*(1/(1-exp(-Lam48*(1/24))));
Ti50_Sc48_A=Ti50_Sc48_R*(1/(1-exp(-Lam48*(1/24))));
VNat_Sc46_A=VNat_Sc46_R*(1/(1-exp(-Lam46*(1/24))));
TiNat_Sc46_A=TiNat_Sc46_R*(1/(1-exp(-Lam46*(1/24))));
Ti47_Sc46_A=Ti47_Sc46_R*(1/(1-exp(-Lam46*(1/24))));
Ti50_Sc46_A=Ti50_Sc46_R*(1/(1-exp(-Lam46*(1/24))));
TiNat_Ca47_A=TiNat_Ca47_R*(1/(1-exp(-LamCa*(1/24))));
Ti47_Ca47_A=Ti47_Ca47_R*(1/(1-exp(-LamCa*(1/24))));
Ti50_Ca47_A=Ti50_Ca47_R*(1/(1-exp(-LamCa*(1/24))));
VNat_Ca47_A=VNat_Ca47_R*(1/(1-exp(-LamCa*(1/24))));
if n==2;
   Ti48_Sc47_A=Ti48_Sc47_R*(1/(1-exp(-Lam47*(1/24))));
   Ti49_Sc47_A=Ti49_Sc47_R*(1/(1-exp(-Lam47*(1/24))));
```

```matlab
    Ti48_Sc48_A=Ti48_Sc48_R*(1/(1-exp(-Lam48*(1/24))));
    Ti49_Sc48_A=Ti49_Sc48_R*(1/(1-exp(-Lam48*(1/24))));
    Ti48_Sc46_A=Ti48_Sc46_R*(1/(1-exp(-Lam46*(1/24))));
    Ti49_Sc46_A=Ti49_Sc46_R*(1/(1-exp(-Lam46*(1/24))));
end
% Production Plot (Days)
ProdTime = [0: 0.01:10];
%%
%%%%%%%%%%%%%%%%%%%%%%%%%%%%%%%%%%%%%%%%%%%%
%%%%%%%%%%%%%%%%%%%%%%%%%%%%%%%%%%%%%%%%%
%     Vanadium FOIL
%%%%%%%%%%%%%%%%%%%%%%%%%%%%%%%%%%%%%%%%%%%%
%%%%%%%%%%%%%%%%%%%%%%%%%%%%%%%%%%%%%%%%%
% initialize & set zeros
VNatActSc47 = zeros(1,numel(ProdTime));
VNatActSc48 = zeros(1,numel(ProdTime));
VNatActSc46 = zeros(1,numel(ProdTime));
VNatActCa47 = zeros(1,numel(ProdTime));
VNatActSc47(1)=0;
VNatActSc48(1)=0;
VNatActSc46(1)=0;
VNatActCa47(1)=0;
VRatio_Check(1)=0;
for i = 1:1:numel(ProdTime)-1;
    % Activity Calcs
VNatActSc47(i+1) = VNat_Sc47_A*(1-exp(-Lam47*ProdTime(i+1)));
VNatActSc48(i+1) = VNat_Sc48_A*(1-exp(-Lam48*ProdTime(i+1)));
VNatActSc46(i+1) = VNat_Sc46_A*(1-exp(-Lam46*ProdTime(i+1)));
VNatActCa47(i+1) = VNat_Ca47_A*(1-exp(-LamCa*ProdTime(i+1)));
    VNatSc47_N1 = VNatActSc47(i+1);
    VNatSc48_N1 = VNatActSc48(i+1);
    VNatSc46_N1 = VNatActSc46(i+1);
    VNatCa47_N1 = VNatActCa47(i+1);
    VRatio_Check(i+1) = VNatSc47_N1/(VNatSc47_N1+VNatSc48_N1+VNatSc46_N1);
    if VRatio_Check(i+1) >= VRatio_Check(i);
      VNatSc47_N0 = VNatActSc47(i+1);
      VNatSc48_N0 = VNatActSc48(i+1);
      VNatSc46_N0 = VNatActSc46(i+1);
      VNatCa47_N0 = VNatActCa47(i+1);
      BeamTime = ProdTime(i+1);
    end
end
BeamTime
PostEOBTime = [0:0.01:10];
VNatSc47Decay=zeros(1,numel(PostEOBTime));
VNatSc48Decay=zeros(1,numel(PostEOBTime));
```

```matlab
VNatSc46Decay=zeros(1,numel(PostEOBTime));
VNatCa47Decay=zeros(1,numel(PostEOBTime));
VRatio = zeros(1,numel(PostEOBTime));
VNatSc47Decay(1)=VNatSc47_N0;
VNatSc48Decay(1)=VNatSc48_N0;
VNatSc46Decay(1)=VNatSc46_N0;
VNatCa47Decay(1)=VNatCa47_N0;
VRatio(1) = 0;
for j = 0:1:numel(PostEOBTime)-1;
   VNatCa47Decay(j+1) = VNatCa47_N0*exp(-LamCa*PostEOBTime(j+1));
   VNatSc47Decay(j+1) = VNatCa47_N0*(LamCa/(Lam47-LamCa))*exp(-
LamCa*PostEOBTime(j+1))+(VNatSc47_N0+VNatCa47_N0*(LamCa/(LamCa-
Lam47)))*exp(-Lam47*PostEOBTime(j+1));
   VNatSc48Decay(j+1) = VNatSc48_N0*exp(-Lam48*PostEOBTime(j+1));
   VNatSc46Decay(j+1) = VNatSc46_N0*exp(-Lam46*PostEOBTime(j+1));
   VRatio(j+1) =
VNatSc47Decay(j+1)/(VNatSc47Decay(j+1)+VNatSc48Decay(j+1)+VNatSc46Decay(j
+1));
end
VRatioMax = max(VRatio)*100
%% Create VNat Figure
% Create figure
figure1 = figure;

% Create subplot
subplot1 = subplot(3,1,1,'Parent',figure1);
box(subplot1,'on');
hold(subplot1,'all');

% Create multiple lines using matrix input to plot
plot1 = plot(ProdTime, VNatActSc47, ProdTime, VNatActSc46, ProdTime,
VNatActSc48, ProdTime,VNatActCa47);
set(plot1(1),'LineWidth',2,'DisplayName','^{47}Sc');
set(plot1(2),'Color',[1 0 0],'LineWidth',2,'DisplayName','^{46}Sc');
set(plot1(3),'Color',[0 1 0],'LineWidth',2,'DisplayName','^{48}Sc');
 set(plot1(4),'Color',[1 1 0],'LineWidth',2,'DisplayName','^{47}Ca');

% Create title
title('Sc Production from ^{nat}V Foil Target','FontSize',14);

% Create xlabel
xlabel('Time (d)','FontSize',12);

% Create ylabel
ylabel('Activity (\muCi/g per \muA)','FontSize',12);
```

```matlab
% Create subplot
subplot2 = subplot(3,1,2,'Parent',figure1);
box(subplot2,'on');
hold(subplot2,'all');

% Create multiple lines using matrix input to plot
plot2 = plot(PostEOBTime, VNatSc47Decay, PostEOBTime, VNatSc46Decay,
PostEOBTime, VNatSc48Decay, PostEOBTime, VNatCa47Decay);
set(plot2(1),'LineWidth',2,'DisplayName','^{47}Sc');
set(plot2(2),'Color',[1 0 0],'LineWidth',2,'DisplayName','^{46}Sc');
set(plot2(3),'Color',[0 1 0],'LineWidth',2,'DisplayName','^{48}Sc');
set(plot2(4),'Color',[0 1 0],'LineWidth',2,'DisplayName','^{47}Ca');

% Create title
title('Sc Decay from ^{nat}V Foil Target','FontSize',14);
%
% Create xlabel
xlabel('Time after EoB (d)','FontSize',12);

% Create ylabel
ylabel('Activity (\muCi/g per \muA)','FontSize',12);

% Create subplot
subplot3 = subplot(3,1,3,'Parent',figure1);
box(subplot3,'on');
hold(subplot3,'all');

% Create multiple lines using matrix input to plot
plot3 = plot(PostEOBTime, VRatio,'LineWidth',2,'Color',[0 1 0],...
   'DisplayName','^{47}Sc');
set(plot3(1),'DisplayName','^{47}Sc Purity');
% Create title
title('Radioisotopic Purity of ^{47}Sc Relative to ^{46}Sc and
^{48}Sc','FontSize',14);
%
% Create xlabel
xlabel('Time after EoB (d)','FontSize',12);

% Create ylabel
ylabel('Purity','FontSize',12);
% Create legend
legend1 = legend(subplot3,'show');
set(legend1,...
   'Position',[0.829367480002688 0.130979085944758 0.0617360226195226
0.0335513611633522]);
```

```matlab
% Create legend
legend(subplot2,'show');

% Create legend
legend2 = legend(subplot1,'show');
set(legend2,...
   'Position',[0.142434630637896 0.84104235429774 0.0617360226195226
0.0615072621394421]);
%%
%%%%%%%%%%%%%%%%%%%%%%%%%%%%%%%%%%%%%%%%%%%%%
%%%%%%%%%%%%%%%%%%%%%%%%%%%%%%%%%%%%%%%%%%
%     TITANIUM FOIL
%%%%%%%%%%%%%%%%%%%%%%%%%%%%%%%%%%%%%%%%%%%%%%
%%%%%%%%%%%%%%%%%%%%%%%%%%%%%%%%%%%%%%%%%%
% initialize & set zeros
TiNatActSc47 = zeros(1,numel(ProdTime));
TiNatActSc48 = zeros(1,numel(ProdTime));
TiNatActSc46 = zeros(1,numel(ProdTime));
TiNatActCa47 = zeros(1,numel(ProdTime));
TiNatActSc47(1)=0;
TiNatActSc48(1)=0;
TiNatActSc46(1)=0;
TiNatActCa47(1)=0;
for i = 1:1:numel(ProdTime)-1;
   % Activity Calcs
TiNatActSc47(i+1) = TiNat_Sc47_A*(1-exp(-Lam47*ProdTime(i+1)));
TiNatActSc48(i+1) = TiNat_Sc48_A*(1-exp(-Lam48*ProdTime(i+1)));
TiNatActSc46(i+1) = TiNat_Sc46_A*(1-exp(-Lam46*ProdTime(i+1)));
TiNatActCa47(i+1) = TiNat_Ca47_A*(1-exp(-LamCa*ProdTime(i+1)));
   TiNatSc47_N1 = TiNatActSc47(i+1);
   TiNatSc48_N1 = TiNatActSc48(i+1);
   TiNatSc46_N1 = TiNatActSc46(i+1);
   TiNatCa47_N1 = TiNatActCa47(i+1);
   TiRatio_Check(i+1) =
TiNatSc47_N1/(TiNatSc47_N1+TiNatSc48_N1+TiNatSc46_N1);
   if VRatio_Check(i+1) >= VRatio_Check(i);
     TiNatSc47_N0 = TiNatActSc47(i+1);
     TiNatSc48_N0 = TiNatActSc48(i+1);
     TiNatSc46_N0 = TiNatActSc46(i+1);
     TiNatCa47_N0 = TiNatActCa47(i+1);
     BeamTime = ProdTime(i+1);
   end
end
BeamTime
PostEOBTime = [0:0.01:10];
TiNatSc47Decay=zeros(1,numel(PostEOBTime));
```

```matlab
TiNatSc48Decay=zeros(1,numel(PostEOBTime));
TiNatSc46Decay=zeros(1,numel(PostEOBTime));
TiNatCa47Decay=zeros(1,numel(PostEOBTime));
TiRatio = zeros(1,numel(PostEOBTime));
TiNatSc47Decay(1)=TiNatSc47_N0;
TiNatSc48Decay(1)=TiNatSc48_N0;
TiNatSc46Decay(1)=TiNatSc46_N0;
TiNatCa47Decay(1)=TiNatCa47_N0;
TiRatio(1) = 0;
for j = 0:1:numel(PostEOBTime)-1;
   TiNatCa47Decay(j+1) = TiNatCa47_N0*exp(-LamCa*PostEOBTime(j+1));
   TiNatSc47Decay(j+1) = TiNatCa47_N0*(LamCa/(Lam47-LamCa))*exp(-
LamCa*PostEOBTime(j+1))+(TiNatSc47_N0+TiNatCa47_N0*(LamCa/(LamCa-
Lam47)))*exp(-Lam47*PostEOBTime(j+1));
   TiNatSc48Decay(j+1) = TiNatSc48_N0*exp(-Lam48*PostEOBTime(j+1));
   TiNatSc46Decay(j+1) = TiNatSc46_N0*exp(-Lam46*PostEOBTime(j+1));
   TiRatio(j+1) =
TiNatSc47Decay(j+1)/(TiNatSc47Decay(j+1)+TiNatSc48Decay(j+1)+TiNatSc46Deca
y(j+1));
end
TiRatioMax = max(TiRatio)*100
%% Create VNat Figure
% Create figure
figure1 = figure;

% Create subplot
subplot1 = subplot(3,1,1,'Parent',figure1);
box(subplot1,'on');
hold(subplot1,'all');

% Create multiple lines using matrix input to plot
plot1 = plot(ProdTime, TiNatActSc47, ProdTime, TiNatActSc46, ProdTime,
TiNatActSc48, ProdTime, TiNatActCa47);
set(plot1(1),'LineWidth',2,'DisplayName','^{47}Sc');
set(plot1(2),'Color',[1 0 0],'LineWidth',2,'DisplayName','^{46}Sc');
set(plot1(3),'Color',[0 1 0],'LineWidth',2,'DisplayName','^{48}Sc');
set(plot1(4),'Color',[1 1 0],'LineWidth',2,'DisplayName','^{47}Ca');
% Create title
title('Sc Production from ^{nat}Ti Foil Target','FontSize',14);

% Create xlabel
xlabel('Time (d)','FontSize',12);

% Create ylabel
ylabel('Activity (\muCi/g per \muA)','FontSize',12);
```

```matlab
% Create subplot
subplot2 = subplot(3,1,2,'Parent',figure1);
box(subplot2,'on');
hold(subplot2,'all');

% Create multiple lines using matrix input to plot
plot2 = plot(PostEOBTime, TiNatSc47Decay, PostEOBTime, TiNatSc46Decay,
PostEOBTime, TiNatSc48Decay);
set(plot2(1),'LineWidth',2,'DisplayName','^{47}Sc');
set(plot2(2),'Color',[1 0 0],'LineWidth',2,'DisplayName','^{46}Sc');
set(plot2(3),'Color',[0 1 0],'LineWidth',2,'DisplayName','^{48}Sc');

% Create title
title('Sc Decay from ^{nat}Ti Foil Target','FontSize',14);
%
% Create xlabel
xlabel('Time after EoB (d)','FontSize',12);

% Create ylabel
ylabel('Activity (\muCi/g per \muA)','FontSize',12);

% Create subplot
subplot3 = subplot(3,1,3,'Parent',figure1);
box(subplot3,'on');
hold(subplot3,'all');

% Create multiple lines using matrix input to plot
plot3 = plot(PostEOBTime, TiRatio,'LineWidth',2,'Color',[0 1 0],...
    'DisplayName','^{47}Sc %Purity');
set(plot3(1),'DisplayName','^{47}Sc Purity');
% Create title
title('Radioisotopic Purity of ^{47}Sc Relative to ^{46}Sc and
^{48}Sc','FontSize',14);
%
% Create xlabel
xlabel('Time after EoB (d)','FontSize',12);

% Create ylabel
ylabel('Purity','FontSize',12);
% Create legend
legend1 = legend(subplot3,'show');
set(legend1,...
    'Position',[0.829367480002688 0.130979085944758 0.0617360226195226
0.0335513611633522]);

% Create legend
```

```matlab
legend(subplot2,'show');

% Create legend
legend2 = legend(subplot1,'show');
set(legend2,...
   'Position',[0.142434630637896 0.84104235429774 0.0617360226195226
0.0615072621394421]);
%%
%%%%%%%%%%%%%%%%%%%%%%%%%%%%%%%%%%%%%%%%%%%%%
%%%%%%%%%%%%%%%%%%%%%%%%%%%%%%%%%%%%%%%%%%
%     Ti47 OXIDE
%%%%%%%%%%%%%%%%%%%%%%%%%%%%%%%%%%%%%%%%%%%%%
%%%%%%%%%%%%%%%%%%%%%%%%%%%%%%%%%%%%%%%%%%
% initialize & set zeros
Ti47ActSc47 = zeros(1,numel(ProdTime));
Ti47ActSc48 = zeros(1,numel(ProdTime));
Ti47ActSc46 = zeros(1,numel(ProdTime));
Ti47ActCa47 = zeros(1,numel(ProdTime));
Ti47ActSc47(1)=0;
Ti47ActSc48(1)=0;
Ti47ActSc46(1)=0;
Ti47ActCa47(1)=0;
for i = 1:1:numel(ProdTime)-1;
   % Activity Calcs
Ti47ActSc47(i+1) = Ti47_Sc47_A*(1-exp(-Lam47*ProdTime(i+1)));
Ti47ActSc48(i+1) = Ti47_Sc48_A*(1-exp(-Lam48*ProdTime(i+1)));
Ti47ActSc46(i+1) = Ti47_Sc46_A*(1-exp(-Lam46*ProdTime(i+1)));
Ti47ActCa47(i+1) = Ti47_Ca47_A*(1-exp(-LamCa*ProdTime(i+1)));
   Ti47Sc47_N1 = Ti47ActSc47(i+1);
   Ti47Sc48_N1 = Ti47ActSc48(i+1);
   Ti47Sc46_N1 = Ti47ActSc46(i+1);
   Ti47Ca47_N1 = Ti47ActCa47(i+1);
   Ti47Ratio_Check(i+1) =
Ti47Sc47_N1/(Ti47Sc47_N1+Ti47Sc48_N1+Ti47Sc46_N1);
   if Ti47Ratio_Check(i+1) >= Ti47Ratio_Check(i);
     Ti47Sc47_N0 = Ti47ActSc47(i+1);
     Ti47Sc48_N0 = Ti47ActSc48(i+1);
     Ti47Sc46_N0 = Ti47ActSc46(i+1);
     Ti47Ca47_N0 = Ti47ActCa47(i+1);
     BeamTime = ProdTime(i+1);
   end
end
BeamTime
PostEOBTime = [0:0.01:10];
Ti47Sc47Decay=zeros(1,numel(PostEOBTime));
Ti47Sc48Decay=zeros(1,numel(PostEOBTime));
```

```matlab
Ti47Sc46Decay=zeros(1,numel(PostEOBTime));
Ti47Ca47Decay=zeros(1,numel(PostEOBTime));
Ti47Ratio = zeros(1,numel(PostEOBTime));
Ti47Sc47Decay(1)=Ti47Sc47_N0;
Ti47Sc48Decay(1)=Ti47Sc48_N0;
Ti47Sc46Decay(1)=Ti47Sc46_N0;
Ti47Ca47Decay(1)=Ti47Sc46_N0;
Ti47Ratio(1) = 0;
for j = 0:1:numel(PostEOBTime)-1;
   Ti47Ca47Decay(j+1) = Ti47Ca47_N0*exp(-LamCa*PostEOBTime(j+1));
   Ti47Sc47Decay(j+1) = Ti47Ca47_N0*(LamCa/(Lam47-LamCa))*exp(-
LamCa*PostEOBTime(j+1))+(Ti47Sc47_N0+Ti47Ca47_N0*(LamCa/(LamCa-
Lam47)))*exp(-Lam47*PostEOBTime(j+1));
   Ti47Sc48Decay(j+1) = Ti47Sc48_N0*exp(-Lam48*PostEOBTime(j+1));
   Ti47Sc46Decay(j+1) = Ti47Sc46_N0*exp(-Lam46*PostEOBTime(j+1));
   Ti47Ratio(j+1) =
Ti47Sc47Decay(j+1)/(Ti47Sc47Decay(j+1)+Ti47Sc48Decay(j+1)+Ti47Sc46Decay(j
+1));
end
Ti47RatioMax = max(Ti47Ratio)*100
 %% Create VNat Figure
 % Create figure
 figure1 = figure;

 % Create subplot
 subplot1 = subplot(3,1,1,'Parent',figure1);
 box(subplot1,'on');
 hold(subplot1,'all');

 % Create multiple lines using matrix input to plot
 plot1 = plot(ProdTime, Ti47ActSc47, ProdTime, Ti47ActSc46, ProdTime,
Ti47ActSc48, ProdTime, Ti47ActCa47);
 set(plot1(1),'LineWidth',2,'DisplayName','^{47}Sc');
 set(plot1(2),'Color',[1 0 0],'LineWidth',2,'DisplayName','^{46}Sc');
 set(plot1(3),'Color',[0 1 0],'LineWidth',2,'DisplayName','^{48}Sc');
   set(plot1(4),'Color',[0 1 0],'LineWidth',2,'DisplayName','^{47}Ca');
 % Create title
 title('Sc Production from ^{47}Ti Oxide Target','FontSize',14);

 % Create xlabel
 xlabel('Time (d)','FontSize',12);

 % Create ylabel
 ylabel('Activity (\muCi/g per \muA)','FontSize',12);

 % Create subplot
```

```matlab
subplot2 = subplot(3,1,2,'Parent',figure1);
box(subplot2,'on');
hold(subplot2,'all');

% Create multiple lines using matrix input to plot
plot2 = plot(PostEOBTime, Ti47Sc47Decay, PostEOBTime, Ti47Sc46Decay,
PostEOBTime, Ti47Sc48Decay, PostEOBTime, Ti47Ca47Decay);
set(plot2(1),'LineWidth',2,'DisplayName','^{47}Sc');
set(plot2(2),'Color',[1 0 0],'LineWidth',2,'DisplayName','^{46}Sc');
set(plot2(3),'Color',[0 1 0],'LineWidth',2,'DisplayName','^{48}Sc');
set(plot2(4),'Color',[1 1 0],'LineWidth',2,'DisplayName','^{47}Ca');
% Create title
title('Sc Decay from ^{47}Ti Oxide Target','FontSize',14);
%
% Create xlabel
xlabel('Time after EoB (d)','FontSize',12);

% Create ylabel
ylabel('Activity (\muCi/g per \muA)','FontSize',12);

% Create subplot
subplot3 = subplot(3,1,3,'Parent',figure1);
box(subplot3,'on');
hold(subplot3,'all');

% Create multiple lines using matrix input to plot
plot3 = plot(PostEOBTime, Ti47Ratio,'LineWidth',2,'Color',[0 1 0],...
  'DisplayName','^{47}Sc');
set(plot3(1),'DisplayName','^{47}Sc Purity');
 % Create title
title('Radioisotopic Purity of ^{47}Sc Relative to ^{46}Sc and
^{48}Sc','FontSize',14);
%
% Create xlabel
xlabel('Time after EoB (d)','FontSize',12);

% Create ylabel
ylabel('Purity','FontSize',12);
% Create legend
legend1 = legend(subplot3,'show');
set(legend1,...
  'Position',[0.829367480002688 0.130979085944758 0.0617360226195226
0.0335513611633522]);

% Create legend
legend(subplot2,'show');
```

```matlab
% Create legend
legend2 = legend(subplot1,'show');
set(legend2,...
    'Position',[0.142434630637896 0.84104235429774 0.0617360226195226
0.0615072621394421]);
%%
%%%%%%%%%%%%%%%%%%%%%%%%%%%%%%%%%%%%%%%%%%%%%
%%%%%%%%%%%%%%%%%%%%%%%%%%%%%%%%%%%%%%%%%%%
%       Ti50 OXIDE
%%%%%%%%%%%%%%%%%%%%%%%%%%%%%%%%%%%%%%%%%%%%%
%%%%%%%%%%%%%%%%%%%%%%%%%%%%%%%%%%%%%%%%%%%
% initialize & set zeros
Ti50ActSc47 = zeros(1,numel(ProdTime));
Ti50ActSc48 = zeros(1,numel(ProdTime));
Ti50ActSc46 = zeros(1,numel(ProdTime));
Ti50ActSc47(1)=0;
Ti50ActSc48(1)=0;
Ti50ActSc46(1)=0;
for i = 1:1:numel(ProdTime)-1;
    % Activity Calcs
Ti50ActSc47(i+1) = Ti50_Sc47_A*(1-exp(-Lam47*ProdTime(i+1)));
Ti50ActSc48(i+1) = Ti50_Sc48_A*(1-exp(-Lam48*ProdTime(i+1)));
Ti50ActSc46(i+1) = Ti50_Sc46_A*(1-exp(-Lam46*ProdTime(i+1)));
Ti50ActCa47(i+1) = Ti50_Ca47_A*(1-exp(-LamCa*ProdTime(i+1)));
    Ti50Sc47_N1 = Ti50ActSc47(i+1);
    Ti50Sc48_N1 = Ti50ActSc48(i+1);
    Ti50Sc46_N1 = Ti50ActSc46(i+1);
    Ti50Ca47_N1 = Ti50ActCa47(i+1);
    Ti50Ratio_Check(i+1) =
Ti50Sc47_N1/(Ti50Sc47_N1+Ti50Sc48_N1+Ti50Sc46_N1);
    if Ti50Ratio_Check(i+1) >= Ti50Ratio_Check(i);
      Ti50Sc47_N0 = Ti50ActSc47(i+1);
      Ti50Sc48_N0 = Ti50ActSc48(i+1);
      Ti50Sc46_N0 = Ti50ActSc46(i+1);
      Ti50Ca47_N0 = Ti50ActCa47(i+1);
      BeamTime = ProdTime(i+1);
    end
end
BeamTime
PostEOBTime = [0:0.01:10];
Ti50Ca47Decay=zeros(1,numel(PostEOBTime));
Ti50Sc47Decay=zeros(1,numel(PostEOBTime));
Ti50Sc48Decay=zeros(1,numel(PostEOBTime));
Ti50Sc46Decay=zeros(1,numel(PostEOBTime));
Ti50Ratio = zeros(1,numel(PostEOBTime));
```

```matlab
Ti50Sc47Decay(1)=Ti50Sc47_N0;
Ti50Sc48Decay(1)=Ti50Sc48_N0;
Ti50Sc46Decay(1)=Ti50Sc46_N0;
Ti50Ca47Decay(1)=Ti50Ca47_N0;
Ti50Ratio(1) = 0;
for j = 0:1:numel(PostEOBTime)-1;
   Ti50Ca47Decay(j+1) = Ti50Ca47_N0*exp(-LamCa*PostEOBTime(j+1));
   Ti50Sc47Decay(j+1) = Ti50Ca47_N0*(LamCa/(Lam47-LamCa))*exp(-
LamCa*PostEOBTime(j+1))+(Ti50Sc47_N0+Ti50Ca47_N0*(LamCa/(LamCa-
Lam47)))*exp(-Lam47*PostEOBTime(j+1));
   Ti50Sc48Decay(j+1) = Ti50Sc48_N0*exp(-Lam48*PostEOBTime(j+1));
   Ti50Sc46Decay(j+1) = Ti50Sc46_N0*exp(-Lam46*PostEOBTime(j+1));
   Ti50Ratio(j+1) =
Ti50Sc47Decay(j+1)/(Ti50Sc47Decay(j+1)+Ti50Sc48Decay(j+1)+Ti50Sc46Decay(j
+1));
end
Ti50RatioMax = max(Ti50Ratio)*100
%% Create VNat Figure
% Create figure
figure1 = figure;

% Create subplot
subplot1 = subplot(3,1,1,'Parent',figure1);
box(subplot1,'on');
hold(subplot1,'all');

% Create multiple lines using matrix input to plot
plot1 = plot(ProdTime, Ti50ActSc47, ProdTime, Ti50ActSc46, ProdTime,
Ti50ActSc48, ProdTime, Ti50ActCa47);
set(plot1(1),'LineWidth',2,'DisplayName','^{47}Sc');
set(plot1(2),'Color',[1 0 0],'LineWidth',2,'DisplayName','^{46}Sc');
set(plot1(3),'Color',[0 1 0],'LineWidth',2,'DisplayName','^{48}Sc');
set(plot1(4),'Color',[1 1 0],'LineWidth',2,'DisplayName','^{47}Ca');
% Create title
title('Sc and Ca Production from ^{50}Ti Oxide Target','FontSize',14);

% Create xlabel
xlabel('Time (d)','FontSize',12);

% Create ylabel
ylabel('Activity (\muCi/g per \muA)','FontSize',12);

% Create subplot
subplot2 = subplot(3,1,2,'Parent',figure1);
box(subplot2,'on');
hold(subplot2,'all');
```

```matlab
 % Create multiple lines using matrix input to plot
 plot2 = plot(PostEOBTime, Ti50Sc47Decay, PostEOBTime, Ti50Sc46Decay,
PostEOBTime, Ti50Sc48Decay, PostEOBTime, Ti50Ca47Decay);
set(plot2(1),'LineWidth',2,'DisplayName','^{47}Sc');
set(plot2(2),'Color',[1 0 0],'LineWidth',2,'DisplayName','^{46}Sc');
set(plot2(3),'Color',[0 1 0],'LineWidth',2,'DisplayName','^{48}Sc');
set(plot2(4),'Color',[1 1 0],'LineWidth',2,'DisplayName','^{47}Ca');

 % Create title
 title('Sc and Ca Decay from ^{50}Ti Oxide Target','FontSize',14);
%
 % Create xlabel
 xlabel('Time after EoB (d)','FontSize',12);

 % Create ylabel
 ylabel('Activity (\muCi/g per \muA)','FontSize',12);

 % Create subplot
 subplot3 = subplot(3,1,3,'Parent',figure1);
 box(subplot3,'on');
 hold(subplot3,'all');

 % Create multiple lines using matrix input to plot
 plot3 = plot(PostEOBTime, Ti50Ratio,'LineWidth',2,'Color',[0 1 0],...
   'DisplayName','^{47}Sc');
 set(plot3(1),'DisplayName','^{47}Sc Purity');
 % Create title
 title('Radioisotopic Purity of ^{47}Sc Relative to ^{46}Sc and
^{48}Sc','FontSize',14);
%
 % Create xlabel
 xlabel('Time after EoB (d)','FontSize',12);

 % Create ylabel
 ylabel('Purity','FontSize',12);
% Create legend
legend1 = legend(subplot3,'show');
set(legend1,...
   'Position',[0.829367480002688 0.130979085944758 0.0617360226195226
0.0335513611633522]);

% Create legend
legend(subplot2,'show');

% Create legend
```

```matlab
legend2 = legend(subplot1,'show');
set(legend2,...
    'Position',[0.142434630637896 0.84104235429774 0.0617360226195226
0.0615072621394421]);
%% Cinder90 Extras
if n==2
 %%
%%%%%%%%%%%%%%%%%%%%%%%%%%%%%%%%%%%%%%%%%%%%
%%%%%%%%%%%%%%%%%%%%%%%%%%%%%%%%%%%%%%%
%     Ti48 OXIDE
%%%%%%%%%%%%%%%%%%%%%%%%%%%%%%%%%%%%%%%%%%%%
%%%%%%%%%%%%%%%%%%%%%%%%%%%%%%%%%%%%%%%
% initialize & set zeros
Ti48ActSc47 = zeros(1,numel(ProdTime));
Ti48ActSc48 = zeros(1,numel(ProdTime));
Ti48ActSc46 = zeros(1,numel(ProdTime));
Ti48ActSc47(1)=0;
Ti48ActSc48(1)=0;
Ti48ActSc46(1)=0;
for i = 1:1:numel(ProdTime)-1;
    % Activity Calcs
Ti48ActSc47(i+1) = Ti48_Sc47_A*(1-exp(-Lam47*ProdTime(i+1)));
Ti48ActSc48(i+1) = Ti48_Sc48_A*(1-exp(-Lam48*ProdTime(i+1)));
Ti48ActSc46(i+1) = Ti48_Sc46_A*(1-exp(-Lam46*ProdTime(i+1)));
    BeamTime = ProdTime(i+1);
    Ti48Sc47_N0 = Ti48ActSc47(i+1);
    Ti48Sc48_N0 = Ti48ActSc48(i+1);
    Ti48Sc46_N0 = Ti48ActSc46(i+1);
end
BeamTime
PostEOBTime = [0:0.01:10];
Ti48Sc47Decay=zeros(1,numel(PostEOBTime));
Ti48Sc48Decay=zeros(1,numel(PostEOBTime));
Ti48Sc46Decay=zeros(1,numel(PostEOBTime));
Ti48Ratio = zeros(1,numel(PostEOBTime));
Ti48Sc47Decay(1)=Ti48Sc47_N0;
Ti48Sc48Decay(1)=Ti48Sc48_N0;
Ti48Sc46Decay(1)=Ti48Sc46_N0;
Ti48Ratio(1) = 0;
for j = 0:1:numel(PostEOBTime)-1;
    Ti48Sc47Decay(j+1) = Ti48Sc47_N0*exp(-Lam47*PostEOBTime(j+1));
    Ti48Sc48Decay(j+1) = Ti48Sc48_N0*exp(-Lam48*PostEOBTime(j+1));
    Ti48Sc46Decay(j+1) = Ti48Sc46_N0*exp(-Lam46*PostEOBTime(j+1));
    Ti48Ratio(j+1) =
Ti48Sc47Decay(j+1)/(Ti48Sc47Decay(j+1)+Ti48Sc48Decay(j+1)+Ti48Sc46Decay(j
+1));
```

```matlab
end
Ti48RatioMax = max(Ti48Ratio)*100
%% Create VNat Figure
% Create figure
figure1 = figure;

% Create subplot
subplot1 = subplot(3,1,1,'Parent',figure1);
box(subplot1,'on');
hold(subplot1,'all');

% Create multiple lines using matrix input to plot
plot1 = plot(ProdTime, Ti48ActSc47, ProdTime, Ti48ActSc46, ProdTime,
Ti48ActSc48);
set(plot1(1),'LineWidth',2,'DisplayName','^{47}Sc');
set(plot1(2),'Color',[1 0 0],'LineWidth',2,'DisplayName','^{46}Sc');
set(plot1(3),'Color',[0 1 0],'LineWidth',2,'DisplayName','^{48}Sc');
% Create title
title('Sc Production from ^{48}Ti Oxide Target','FontSize',14);

% Create xlabel
xlabel('Time (d)','FontSize',12);

% Create ylabel
ylabel('Activity (\muCi/g per \muA)','FontSize',12);

% Create subplot
subplot2 = subplot(3,1,2,'Parent',figure1);
box(subplot2,'on');
hold(subplot2,'all');

% Create multiple lines using matrix input to plot
plot2 = plot(PostEOBTime, Ti48Sc47Decay, PostEOBTime, Ti48Sc46Decay,
PostEOBTime, Ti48Sc48Decay);
set(plot2(1),'LineWidth',2,'DisplayName','^{47}Sc');
set(plot2(2),'Color',[1 0 0],'LineWidth',2,'DisplayName','^{46}Sc');
set(plot2(3),'Color',[0 1 0],'LineWidth',2,'DisplayName','^{48}Sc');
% Create title
title('Sc Decay from ^{48}Ti Oxide Target','FontSize',14);
%
% Create xlabel
xlabel('Time after EoB (d)','FontSize',12);

% Create ylabel
ylabel('Activity (\muCi/g per \muA)','FontSize',12);
```

```matlab
% Create subplot
subplot3 = subplot(3,1,3,'Parent',figure1);
box(subplot3,'on');
hold(subplot3,'all');

% Create multiple lines using matrix input to plot
plot3 = plot(PostEOBTime, Ti48Ratio,'LineWidth',2,'Color',[0 1 0],...
  'DisplayName','^{47}Sc');
set(plot3(1),'DisplayName','^{47}Sc Purity');
 % Create title
title('Radioisotopic Purity of ^{48}Sc Relative to ^{46}Sc and
^{48}Sc','FontSize',14);
%
% Create xlabel
xlabel('Time after EoB (d)','FontSize',12);

% Create ylabel
ylabel('Purity','FontSize',12);
% Create legend
legend1 = legend(subplot3,'show');
set(legend1,...
  'Position',[0.829367480002688 0.130979085944758 0.0617360226195226
0.0335513611633522]);

% Create legend
legend(subplot2,'show');
%
% % Create legend
legend2 = legend(subplot1,'show');
 set(legend2,...
   'Position',[0.142434630637896 0.84104235429774 0.0617360226195226
0.0615072621394421]);
%%
%%%%%%%%%%%%%%%%%%%%%%%%%%%%%%%%%%%%%%%%%%%%
%%%%%%%%%%%%%%%%%%%%%%%%%%%%%%%%%%%%%%%%
%     Ti49 OXIDE
%%%%%%%%%%%%%%%%%%%%%%%%%%%%%%%%%%%%%%%%%%%%
%%%%%%%%%%%%%%%%%%%%%%%%%%%%%%%%%%%%%%%%
% initialize & set zeros
Ti49ActSc47 = zeros(1,numel(ProdTime));
Ti49ActSc48 = zeros(1,numel(ProdTime));
Ti49ActSc46 = zeros(1,numel(ProdTime));
Ti49ActSc47(1)=0;
Ti49ActSc48(1)=0;
Ti49ActSc46(1)=0;
for i = 1:1:numel(ProdTime)-1;
```

```matlab
    % Activity Calcs
Ti49ActSc47(i+1) = Ti49_Sc47_A*(1-exp(-Lam47*ProdTime(i+1)));
Ti49ActSc48(i+1) = Ti49_Sc48_A*(1-exp(-Lam48*ProdTime(i+1)));
Ti49ActSc46(i+1) = Ti49_Sc46_A*(1-exp(-Lam46*ProdTime(i+1)));
    Ti49Sc47_N0 = Ti49ActSc47(i+1);
    Ti49Sc48_N0 = Ti49ActSc48(i+1);
    Ti49Sc46_N0 = Ti49ActSc46(i+1);
end
BeamTime
PostEOBTime = [0:0.01:10];
Ti49Sc47Decay=zeros(1,numel(PostEOBTime));
Ti49Sc48Decay=zeros(1,numel(PostEOBTime));
Ti49Sc46Decay=zeros(1,numel(PostEOBTime));
Ti49Ratio = zeros(1,numel(PostEOBTime));
Ti49Sc47Decay(1)=Ti49Sc47_N0;
Ti49Sc48Decay(1)=Ti49Sc48_N0;
Ti49Sc46Decay(1)=Ti49Sc46_N0;
Ti49Ratio(1) = 0;
for j = 0:1:numel(PostEOBTime)-1;
  Ti49Sc47Decay(j+1) = Ti49Sc47_N0*exp(-Lam47*PostEOBTime(j+1));
  Ti49Sc48Decay(j+1) = Ti49Sc48_N0*exp(-Lam48*PostEOBTime(j+1));
  Ti49Sc46Decay(j+1) = Ti49Sc46_N0*exp(-Lam46*PostEOBTime(j+1));
  Ti49Ratio(j+1) =
Ti49Sc47Decay(j+1)/(Ti49Sc47Decay(j+1)+Ti49Sc48Decay(j+1)+Ti49Sc46Decay(j
+1));
end
Ti49RatioMax = max(Ti49Ratio)*100
 %% Create Ti49 Figure
 % Create figure
 figure1 = figure;

 % Create subplot
 subplot1 = subplot(3,1,1,'Parent',figure1);
 box(subplot1,'on');
 hold(subplot1,'all');

 % Create multiple lines using matrix input to plot
 plot1 = plot(ProdTime, Ti49ActSc47, ProdTime, Ti49ActSc46, ProdTime,
Ti49ActSc48);
 set(plot1(1),'LineWidth',2,'DisplayName','^{47}Sc');
 set(plot1(2),'Color',[1 0 0],'LineWidth',2,'DisplayName','^{46}Sc');
 set(plot1(3),'Color',[0 1 0],'LineWidth',2,'DisplayName','^{48}Sc');
 % Create title
 title('Sc Production from ^{49}Ti Oxide Target','FontSize',14);

 % Create xlabel
```

```matlab
xlabel('Time (d)','FontSize',12);

% Create ylabel
ylabel('Activity (\muCi/g per \muA)','FontSize',12);

% Create subplot
subplot2 = subplot(3,1,2,'Parent',figure1);
box(subplot2,'on');
hold(subplot2,'all');

% Create multiple lines using matrix input to plot
plot2 = plot(PostEOBTime, Ti49Sc47Decay, PostEOBTime, Ti49Sc46Decay,
PostEOBTime, Ti49Sc48Decay);
set(plot2(1),'LineWidth',2,'DisplayName','^{47}Sc');
set(plot2(2),'Color',[1 0 0],'LineWidth',2,'DisplayName','^{46}Sc');
set(plot2(3),'Color',[0 1 0],'LineWidth',2,'DisplayName','^{48}Sc');
% Create title
title('Sc Decay from ^{49}Ti Oxide Target','FontSize',14);
%
% Create xlabel
xlabel('Time after EoB (d)','FontSize',12);

% Create ylabel
ylabel('Activity (\muCi/g per \muA)','FontSize',12);

% Create subplot
subplot3 = subplot(3,1,3,'Parent',figure1);
box(subplot3,'on');
hold(subplot3,'all');

% Create multiple lines using matrix input to plot
plot3 = plot(PostEOBTime, Ti49Ratio,'LineWidth',2,'Color',[0 1 0],...
    'DisplayName','^{47}Sc');
set(plot3(1),'DisplayName','^{47}Sc Purity');
% Create title
title('Radioisotopic Purity of ^{47}Sc Relative to ^{46}Sc and
^{48}Sc','FontSize',14);
%
% Create xlabel
xlabel('Time after EoB (d)','FontSize',12);

% Create ylabel
ylabel('Purity','FontSize',12);
% Create legend
legend1 = legend(subplot3,'show');
set(legend1,...
```

```
    'Position',[0.829367480002688 0.130979085944758 0.0617360226195226
0.0335513611633522]);

% Create legend
legend(subplot2,'show');

% Create legend
legend2 = legend(subplot1,'show');
set(legend2,...
    'Position',[0.142434630637896 0.84104235429774 0.0617360226195226
0.0615072621394421]);
end
```

E. MATLAB Script: MCNP Cross Section Derivation

The following script was written to derive cross sections from the MCNP Ft8 Res tally outputs for each individual energy. Bash scripting was then used to run through each energy and extract the proper data in order to generate excitation functions. Further discussion of this script may be found in Chapter 3.

```matlab
%% Import data from text file.
% Script for importing data from the following text file:
%
%    /Users/kadelorm/Documents/Research/MCNPInputs/2.2313tallyVNat.txt
%
% To extend the code to different selected data or a different text file,
% generate a function instead of a script.

% Auto-generated by MATLAB on 2013/11/24 22:49:05

%% Initialize variables.
filename = '2.2313tallyVNat.txt';
%% Use Import Function
%# ask for inputs
% % tmp = input(sprintf('Please give file name - if in a differnt path, input entire
path: ',filename));
% %# if the user hits 'return' without writing anything, tmp is empty and the default
is used
% if ~isempty(tmp)
% filename = tmp;
%end
delimiter = ' ';
startRow = 27;
endRow = 40;

%% Format string for each line of text:
%   column1: double (%f)
%       column2: double (%f)
%   column3: double (%f)
%       column4: double (%f)
%   column5: double (%f)
%       column6: double (%f)
%   column7: double (%f)
%       column8: double (%f)
% For more information, see the TEXTSCAN documentation.
formatSpec =
'%f%f%f%f%f%f%f%f%*s%*s%*s%*s%*s%*s%*s%*s%*s%*s%*s%*s%*s%*s%*s
%*s%*s%*s%*s%*s%*s%*s%*s%*s%*s%*s%*s%*s%*s%[^\n\r]';

%% Open the text file.
fileID = fopen(filename,'r');

%% Read columns of data according to format string.
% This call is based on the structure of the file used to generate this
% code. If an error occurs for a different file, try regenerating the code
% from the Import Tool.
```

```matlab
dataArray = textscan(fileID, formatSpec, endRow-startRow+1, 'Delimiter', delimiter,
'MultipleDelimsAsOne', true, 'HeaderLines', startRow-1, 'ReturnOnError', false);

%% Close the text file.
fclose(fileID);

%% Post processing for unimportable data.
% No unimportable data rules were applied during the import, so no post
% processing code is included. To generate code which works for
% unimportable data, select unimportable cells in a file and regenerate the
% script.

%% Allocate imported array to column variable names
RES1 = dataArray{:, 1};
RES1Err = dataArray{:, 2};
RES2 = dataArray{:, 3};
RES2Err = dataArray{:, 4};
RES3 = dataArray{:, 5};
RES3Err = dataArray{:, 6};
RES4 = dataArray{:, 7};
RES4Err = dataArray{:, 8};
Res=[RES1(1),RES2(1),RES3(1),RES4(1),RES1(2),RES2(2),RES3(2),RES4(2),RES1(3
),RES2(3),RES3(3),RES4(3), ...

RES1(4),RES2(4),RES3(4),RES4(4),RES1(5),RES2(5),RES3(5),RES4(5),RES1(6),RES
2(6),RES3(6),RES4(6), ...

RES1(7),RES2(7),RES3(7),RES4(7),RES1(8),RES2(8),RES3(8),RES4(8),RES1(9),RES
2(9),RES3(9),RES4(9),RES1(10),RES2(10),RES3(10),RES4(10), ...

RES1(11),RES2(11),RES3(11),RES4(11),RES1(12),RES2(12),RES3(12),RES4(12),RE
S1(13),RES2(13),RES3(13),RES4(13), ...
    RES1(14),RES2(14),RES3Err(14)]';
Err =
[RES1Err(1),RES2Err(1),RES3Err(1),RES4Err(1),RES1Err(2),RES2Err(2),RES3Err(2
),RES4Err(2),RES1Err(3),RES2Err(3),RES3Err(3),RES4Err(3), ...

RES1Err(4),RES2Err(4),RES3Err(4),RES4Err(4),RES1Err(5),RES2Err(5),RES3Err(5)
,RES4Err(5),RES1Err(6),RES2Err(6),RES3Err(6),RES4Err(6), ...

RES1Err(7),RES2Err(7),RES3Err(7),RES4Err(7),RES1Err(8),RES2Err(8),RES3Err(8)
,RES4Err(8),RES1Err(9),RES2Err(9),RES3Err(9),RES4Err(9),RES1Err(10),RES2Err(
10),RES3Err(10),RES4Err(10), ...

RES1Err(11),RES2Err(11),RES3Err(11),RES4Err(11),RES1Err(12),RES2Err(12),RE
S3Err(12),RES4Err(12),RES1Err(13),RES2Err(13),RES3Err(13),RES4Err(13), ...
```

```matlab
    RES1Err(14),RES2Err(14),RES3Err(14)]'.*Res;
ResErr = [Res,Err];
%%% Nuclide String
%%% Import data from text file.
% Script for importing data from the following text file:
%
%    /Users/kadelorm/Documents/Research/MCNPInputs/2.2313tallyVNat.txt
%
% To extend the code to different selected data or a different text file,
% generate a function instead of a script.

% Auto-generated by MATLAB on 2013/11/24 23:10:40

%%% Initialize variables.
delimiter = ' ';
startRow = 11;
endRow = 20;

%%% Format string for each line of text:
%   column1: double (%f)
%       column2: double (%f)
%   column3: double (%f)
%       column4: double (%f)
%   column5: double (%f)
%       column6: double (%f)
% For more information, see the TEXTSCAN documentation.
formatSpec =
'%f%f%f%f%f%f%*s%*s%*s%*s%*s%*s%*s%*s%*s%*s%*s%*s%*s%*s%*s%*s%*s
%*s%*s%*s%*s%*s%*s%*s%*s%*s%*s%*s%*s%*s%*s%*s%[^\n\r]';

%%% Open the text file.
fileID = fopen(filename,'r');

%%% Read columns of data according to format string.
% This call is based on the structure of the file used to generate this
% code. If an error occurs for a different file, try regenerating the code
% from the Import Tool.
dataArray = textscan(fileID, formatSpec, endRow-startRow+1, 'Delimiter', delimiter,
'MultipleDelimsAsOne', true, 'HeaderLines', startRow-1, 'ReturnOnError', false);

%%% Close the text file.
fclose(fileID);

%%% Post processing for unimportable data.
% No unimportable data rules were applied during the import, so no post
% processing code is included. To generate code which works for
```

```matlab
% unimportable data, select unimportable cells in a file and regenerate the
% script.

%% Allocate imported array to column variable names
VarName1 = dataArray{:, 1};
VarName2 = dataArray{:, 2};
VarName3 = dataArray{:, 3};
VarName4 = dataArray{:, 4};
VarName5 = dataArray{:, 5};
VarName6 = dataArray{:, 6};
Nuclides=[VarName1(1), VarName2(1), VarName3(1), VarName4(1), VarName5(1),
VarName6(1), ...
    VarName1(2), VarName2(2), VarName3(2), VarName4(2), VarName5(2),
VarName6(2), ...
    VarName1(3), VarName2(3), VarName3(3), VarName4(3), VarName5(3),
VarName6(3), ...
    VarName1(4), VarName2(4), VarName3(4), VarName4(4), VarName5(4),
VarName6(4), ...
    VarName1(5), VarName2(5), VarName3(5), VarName4(5), VarName5(5),
VarName6(5), ...
    VarName1(6), VarName2(6), VarName3(6), VarName4(6), VarName5(6),
VarName6(6), ...
    VarName1(7), VarName2(7), VarName3(7), VarName4(7), VarName5(7),
VarName6(7), ...
    VarName1(8), VarName2(8), VarName3(8), VarName4(8), VarName5(8),
VarName6(8), ...
    VarName1(9), VarName2(9), VarName3(9), VarName4(9), VarName5(9),
VarName6(9), ...
    VarName1(10)]';
%% Calcualte Cross Section
% Specify Sample
% n=1;
% %# ask for inputs
% tmp = input(sprintf('Select Sample: V-nat = 1; Ti-nat = 2; Ti-47 = 3; Ti-50 =4: ',n));
% %# if the user hits 'return' without writing anything, tmp is empty and the default
is used
% if ~isempty(tmp)
% n = tmp;
% if n ==1;
  rho = 6.0; %g/cm^3
   A = 50.9415;
% elseif n=1=2;
%   rho = 4.506; %g/cm&3
%   A = 47.867;
% elseif n ==3;
%    rho = 4.11;
```

```matlab
%    A = 47;
% elseif n == 4;
%    rho = 4.11;
%    A = 50;
% end
Avagadro = 6.0221413e+23; % atoms/mol
Volume = pi*((0.01)^2)*0.0133; % cm^3
GramsofTarget = Volume*rho; % g
Res2 = Res/Volume;% nuclide/cm^2
Err2 = Err/Volume;% nuclide/cm^2
NTarg = ((rho*Avagadro)/A); %atoms/cm^3
Flux = 10000000; % neutrons/cm^2
CrossSections = (Res2/(NTarg*Flux))*10^24; % barns
CSErr = (Err2/(NTarg*Flux))*10^24;
Table=[Nuclides/10000 Res Err CrossSections CSErr];
SF=5;
ProductTable=sortrows(Table);
% ProductTable2=spa_sf(ProductTable,SF);
% indices = find(ProductTable2(:,2)==0);
% ProductTable2(indices,:) = [];
%% Just ZAID & Cross Section
% Table2 = [Nuclides/10000 CrossSections CSErr];
% SF=5;
% ProductTable3=sortrows(Table2);
% ProductTable4=spa_sf(ProductTable3,SF);
% indices = find(ProductTable4(:,2)==0);
% ProductTable4(indices,:) = [];

%% Create Table For Displate
Titles = ['Nuclide(ZAID)|Tally|Error'];
%disptable(ProductTable2,'Nuclide(ZAID)|Tally|Tally Error|Cross
Section(barns)|CS Error',zeros(length(Nuclides),0))
%disptable(ProductTable4,'Nuclide(ZAID)|Cross Section(barns)|CS
Error',zeros(length(Nuclides),0))
NuclidesMade = ProductTable(:,1);
%% Clear temporary variables
clearvars filename delimiter startRow endRow formatSpec fileID dataArray ans;
%% Clear temporary variables
clearvars filename delimiter startRow endRow formatSpec fileID dataArray ans raw
col numericData rawData row regexstr result numbers invalidThousandsSeparator
thousandsRegExp me rawNumericColumns rawCellColumns R;
%% export to textfile
%# ask for output
fprintf('\n Nuclide    Tally    TallyError XSection    CSErr:\n');
for j=1:length(ProductTable(:,1))
```

```
fprintf('%8.4f %13.4e %13.4e %13.4e %13.4e \n',
ProductTable(j,1),ProductTable(j,2),ProductTable(j,3),ProductTable(j,4),
ProductTable(j,5));
end
% fileout = '2.2313tallyVNat.txt';
%  tmp = input(sprintf('Please give fileoutname: ',fileout));
% % %# if the user hits 'return' without writing anything, tmp is empty and the
default is used
%  if ~isempty(tmp)
%  fileout = tmp;
%  end
Table = table(ProductTable(:,1),
ProductTable(:,2),ProductTable(:,3),ProductTable(:,4),ProductTable(:,5))
writetable(Table, 'fileout.txt')
```

F. MATLAB Script: MCNP Instantaneous Production Rate Estimation

The following script was written to determine the estimated instantaneous production rate from the cross sections derived from the MCNP Ft8 Res tally and the CEM3.03 neutron flux characterization. outputs for each individual energy. Bash scripting was then used to run through each energy and extract the proper data in order to generate excitation functions. Further discussion of this script may be found in Chapter 3.

%% MCNP Yield and Activation Prediction
% K. Austin DeLorme
% December 2013
% Masters Thesis at AFIT in collaboration with Los Alamos Nation Labs and
% DTRA
%% Description of MCNP Cross Section Calculation
% MCNPX (and MCNP6) allow for the generation of double differentiable cross
% sections from a residual nuclide tally. The LCA card is a part of the specification
% of which physics model is to be used for calcuation. The 8th option to be
% specified on this card is NOACT. If set to -2, source particles
% immediately collide, and single interaction physics modeling will occur.
% Source particles will have a zero-distance to collision, and that of all
% subsequent particles will be infinity. When utilizing the FT8 Res tally,
% which provides a count of residual nuclides resulting from a specified
% irradiation, and by specifying a monoenergetic single particle source,
% cross section my be caluculated directly. (citation: MCNP Extensions:
% Version 2.5.0, Hendricks + multiple authors)

% A sample input file is shown below. This file will output the number of
% residual nuclei with Z numbers ranging from 19-23 resulting from the interaction
% of 10^7 neutrons with an energy of 50 MeV.
% Residual Nuclide File for Ti-47 Oxide
% 1 1 -10. -1 imp:n=1
% 2 0   1 imp:n=0
%
% c Surface
% 1 so .01
%
% c Material Cards
% m1   22046   0.0041
%   22047   0.9570
%   22048   0.0357
%   22049   0.0180
%   22050   0.0140
% mode n p
% PHYS:P 110 0 0 0 1 0 0
% PHYS:N 110 0 1 0
% c Physics Models
% LCA   2 1 1 23 1 1 0 -2 0
% c Source Information
% SDEF POS 0 0 0 DIR=-1 VEC=0 0 1 PAR=1 erg 50
% NPS 10000000
% c Tally
% f8:n 1
% ft8 res 19 23
% PRDMP 2j -1

%% Bash Script
% The input deck for each target material of interest must be run for the
% energy range of interest - the results for each individual nuclide may then
% be interpolated if desired.

% Sample Bash File:
% #!/bin/sh
% # Purpose: Runs MCNP6 F8 Res Tally for energies in k - renames output and
% Tally and saves them in appropriate directories
% #Author: K. Austin DeLorme
%
% mkdir Ti47Tally
% mkdir Ti47Outs
% export INP="Ti47Res.i"
%
% for k in 0.00000000001 0.000000005 0.00000001 0.000000015 0.00000002
0.000000025
%   0.00000003 0.000000035 0.000000042 0.00000005 0.000000058
0.000000067 0.00000008
%   0.0000001 0.000000152 0.000000251 0.000000414 0.000000683
0.000001125 0.000001855
%   0.000003059 0.000005043 0.000008315 0.00001371 0.00003727 0.00006144
0.0001013 0.000167
%   0.0002754 0.000454 0.0007485 0.001234 0.002035 0.002404 0.00284
0.04087 0.0673 0.1111
%   0.1832 0.302 0.3887 0.4979 0.63928 0.82085 1.108 1.3534 1.7377 2.2313
2.86510 3.6788
%   4.9658 6.065 10 14.918 16.905 20 22 24 26 28 30 32 34 36 38 40 42 44 46 48
50 52 54
%   56 58 60 62 64 66 68 70 72 74 76 78 80 82 84 86 88 90 92 94 96 98 100
% do sed "s/erg [^]*/erg $k/" $INP > temp
% rm $INP
% mv temp $INP
% mcnp6 i=$INP o=$k"MeV_out_Ti47"
% mv mctal $k"tallyTi47"
% mv $k"tallyTi47" Ti47Tally
% mv $k"MeV_out_Ti47" Ti47Outs
% rm runtpe
% done

%% Derive Cross Section
% From here a script was written in MATLAB to take the 'mctal' output and
% calculate the crosssection and associated error. The cross section
% outputs for each energy are then run through a script to exctract a particular
% residual nuclei at all energies and compile them into a file.

```matlab
%% Generate Neutron Flux
% An input deck created by J. Engle was modified to obtain the neutron flux
% in the location of the samples of interest. This input deck captures the
% character of the proton beam interacting with the RbCl Ga target stack
% and tally's the neutron flux by residual neutrons
%% CEM3.03
% In MCNP6 the CEM.03 model was developed. There are many physics models
% which may be used.  The CEM2k is ideal as it has been developed
% specifically to deal with the medium energy range between 20-400 MeV.
% Tabulated data from ENSDF can be used up to 20-25 MeV, and the Bertini
% and INCL models were intended to deal with high energies (above 400MeV)
%% Initialize
 clear all
 clc
%% Import Neutron flus and repeat steps above to put into column form:
Fluxdata =
xlsread('/Users/kadelorm/Documents/Research/Flux/IsotopeCrossSections.xlsx','
Flux');
FluxEnergy = Fluxdata(:,1);
NFlux = Fluxdata(:,2);
NFluxErr = Fluxdata(:,3);
%% Import Cross Section Data
format long
% Specify Sample
 n=1;
%# ask for inputs if used by hand vs scriped
 tmp = input(sprintf('Select Sample: V-nat = 1; Ti-nat = 2; Ti-47 = 3; Ti-50 =4: ',n));
% %# if the user hits 'return' without writing anything, tmp is empty and the default
is used
if ~isempty(tmp)
n = tmp;
end
if n ==1;
   VNat =
xlsread('/Users/kadelorm/Documents/Research/Flux/IsotopeCrossSections.xlsx','
VNat');
  CS = VNat(:,4);
  CSErr = VNat(:,5);
  Ti44CS = CS(1:93);
  Ti44CSErr = CSErr(1:93);
  Sc46CS = CS(94:186);
  Sc46CSErr = CSErr(94:186);
  Sc47CS = CS(187:279);
  Sc47CSErr = CSErr(187:279);
  Sc48CS = CS(280:372);
  Sc48CSErr = CSErr(280:372);
```

```matlab
    rho = 6.0; %g/cm^3
    A = 50.9415;
elseif n==2;
    TiNat =
xlsread('/Users/kadelorm/Documents/Research/Flux/IsotopeCrossSections.xlsx','
TiNat');
    CS = TiNat(:,4);
    CSErr = TiNat(:,5);
    Ti44CS = CS(1:93);
    Ti44CSErr = CSErr(1:93);
    Sc46CS = CS(94:186);
    Sc46CSErr = CSErr(94:186);
    Sc47CS = CS(187:279);
    Sc47CSErr = CSErr(187:279);
    Sc48CS = CS(280:372);
    Sc48CSErr = CSErr(280:372);
   rho = 4.506; %g/cm&3
   A = 47.867;
elseif n ==3;
    Ti47 =
xlsread('/Users/kadelorm/Documents/Research/Flux/IsotopeCrossSections.xlsx','
Ti47');
    CS = Ti47(:,4);
    CSErr = Ti47(:,5);
    Ti44CS = CS(1:93);
    Ti44CSErr = CSErr(1:93);
    Ca47CS = CS(94:186);
    Ca47CSErr = CSErr(94:186);
    Sc46CS = CS(187:279);
    Sc46CSErr = CSErr(187:279);
    Sc47CS = CS(280:372);
    Sc47CSErr = CSErr(280:372);
    Sc48CS = CS(373:465);
    Sc48CSErr = CSErr(373:465);
    rho = 4.23*.599408;
    A = 46.9518;
elseif n == 4;
    Ti50 =
xlsread('/Users/kadelorm/Documents/Research/Flux/IsotopeCrossSections.xlsx','
Ti50');
    CS = Ti50(:,4);
    CSErr = Ti50(:,5);
    Ti44CS = CS(1:93);
    Ti44CSErr = CSErr(1:93);
    Ca47CS = CS(94:186);
    Ca47CSErr = CSErr(94:186);
```

```matlab
    Sc46CS = CS(187:279);
    Sc46CSErr = CSErr(187:279);
    Sc47CS = CS(280:372);
    Sc47CSErr = CSErr(280:372);
    Sc48CS = CS(373:465);
    Sc48CSErr = CSErr(373:465);
    rho = 4.32*.599408;
    A = 49.9448;
end
%%% Ensure Data matches Energy
Interpdiv1 = (length(Sc47CS)-1)/(length(NFlux));
xi = 1:Interpdiv1: (length(Sc47CS))-2*Interpdiv1;
Interpdiv2 = (length(Sc46CS)-1)/(length(NFlux));
xi2 = 1:Interpdiv2: (length(Sc46CS))-2*Interpdiv2;
Interpdiv3 = (length(Sc48CS)-1)/(length(NFlux));
xi3 = 1:Interpdiv3: (length(Sc48CS))-2*Interpdiv3;
if n == 3 && 4;
Interpdiv4 = (length(Ca47CS)-1)/(length(NFlux));
xi4 = 1:Interpdiv4: (length(Ca47CS))-2*Interpdiv4;
end
Interpdiv5 = (length(Ti44CS)-1)/(length(NFlux));
xi5 = 1:Interpdiv5: (length(Ti44CS)) - 2*Interpdiv5;
Ti44CSi = [interp1(1:length(Ti44CS), Ti44CS, xi5)';Ti44CS(end)];
Ti44CSerri = [interp1(1:length(Ti44CSErr), Ti44CSErr, xi5)';Ti44CSErr(end)];
Sc47CSi = [interp1(1:length(Sc47CS), Sc47CS, xi)';Sc47CS(end)];
Sc47CSerri = [interp1(1:length(Sc47CSErr), Sc47CSErr, xi)';Sc47CSErr(end)];
Sc46CSi = [interp1(1:length(Sc46CS), Sc46CS, xi2)'; Sc46CS(end)];
Sc46CSerri = [interp1(1:length(Sc46CSErr), Sc46CSErr, xi2)';Sc46CSErr(end)];
Sc48CSi = [interp1(1:length(Sc48CS), Sc48CS, xi3)';Sc48CS(end)];
Sc48CSerri = [interp1(1:length(Sc48CSErr), Sc48CSErr, xi3)';Sc48CSErr(end)];
if n == 3 && 4;
Ca47CSi = [interp1(1:length(Ca47CS), Ca47CS, xi4)';Ca47CS(end)];
Ca47CSerri = [interp1(1:length(Ca47CSErr), Ca47CSErr, xi4)';Ca47CSErr(end)];
end
%%% Plot Cross Sections as a Function of Energy
hold off
figure1=figure;
axes1 = axes('Parent',figure1,'YScale','log','YMinorTick','on',...
    'FontSize',16);
box(axes1,'on');
hold(axes1,'all');

% Create title
if n==1;
title('Excitation function for ^{44}Ti Produced by Neutron Interaction with
^{nat}V',...
```

```matlab
    'FontSize',18);
elseif n==2;
title('Excitation function for ^{44}Ti Produced by Neutron Interaction with
^{nat}Ti',...
    'FontSize',18);
elseif n==3;
title('Excitation function for ^{44}Ti Produced by Neutron Interaction with ^{47}Ti
Oxide',...
    'FontSize',18);
elseif n==4;
title('Excitation function for ^{44}Ti Produced by Neutron Interaction with ^{50}Ti
Oxide',...
    'FontSize',18);
end
% Create xlabel
xlabel('Neutron Energy (MeV)','FontSize',18);

% Create ylabel
ylabel('Neutron Cross Section (barns)','FontSize',18);
semilogy([0;FluxEnergy], [0;Ti44CSi],'MarkerEdgeColor',[0 0
1],'LineWidth',3,'Color',[0 0 1])
%%
hold off
figure2=figure;
axes2 = axes('Parent',figure2,'YScale','log','YMinorTick','on',...
    'FontSize',16);
box(axes2,'on');
hold(axes2,'all');

% Create title
if n==1;
title('Excitation function for ^{47}Sc Produced by Neutron Interaction with
^{nat}V',...
    'FontSize',18);
elseif n==2;
title('Excitation function for ^{47}Sc Produced by Neutron Interaction with
^{nat}Ti',...
    'FontSize',18);
elseif n==3;
title('Excitation function for ^{47}Sc Produced by Neutron Interaction with ^{47}Ti
Oxide',...
    'FontSize',18);
elseif n==4;
title('Excitation function for ^{47}Sc Produced by Neutron Interaction with ^{50}Ti
Oxide',...
    'FontSize',18);
```

```matlab
end
% Create xlabel
xlabel('Neutron Energy (MeV)','FontSize',18);

% Create ylabel
ylabel('Neutron Cross Section (barns)','FontSize',18);
semilogy([0;FluxEnergy], [0;Sc47CSi],'LineWidth',3,'Color',[0 1 0])
%%
hold off
figure3=figure;
axes3 = axes('Parent',figure2,'YScale','log','YMinorTick','on',...
    'FontSize',16);
box(axes3,'on');
hold(axes3,'all');

% Create title
if n==1;
title('Excitation function for ^{46}Sc Produced by Neutron Interaction with
^{nat}V',...
    'FontSize',18);
elseif n==2;
title('Excitation function for ^{46}Sc Produced by Neutron Interaction with
^{nat}Ti',...
    'FontSize',18);
elseif n==3;
title('Excitation function for ^{46}Sc Produced by Neutron Interaction with ^{47}Ti
Oxide',...
    'FontSize',18);
elseif n==4;
title('Excitation function for ^{46}Sc Produced by Neutron Interaction with ^{50}Ti
Oxide',...
    'FontSize',18);
end
% Create xlabel
xlabel('Neutron Energy (MeV)','FontSize',18);

% Create ylabel
ylabel('Neutron Cross Section (barns)','FontSize',18);
semilogy([0;FluxEnergy], [0;Sc46CSi],'LineWidth',3,'Color',[1 1 0])
%%
hold off
figure4=figure;
axes4 = axes('Parent',figure4,'YScale','log','YMinorTick','on',...
    'FontSize',16);
box(axes4,'on');
hold(axes4,'all');
```

```matlab
% Create title
if n==1;
title('Excitation function for ^{48}Sc Produced by Neutron Interaction with
^{nat}V',...
    'FontSize',18);
elseif n==2;
title('Excitation function for ^{48}Sc Produced by Neutron Interaction with
^{nat}Ti',...
    'FontSize',18);
elseif n==3;
title('Excitation function for ^{48}Sc Produced by Neutron Interaction with ^{47}Ti
Oxide',...
    'FontSize',18);
elseif n==4;
title('Excitation function for ^{48}Sc Produced by Neutron Interaction with ^{50}Ti
Oxide',...
    'FontSize',18);
end
% Create xlabel
xlabel('Neutron Energy (MeV)','FontSize',18);

% Create ylabel
ylabel('Neutron Cross Section (barns)','FontSize',18);
semilogy([0;FluxEnergy],[0;Sc48CSi],'LineWidth',3,'Color',[1 0 1])
%% Calculating Production Rate from these values
%  The flux values are given per incident proton. Therefore, in order to
%  calculate production rate per second we must calculate the number of
%  incident protons per second based on the specs of the proton beam. The
%  proton beam runs at 220 uAh.
Avagadro = 6.0221413e+23;
NProtons = (220*10^-6)/(1.6*10^-19); % number of protons/s
NFlux2 = NFlux*NProtons;%Number of neutrons by energy / cm2
NFlux2err = NFluxErr*NProtons;
%  Figuring out Units:
%  leaving rho out gets me units of decays s^-1 g^-1
%  Dividing by Curies
Ti44ProdRate = (NFlux2.*Ti44CSi*Avagadro*10^-24)/(A*3.7*10^4);
Ti44PR = sum(Ti44ProdRate)
Sc46ProdRate = (NFlux2.*Sc46CSi*Avagadro*10^-24)/(A*3.7*10^4);
Sc46PR = sum(Sc46ProdRate)
Sc47ProdRate = (NFlux2.*Sc47CSi*Avagadro*10^-24)/(A*3.7*10^4);
Sc47PR = sum(Sc47ProdRate)
Sc48ProdRate = (NFlux2.*Sc48CSi*Avagadro*10^-24)/(A*3.7*10^4);
Sc48PR = sum(Sc48ProdRate)
% Error
```

```
Ti44ProdRateErr = (Ti44PR*sqrt(((NFluxErr./NFlux2).^2) +
((Ti44CSerri./Ti44CSi).^2))*((rho*A*Avagadro*10^-24))/(3.7*10^10));
Ti44PRErr = sum(Ti44ProdRateErr(isfinite(Ti44ProdRateErr(:, 1)),:))
Sc46ProdRateErr = (Sc46PR*sqrt(((NFluxErr./NFlux2).^2) +
((Sc46CSerri./Sc46CSi).^2))*((rho*A*Avagadro*10^-24))/(3.7*10^10));
Sc46PRErr = sum(Sc46ProdRateErr(isfinite(Sc46ProdRateErr(:, 1)),:))
Sc47ProdRateErr = (Sc47PR*sqrt(((NFluxErr./NFlux2).^2) +
((Sc47CSerri./Sc47CSi).^2))*((rho*A*Avagadro*10^-24))/(3.7*10^10));
Sc47PRErr = sum(Sc47ProdRateErr(isfinite(Sc47ProdRateErr(:, 1)),:))
Sc48ProdRateErr = (Sc48PR*sqrt(((NFluxErr./NFlux2).^2) +
((Sc48CSerri./Sc48CSi).^2))*((rho*A*Avagadro*10^-24))/(3.7*10^10));
Sc48PRErr = sum(Sc48ProdRateErr(isfinite(Sc48ProdRateErr(:, 1)),:))
if n == 3 && 4;
Ca47ProdRate = (NFlux2.*Ca47CSi*rho*A*Avagadro*10^-24)/(3.7*10^10);
Ca47PR = sum(Ca47ProdRate)
end
```

G. Foil Measurements

The following data are measurements taken at Los Alamos for additional foil samples prepared for irradiation. Measurements and information regarding the foil samples used in the experiment may be found in Chapter 4.

	Sample 2		
	Dia. (mm)	*Thick. (mm)*	*Mass (g)*
	10.30	0.138	0.0515
	10.35	0.140	0.0514
	10.32	0.136	0.0541
			0.0514
			0.0514
Average	10.323	0.138	0.05142
Std Dev	0.02517	0.00200	0.00004
Error	0.01453	0.00115	0.00002
	Sample 3		
	Dia. (mm)	*Thick. (mm)*	*Mass (g)*
	10.34	0.136	0.0508
	10.34	0.135	0.0510
	10.36	0.144	0.0509
			0.0509
			0.0509
Average	10.346	0.138	0.0509
Std Dev	0.01155	0.00493	0.00007
Error	0.00667	0.00285	0.00003
	Sample 4		
	Dia. (mm)	*Thick. (mm)*	*Mass (g)*
	10.30	0.138	0.0515
	10.36	0.140	0.0514
	10.37	0.136	0.0541
			0.0514
			0.0514
Average	10.343	0.137	0.05116
Std Dev	0.03786	0.00173	0.00005
Error	0.02186	0.00100	0.00002

Table 22. Ti Foil measurements taken on 18 Sept 13.

Sample 2			
	Dia. (mm)	*Thick. (mm)*	*Mass (g)*
	10.25	0.139	0.0704
	10.36	0.139	0.0706
	10.3	0.136	0.0706
			0.0707
			0.0705
Average	10.30333	0.13800	0.07056
Std Dev	0.05508	0.00173	0.00011
Error	0.03180	0.00100	0.00005
Sample 3			
	Dia. (mm)	*Thick. (mm)*	*Mass (g)*
	10.35	0.143	0.0697
	10.27	0.140	0.0700
	10.26	0.139	0.0698
			0.0699
			0.0698
Average	10.29333	0.14067	0.06984
Std Dev	0.04933	0.00208	0.00011
Error	0.02848	0.00120	0.00005
Sample 4			
	Dia. (mm)	*Thick. (mm)*	*Mass (g)*
	10.29	0.140	0.0703
	10.35	0.137	0.0703
	10.32	0.141	0.0703
			0.0704
			0.0704
Average	10.32000	0.13933	0.07034
Std Dev	0.03000	0.00208	0.00005
Error	0.01732	0.00120	0.00002

Table 23. Vanadium Foil measurements taken on 18 Sept 13.

155

H. MATLAB Script: Weighted Nonlinear Model

The following is the MATLAB script generated to perform weighted non-linear fits on the data extracted from unisampo and discussed in Chapter 5.

```matlab
%% Decay Fitting Tool
% K. AUSTIN DELROME
% October 2013
clear all
clc
%% Use Import Function
FileNAME='/Users/kadelorm/Documents/Research/TxtFiles/VNat_Sc47_159.txt';
%# ask for inputs
tmp = input(sprintf('Please give file name - if in a differnt path, input entire path:
',FileNAME));
%# if the user hits 'return' without writing anything, tmp is empty and the default is
used
if ~isempty(tmp)
FileNAME = tmp;
end
[DeltaT,CountLength, PkGamma, Efficiency, PercentError] =
ImportScriptSolution(FileNAME);
%% Input Information about Isotope
% This part of the script will default to information aobut the 159.9 Sc-47
% Peak. It allows the input of the Isotope, HalfLife, Energy Peak, and
% Intensity of that peak.

% Specify Isotope investigated
m=1;
%# ask for inputs
tmp = input(sprintf('Select Isotope: Sc47 = 1; Sc48 = 2; Sc46 = 3; Ca47 =4: ',m));
%# if the user hits 'return' without writing anything, tmp is empty and the default is
used
if ~isempty(tmp)
m = tmp;
if m ==1;
   Isotope = 'Sc47'
elseif m==2;
   Isotope = 'Sc48'
elseif m ==3;
   Isotope = 'Sc46'
elseif m == 4;
   Isotope = 'Ca47'
end
end

% Specify Sample
n=1;
%# ask for inputs
tmp = input(sprintf('Select Sample: V-nat = 1; Ti-nat = 2; Ti-47 = 3; Ti-50 =4: ',n));
```

```matlab
%# if the user hits 'return' without writing anything, tmp is empty and the default is
used
if ~isempty(tmp)
n = tmp;
if n ==1;
   Sample = 'V-nat Foil Sample'
elseif n==2;
   Sample = 'Ti-nat Foil Sample'
elseif n ==3;
   Sample = 'Ti-47 Oxide Sample'
elseif n == 4;
   Sample = 'Ti-50 Oxide Sample'
end
end

% Specify Data Analysis Tool Selected
o=1;
%# ask for inputs
tmp = input(sprintf('Select Data Analysis Tool: Unisampo = 1; RayGun = 2; SPECANL
= 3: ',o));
%# if the user hits 'return' without writing anything, tmp is empty and the default is
used
if ~isempty(tmp)
o = tmp;
if o ==1;
   DatString = 'UNISAMPO Data'
elseif o==2;
   DatString = 'RAYGUN Data'
elseif o ==3;
   DatString = 'SPECANL Data'
end
end
% HalfLife=3.3492;
% %# ask for inputs
% tmp = input(sprintf('Give Half-Life in Days',HalfLife));
% %# if the user hits 'return' without writing anything, tmp is empty and the default
is used
% if ~isempty(tmp)
% HalfLife = tmp;
% end
Sc47 = strcmp(Isotope,'Sc47');
Sc46 = strcmp(Isotope,'Sc46');
Sc48 = strcmp(Isotope,'Sc48');
Ca47 = strcmp(Isotope,'Ca47');
if Sc47==1;
   display(Isotope)
```

```
    HalfLife = 3.3492
    PkEnergy = 159.9
    PkIntensity = .68
elseif Sc46 == 1;
    display(Isotope)
    HalfLife = 83.79
    PkEnergy= 889;
    %# ask for inputs
    tmp = input(sprintf('Give Peak Energy in keV (889 keV or 1120 keV):
',PkEnergy));
    %# if the user hits 'return' without writing anything, tmp is empty and the default
is used
    if ~isempty(tmp)
    PkEnergy = tmp;
    end
    display(PkEnergy)
    PkIntensity = .9998
elseif Sc48 == 1;
    display(Isotope)
    HalfLife = 1.8196
    PkEnergy= 983;
    %# ask for inputs
    tmp = input(sprintf('Give Peak Energy in keV (983 keV or 1312 keV)',PkEnergy));
    %# if the user hits 'return' without writing anything, tmp is empty and the default
is used
    if ~isempty(tmp)
    PkEnergy = tmp;
    end
    display(PkEnergy)
    PkIntensity = 1.001
    if PkEnergy == 983;
        PkIntensityV = .998;
    elseif PkEnergy == 1312;
        PkIntensityV = .982;
    end
elseif Ca47 == 1;
    display(Isotope)
    HalfLife = 4.536
    PkEnergy = 1297
    PkIntensity = .67
end

%% Calculate Decay Constant
% Calculates the decay constant for the specified isotope based on the
% half-life input
```

```matlab
Lambda = log(2)/HalfLife;
%% Calculate Initial Conditions
% Back out the activity at EOB - Currently this is done by simply looking
% at the first count value - a least squares method is being investigated

% Activity converstion - 1 Curie = =3.7*(10^10)decays/second
% Converstion is made to gammas/min
Activity_Conversion = 3.7*60*(10^10);

% Select Peak Gamma from first count-convert units based on count length
% and use decay curve for specified isotope to determine EOB activity
N_GammasperMin = PkGamma./(PkIntensity); % Gamma/min
display('Initial_N in Gammas/min:')
Initial_N = N_GammasperMin.*exp(Lambda*DeltaT)
display('Initial_Activity in Curies:')
Initial_Activity = Initial_N/Activity_Conversion
%% Least Squares
xdata = DeltaT;
ydata = PkGamma;
%Weight = PkGamma.*CountLength/20;
Weight = PercentError;
 xdat2 = [0 xdata' 16]';
if Sc47 == 1;
   FitStr = 'a*exp(-0.2070*x)'
   display('54540*(0.1528/(.2070-.1528))*exp(-.1528*x)+(a+54540*(.1528/(.1528-
.2070)))*exp(-.2070*x)');
   %# ask for inputs
   tmp = input(sprintf('To include Ca-47 enter in form above inserting a value for
N0_Ca....: ',FitStr));
   %# if the user hits 'return' without writing anything, tmp is empty and the default
is used
   if ~isempty(tmp)
   FitStr = tmp;
   end
   f = fittype(FitStr);
   fit1 = fit(xdata,ydata,f, 'StartPoint', [1000000])
   Coeffs = coeffvalues(fit1);
   N_0_Sc47 = Coeffs(1);
   Activity_Sc47 = (N_0_Sc47/(PkIntensity))/Activity_Conversion
elseif Sc46 == 1;
   FitStr = 'a*exp(-0.0083*x)';
   f  = fittype(FitStr);
   fit1 = fit(xdata,ydata,f, 'StartPoint', [2051000])
   Coeffs = coeffvalues(fit1);
   N_0_Sc46 = Coeffs(1);
   Activity_Sc46 = (N_0_Sc46/(PkIntensity))/Activity_Conversion
```

```matlab
elseif Sc48 == 1;
   if n == 1;
   FitStr='a*exp(-0.3809*x)';
   DEL = sum(Weight)*sum(Weight.*xdata.^2)-(sum(Weight.*xdata))^2;
   N0= exp((sum(Weight.*xdata.^2)*sum(Weight.*ydata)-
sum(Weight.*xdata)*sum(Weight.*ydata))/DEL)
   Error_N0 = N0*sqrt(sum(Weight.*xdata.^2)/DEL)
   fit1 = N0*exp(-Lambda*xdat2);
   Activity_Sc48 = (N0/(PkIntensity))/Activity_Conversion
   end
elseif Ca47 == 1;
   DEL = sum(Weight)*sum(Weight.*xdata.^2)-(sum(Weight.*xdata))^2;
   N0= (sum(Weight.*xdata.^2)*sum(Weight.*ydata)-
sum(Weight.*xdata)*sum(Weight.*ydata))/DEL
   Error_N0 = sqrt(sum(Weight.*xdata.^2)/DEL)
   fit1 = N0*exp(-Lambda*xdat2);
end

%% 95 Percent Confidence Interval Inital Concentration Values
   Upper95Percent = N0+2*Error_N0;
   Lower95Percent = N0-2*Error_N0;
   if Sc47 == 1;
   UpConf = 54540*(0.1528/(.2070-.1528))*exp(-
.1528*xdat2)+(Upper95Percent+54540*(.1528/(.1528-.2070)))*exp(-.2070*xdat2);
   display('Ca47(0)*(0.1528/(.2070-.1528))*exp(-
.1528*xdat2)+(Upper95Percent+Ca47(0)*(.1528/(.1528-.2070)))*exp(-
.2070*xdat2)')
   %# ask for inputs
   tmp = input(sprintf('To include Ca-47 enter in form above inserting a value for
Ca47(0)....: ',UpConf));
   %# if the user hits 'return' without writing anything, tmp is empty and the default
is used
   if ~isempty(tmp)
   UpConf = tmp;
   end
   LowConf = 54540*(0.1528/(.2070-.1528))*exp(-
.1528*xdat2)+(Lower95Percent+54540*(.1528/(.1528-.2070)))*exp(-
.2070*xdat2);
   display('Ca47(0)*(0.1528/(.2070-.1528))*exp(-
.1528*xdat2)+(Lower95Percent+Ca47(0)*(.1528/(.1528-.2070)))*exp(-
.2070*xdat2)')
   %# ask for inputs
   tmp = input(sprintf('To include Ca-47 enter in form above inserting a value for
Ca47(0)....: ',LowConf));
   %# if the user hits 'return' without writing anything, tmp is empty and the default
is used
```

```matlab
      if ~isempty(tmp)
      LowConf = tmp;
      end
    elseif Sc46 == 1;
       UpConf = Upper95Percent*exp(-0.0083*xdat2);
       LowConf = Lower95Percent*exp(-0.0083*xdat2);
    elseif Sc48 == 1;
       UpConf = Upper95Percent*exp(-0.3809*xdat2);
       LowConf = Lower95Percent*exp(-0.3809*xdat2);
       end
    elseif Ca47 == 1;
       UpConf = Upper95Percent*exp(-0.1528*xdat2);
       LowConf = Lower95Percent*exp(-0.1528*xdat2);
    end
%% Plots Data against Fit
% Create figure
figure1 = figure;

% Create axes
axes1 = axes('Parent',figure1,'YScale','log','YMinorTick','on',...
    'FontSize',12,...
    'FontName','Arial');
box(axes1,'on');
hold(axes1,'all');

% Create title
if Sc47 == 1;
   PTitle = 'Decay Fit for Sc47 (159 keV Peak)';
elseif Sc46 == 1;
    if PkEnergy==889;
   PTitle = 'Decay Fit for Sc46 (889 keV Peak)';
    else
   PTitle = 'Decay Fit for Sc46 (1120  keV Peak)';
    end
elseif Sc48 == 1;
    if PkEnergy == 983;
   PTitle = 'Decay Fit for Sc48 (983 keV Peak)';
    else
   PTitle = 'Decay Fit for Sc48 (1312 keV Peak)';
    end
elseif Ca47 == 1;
   PTitle = 'Decay Fit for Ca47 (1297 keV Peak)';
end
title(PTitle,'FontSize',20);
% Generate and Plot Error
% Note: Error is given is statistical and given in the UNISAMPO detection
```

```matlab
Error = 2*PercentError.*PkGamma*.01;
errorbar(DeltaT,PkGamma, Error, '.','DisplayName',DatString)
% Plot Fit
plot(xdat2,fit1,'r-')
% Plot Confidences
semilogy(xdat2,UpConf,'--','DisplayName','Upper 95% Confidence')
semilogy(xdat2,LowConf,'g--','DisplayName','Lower 95% Confidence')

% Create xlabel
xlabel('Time (Days)','FontSize',20);

% Create ylabel
ylabel('Activity (Gammas/Min)','FontSize',20);

% Create legend
legend(axes1,'show');

% % Create textbox
% annotation(figure1,'textbox',...
%     [0.359532451177487 0.861212981584445 0.282833436030216
0.0379746835442958],...
%     'String',Sample,...
%     'HorizontalAlignment','center',...
%     'FontSize',20,...
%     'FitBoxToText','off',...
%     'LineStyle','none');
%
% % Create textbox
% if Sc47 == 1;
%     FitString1 = '    NSc47(t) = NCa47(0)*(LamdaCa47/(LambdaSc47-
LambdaCa47))*exp(-
LambdaCa47*x)+(NSc47(0)+NCa47(0)*(LambdaCa47/(LambdaCa47-
LambdaSc47)))*exp(-LambdaSc47*x)';
%     FitString2 = N_0_Sc47;
%     FitString3 = Activity_Sc47;
% elseif Sc46 == 1;
%     FitString1 = '    N(t) = NSc47(0)*exp(-LambdaSc46*t)';
%     FitString2 = N_0_Sc46;
%     FitString3 = Activity_Sc46;
% elseif Sc48 == 1;
%     if n==or(1,3);
%     FitString1 = '    N(t) = NSc48(0)*exp(-LambdaSc48*t)+NV48(0)*exp(-
LambdaV48*t)';
%     else
%     FitString1 = '    N(t) = NSc48(0)*exp(-LambdaSc48*t)';
%     end
```

```matlab
%    FitString2 = N_0_Sc48;
%    FitString3 = Activity_Sc48;
% elseif Ca47 == 1;
%    FitString1 = '    N(t) = NCa47(0)*exp(-LambdaSc47*t)';
%    FitString2 = N_0_Ca47;
%    FitString3 = Activity_Ca47;
% end
% if Sc47 ==1;
%    annotation(figure1,'textbox',...
%    [0.143910972652335 0.0665362035225049 0.776992982149925
0.309810920316418],...
%    'String',{'General Model:','NSc47(t) = NCa47(0)*(LamdaCa47/(LambdaSc47-
LambdaCa47))*exp(-LambdaCa47*x)','
+(NSc47(0)+NCa47(0)*(LambdaCa47/(LambdaCa47-LambdaSc47)))*exp(-
LambdaSc47*x)','Concentration at EOB:','9.50306e+06','Activity at EOB
(Curries):','6.29508e-06'},...
%    'FontSize',14,...
%    'FitBoxToText','off',...
%    'LineStyle','none');
% else
%    annotation(figure1,'textbox',...
%    [0.148430746663634 0.230633802816902 0.401851739212072
0.202464788732394],...
%    'String',{'General Model:',FitString1,'Concentration at EOB:',
FitString2,'Activity at EOB (Curries):',    FitString3},...
%    'FontSize',20,...
%    'FitBoxToText','off',...
%    'LineStyle','none');
% end
```

I. ^{47}Ca Weighted Nonlinear Fits

The following plots are the weighted nonlinear fits generated for the 1297 keV ^{47}Ca peak, generated using the script in Appendix H.
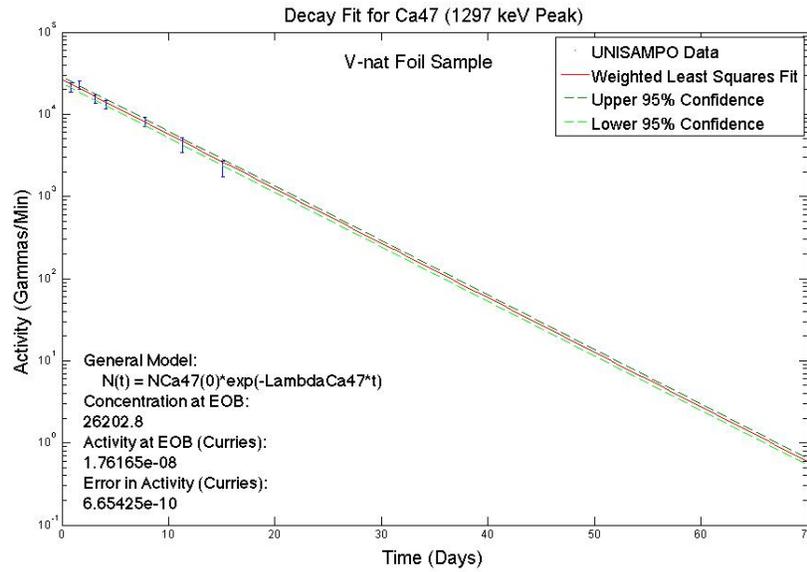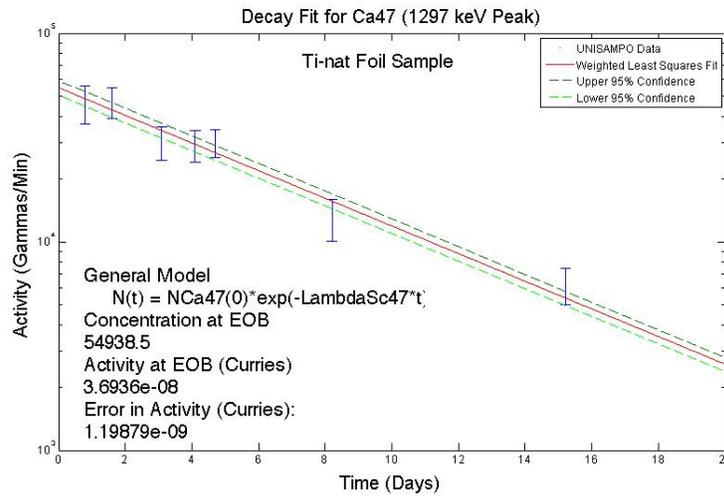

Figure 46. This figure, generated in MATLAB from the peak fitting data extracted by the UNISAMPO data analysis tool shows a weighted nonlinear model fit of the 1297 keV peak of ^{47}Ca within the ^{nat}V sample. It is plotted with **95%** confidence bounds determined by error propagated throughout the fitting process.
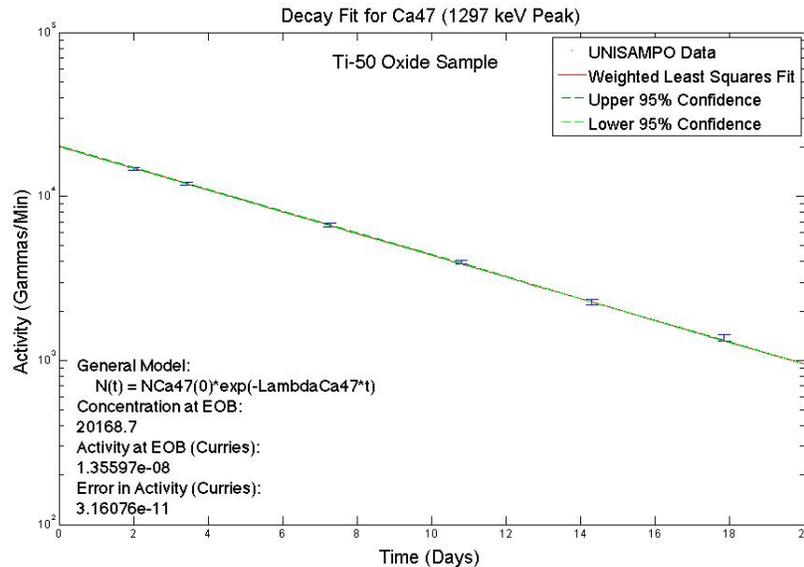
Figure 47. This figure, generated in MATLAB from the peak fitting data extracted by the UNISAMPO data analysis tool shows a weighted nonlinear model fit of the 1297 keV peak of ^{47}Ca within the ^{nat}Ti sample. It is plotted with 95% confidence bounds determined by error propagated throughout the fitting process.
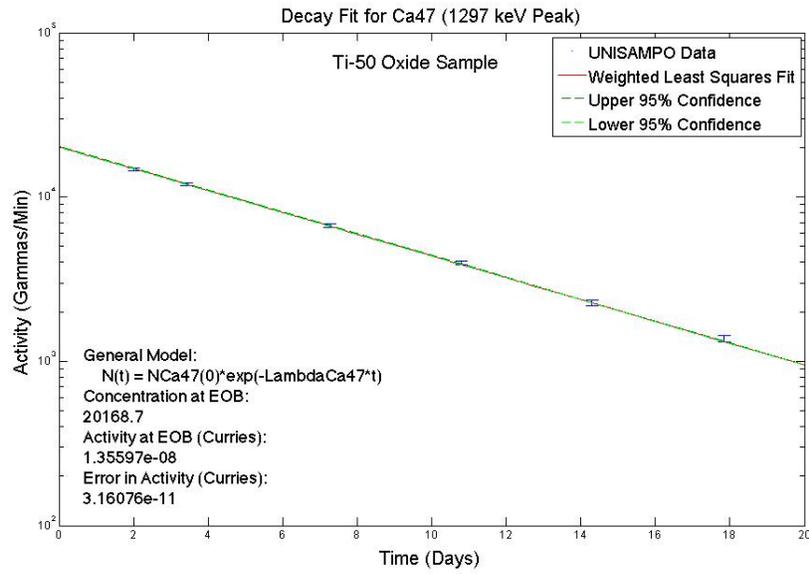

Figure 48. This figure, generated in MATLAB from the peak fitting data extracted by the UNISAMPO data analysis tool shows a weighted nonlinear model fit of the 1297 keV peak of ^{47}Ca within the ^{47}Ti sample. It is plotted with 95% confidence bounds determined by error propagated throughout the fitting process.

Figure 49. This figure, generated in MATLAB from the peak fitting data extracted by the UNISAMPO data analysis tool shows a weighted nonlinear model fit of the 1297 keV peak of ^{47}Ca within the ^{50}Ti sample. It is plotted with 95% confidence bounds determined by error propagated throughout the fitting process.

J. ^{48}Sc Weighted Nonlinear Fits for 983 keV Peak

The following plots are the weighted nonlinear fits generated for the 983 keV ^{48}Sc peak, generated using the script in Appendix H.
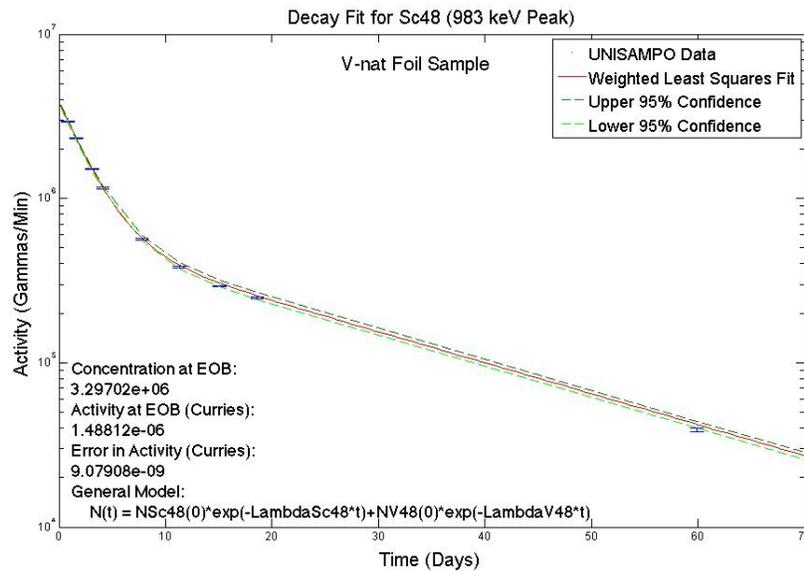

Figure 50. This figure, generated in MATLAB from the peak fitting data extracted by the UNISAMPO data analysis tool shows a weighted nonlinear model fit of the 983 keV peak of ^{48}Sc within the ^{nat}V sample. It is plotted with 95% confidence bounds determined by error propagated throughout the fitting process.
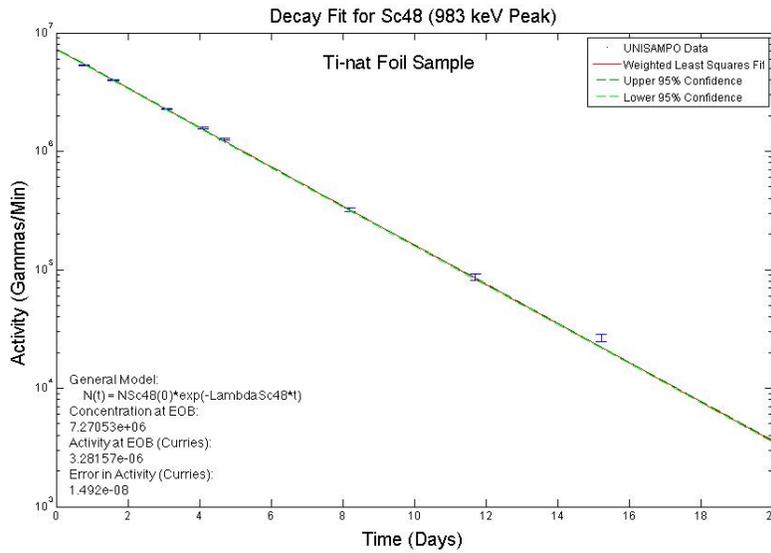
Figure 51. This figure, generated in MATLAB from the peak fitting data extracted by the UNISAMPO data analysis tool shows a weighted nonlinear model fit of the 983 keV peak of ^{48}Sc within the ^{nat}Ti sample. It is plotted with 95% confidence bounds determined by error propagated throughout the fitting process.

Figure 52. This figure, generated in MATLAB from the peak fitting data extracted by the UNISAMPO data analysis tool shows a weighted nonlinear model fit of the 983 keV peak of ^{48}Sc within the ^{47}Ti sample. It is plotted with 95% confidence bounds determined by error propagated throughout the fitting process.
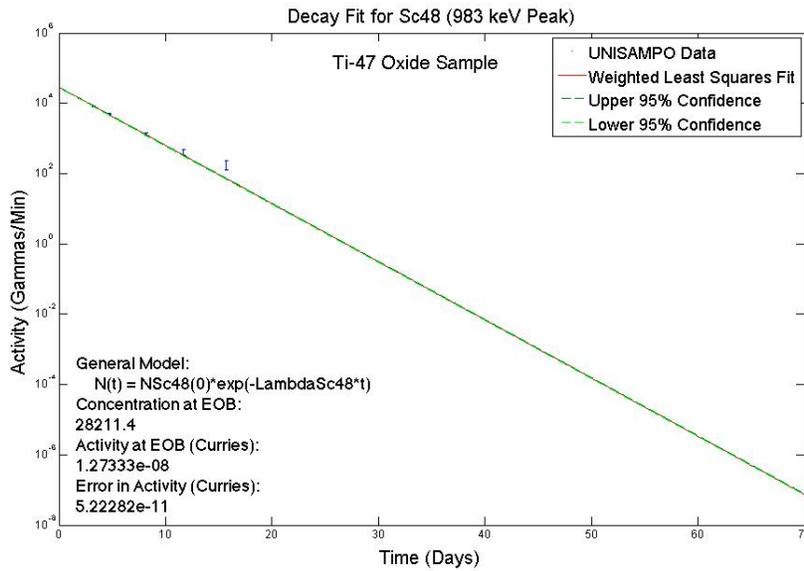
Figure 53. This figure, generated in MATLAB from the peak fitting data extracted by the UNISAMPO data analysis tool shows a weighted nonlinear model fit of the 983 keV peak of ^{48}Sc within the ^{50}Ti sample. It is plotted with 95% confidence bounds determined by error propagated throughout the fitting process.

K. ^{46}Sc Weighted Nonlinear Fits

The following plots are the weighted nonlinear fits generated for both the 889 and 1120 keV ^{46}Sc peaks, generated using the script in Appendix H.
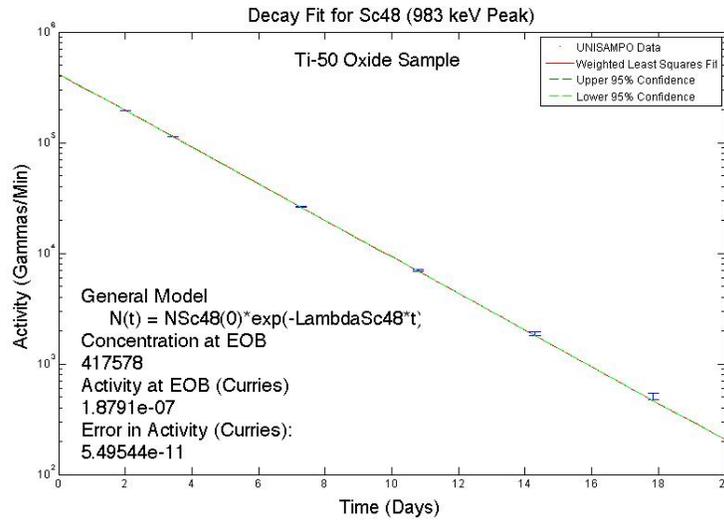

Figure 54. This figure, generated in MATLAB from the peak fitting data extracted by the UNISAMPO data analysis tool shows a weighted nonlinear model fit of the 1120 keV peak of ^{46}Sc within the ^{nat}V sample. It is plotted with 95% confidence bounds determined by error propagated throughout the fitting process.

Figure 55. This figure, generated in MATLAB from the peak fitting data extracted by the UNISAMPO data analysis tool shows a weighted nonlinear model fit of the 1120 keV peak of ^{46}Sc within the ^{nat}Ti sample. It is plotted with 95% confidence bounds determined by error propagated throughout the fitting process.
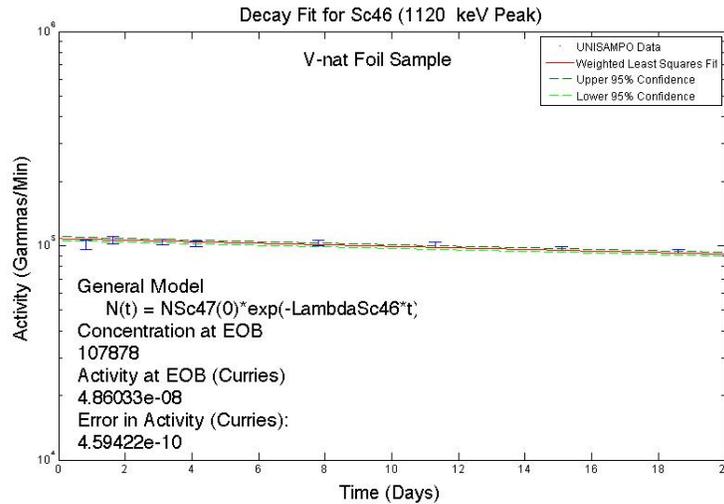

Figure 56. This figure, generated in MATLAB from the peak fitting data extracted by the UNISAMPO data analysis tool shows a weighted nonlinear model fit of the 1120 keV peak of ^{46}Sc within the ^{47}Ti sample. It is plotted with 95% confidence bounds determined by error propagated throughout the fitting process.

172

Figure 57. This figure, generated in MATLAB from the peak fitting data extracted by the UNISAMPO data analysis tool shows a weighted nonlinear model fit of the 1120 keV peak of [46]Sc within the [50]Ti sample. It is plotted with 95% confidence bounds determined by error propagated throughout the fitting process.
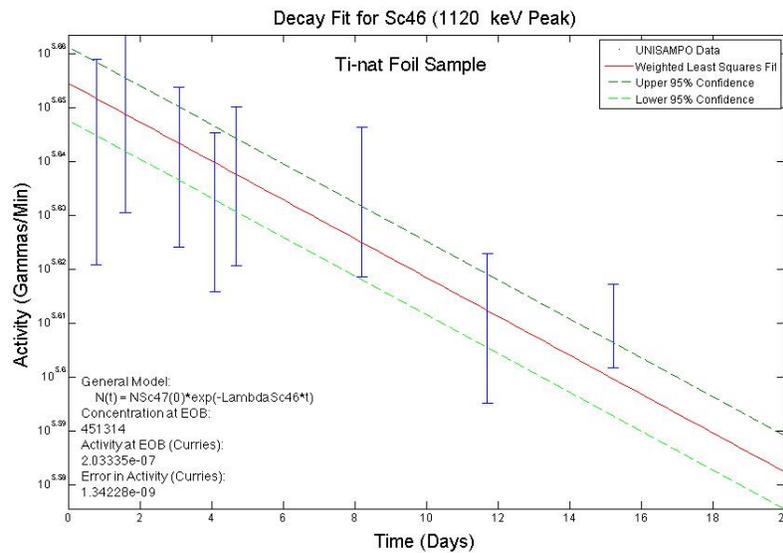

Figure 58. This figure, generated in MATLAB from the peak fitting data extracted by the UNISAMPO data analysis tool shows a weighted nonlinear model fit of the 889 keV peak of [46]Sc within the [nat]V sample. It is plotted with 95% confidence bounds determined by error propagated throughout the fitting process.
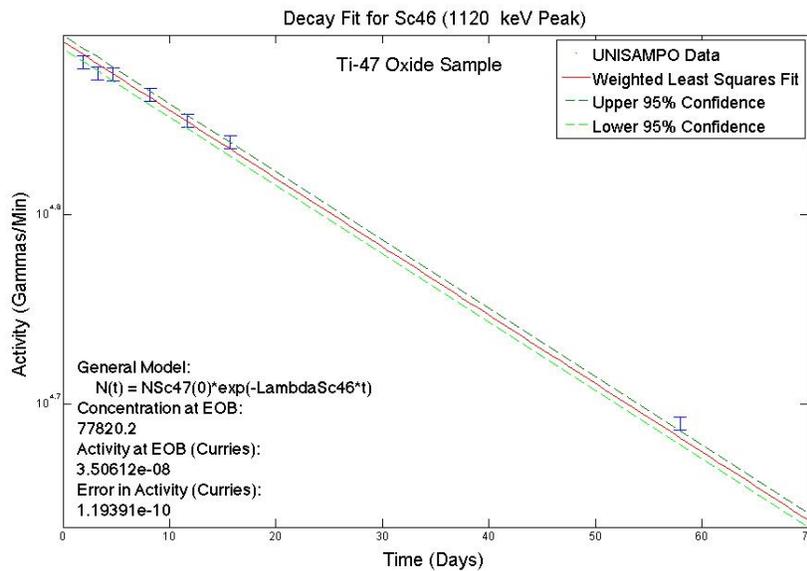
173

Figure 59. This figure, generated in MATLAB from the peak fitting data extracted by the UNISAMPO data analysis tool shows a weighted nonlinear model fit of the 889 keV peak of ^{46}Sc within the ^{nat}Ti sample. It is plotted with 95% confidence bounds determined by error propagated throughout the fitting process.
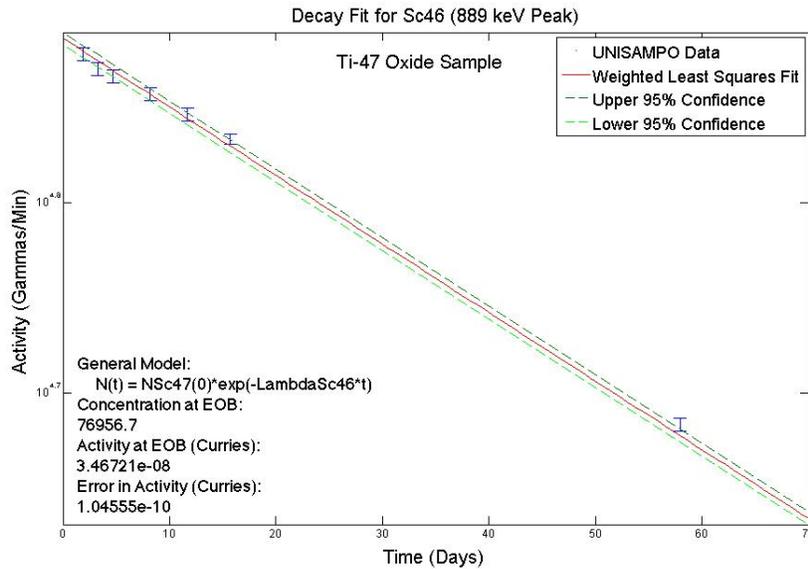
Figure 60. This figure, generated in MATLAB from the peak fitting data extracted by the UNISAMPO data analysis tool shows a weighted nonlinear model fit of the 889 keV peak of ^{46}Sc within the ^{47}Ti sample. It is plotted with 95% confidence bounds determined by error propagated throughout the fitting process.
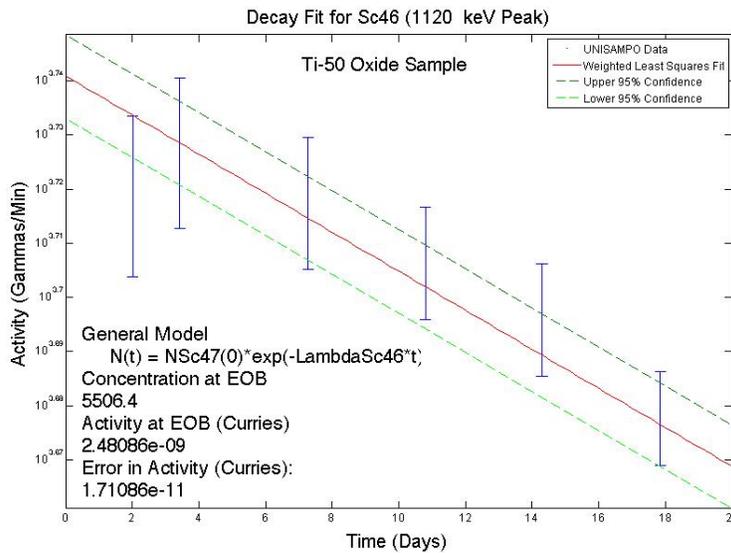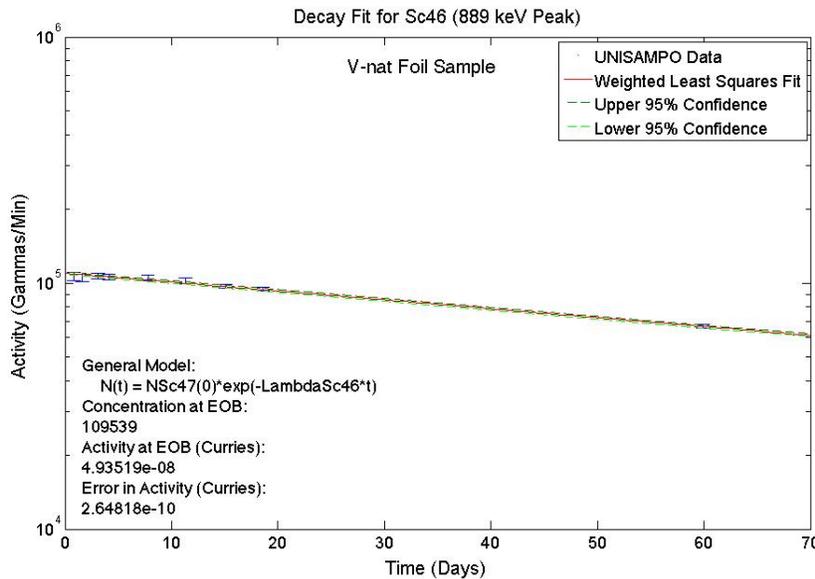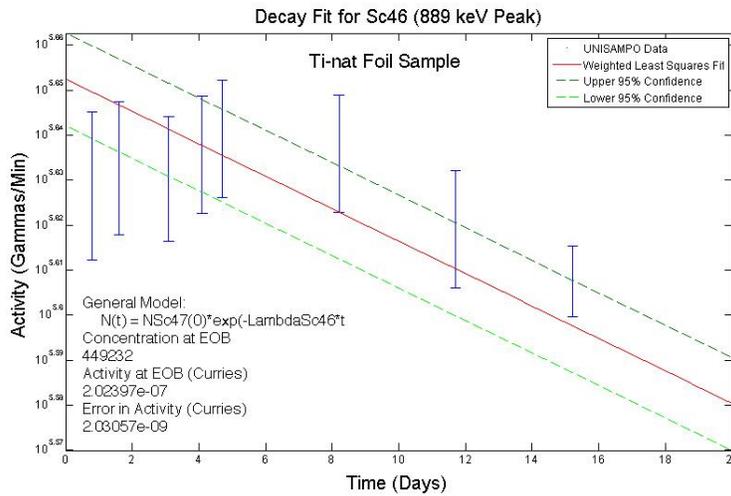
174
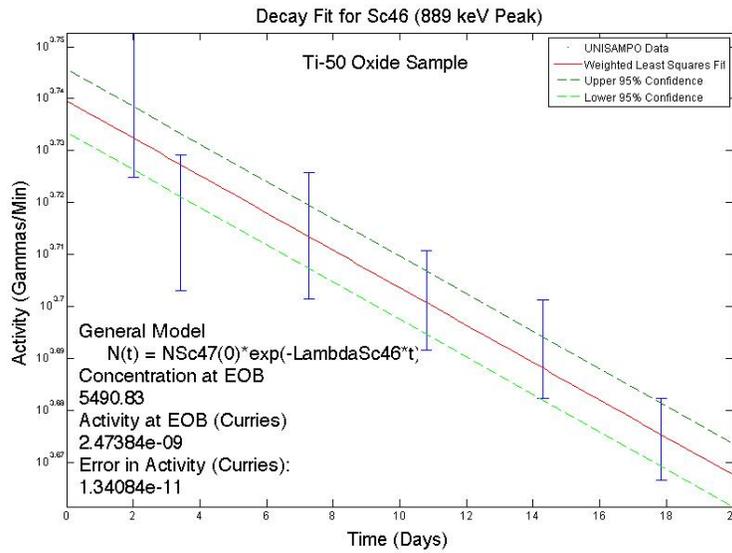
Figure 61. This figure, generated in MATLAB from the peak fitting data extracted by the UNISAMPO data analysis tool shows a weighted nonlinear model fit of the 889 keV peak of ^{46}Sc within the ^{50}Ti sample. It is plotted with 95% confidence bounds determined by error propagated throughout the fitting process.

175

L. MATLAB Script: Peak Fitting and Anylisis of Counter 77 Spectra

The following script was generated to perform a gamma spectrum peak analysis on the data collected using Counter 77 in the hot cells room at the Los Alamos. The first removes the background from raw spectra, then applies a medium filter to remove any contaminating electrons. It then attempts to perform a Gaussian fit to the data and plots the fit along with the residual plot associated. It then prompts the user to accept this fit or to go back to the original background omitted peak and to determine upper and lower bounds and a cutoff value based on visual investigation. From there counts are converted into activity values and output into a table. Further discussion of this process can be found in Chapter 5.

176

```matlab
%%% Import data from text file.
% Script for importing data from the following text file:
%
%    /Users/kadelorm/Documents/Research/AustinSc47/Ti_50_sol1.Txt
%
% To extend the code to different selected data or a different text file,
% generate a function instead of a script.

% Auto-generated by MATLAB on 2013/12/17 12:38:47

%%% Initialize variables.
filename = '/Users/kadelorm/Documents/Research/AustinSc47/Ti_50_sol1.Txt';
%# ask for inputs
tmp = input(sprintf('Please give file name - if in a differnt path, input entire path: ',filename));
%# if the user hits 'return' without writing anything, tmp is empty and the default is used
if ~isempty(tmp)
filename = tmp;
end
delimiter = ' ';
startRow = 13;
endRow = 4108;

%%% Format string for each line of text:
%   column1: double (%f)
% For more information, see the TEXTSCAN documentation.
formatSpec = '%f%*s%*s%*s%*s%*s%*s%*s%*s%*s%[^\n\r]';

%%% Open the text file.
fileID = fopen(filename,'r');

%%% Read columns of data according to format string.
% This call is based on the structure of the file used to generate this
% code. If an error occurs for a different file, try regenerating the code
% from the Import Tool.
dataArray = textscan(fileID, formatSpec, endRow-startRow+1, 'Delimiter', delimiter, 'MultipleDelimsAsOne', true, 'EmptyValue' ,NaN,'HeaderLines', startRow-1, 'ReturnOnError', false);
%%% Post processing for unimportable data.
% No unimportable data rules were applied during the import, so no post
% processing code is included. To generate code which works for
% unimportable data, select unimportable cells in a file and regenerate the
% script.
%%% Close the text file.
fclose(fileID);
```

```matlab
Ti502 = strcmp(filename,'Ti_50_sol1.Txt');
Ti504 = strcmp(filename,'Ti50_Transfer_Vile.txt');
Ti501 = strcmp(filename,'Ti50_Lvile.txt');
Ti503 = strcmp(filename,'Ti50_disVileQz.txt');
Ti505 = strcmp(filename,'Ti50_Cout_Vile_5mL.txt');

Ti473 = strcmp(filename,'Ti47_Transfer_Vile.txt');
Ti471 = strcmp(filename,'Ti47_Lvile.txt');
Ti472 = strcmp(filename,'Ti47_disVileQZ.txt');
Ti474 = strcmp(filename,'Ti47_Count_Vile_5mL.txt');
%%% Input Time Data
% Note: Time is converted to Zulu Julian calendar date to match EOB
% recorded time
if Ti502 == 1;
    Time = 267.8721;
    Shelf = 6;
    CL = 5; %min
    Output = 'Ti50_Vile2_Out.txt';
    FitString = 'Ti50 Vial #2';
elseif Ti504==1;
    Time = 267.9284;
     Shelf = 5;
     CL = 5; %min
     Output = 'Ti50_Vile4_Out.txt';
     FitString = 'Ti50 Vial #4';
elseif Ti501==1;
    Time = 267.8513;
    Shelf = 6;
    CL = 5; %min
    Output = 'Ti50_Vile1_Out.txt';
    FitString = 'Ti50 Vial #1';
elseif Ti503==1;
    Time = 267.8967;
    Shelf = 6;
    CL = 3; %min
    Output = 'Ti50_Vile3_Out.txt';
    FitString = 'Ti50 Vial #3';
elseif Ti505==1;
    Time = 267.9202;
    Shelf = 6;
    CL = 5; %min
    Output = 'Ti50_Vile5_Out.txt';
    FitString = 'Ti50 Vial #5';
elseif Ti473==1;
    Time = 267.9381;
```

```matlab
    Shelf = 5;
    CL = 5; %min
    Output = 'Ti47_Vile3_Out.txt';
    FitString = 'Ti47 Vial #3';
elseif Ti471==1;
    Time = 267.8581;
    Shelf = 6;
    CL = 5; %min
    Output = 'Ti47_Vile1_Out.txt';
    FitString = 'Ti47 Vial #1';
elseif Ti472==1;
    Time = 267.9030;
    Shelf = 6;
    CL = 3; %min
    Output = 'Ti47_Vile2_Out.txt';
    FitString = 'Ti47 Vial #2';
elseif Ti474==1;
    Time = 267.9274;
    Shelf = 6;
    CL = 5; %min
    Output = 'Ti47_Vile4_Out.txt';
    FitString = 'Ti47 Vial #4';
end
EoB = 266.0703;
DeltaT = Time-EoB; %days
%% Background Import
filename = '/Users/kadelorm/Documents/Research/AustinSc47/background.txt';
delimiter = {',',' '};
startRow = 5;
endRow = 4100;

%% Format string for each line of text:
%   column2: double (%f)
% For more information, see the TEXTSCAN documentation.
formatSpec = '%*s%f%*s%*s%*s%*s%*s%*s%*s%*s%*s%[^\n\r]';

%% Open the text file.
fileID = fopen(filename,'r');

%% Read columns of data according to format string.
% This call is based on the structure of the file used to generate this
% code. If an error occurs for a different file, try regenerating the code
% from the Import Tool.
dataArray2 = textscan(fileID, formatSpec, endRow-startRow+1, 'Delimiter',
delimiter, 'EmptyValue' ,NaN,'HeaderLines', startRow-1, 'ReturnOnError', false);
%% Allocate imported array to column variable names
```

```
RawData = dataArray{:, 1};
BG = dataArray2{:, 1};
BGCL = 1000;
BG2 = BG*(CL/BGCL);
Data = RawData-BG2;
EnergyBins = 0.5:.5:2048;
%%% Plot Energy Data
% Create figure
figure1 = figure;

% Create axes
axes1 = axes('Parent',figure1,'FontSize',16);
box(axes1,'on');
hold(axes1,'all');

% Create plot
plot(EnergyBins,Data)

% Create title
title('Gamma Spectra from Counter 77','FontSize',20);

% Create xlabel
xlabel('Energy (keV)','FontSize',20);

% Create ylabel
ylabel('Gamma Counts','FontSize',20);


annotation(figure1,'textbox',...
   [0.326555023923445 0.829932996976502 0.405581947743468
0.0609137055837563],...
   'String',{FitString},...
   'FontSize',20,...
   'LineStyle','none');
saveas(figure1,'figure1.eps','eps')
%%% Using a median filter to remove compton electrons
w=100
%# ask for inputs
tmp = input(sprintf('Set the Window width for median Filter (default w=100): ',w));
%# if the user hits 'return' without writing anything, tmp is empty and the default is
used
if ~isempty(tmp)
w = tmp;
end
Filter = medfilt1(Data,w);
%%% plot the filter
```

```matlab
figure3 =figure;
% Create axes
axes1 = axes('Parent',figure3,'FontSize',16);
box(axes1,'on');
hold(axes1,'all');

% Create plot
plot(EnergyBins,Filter)

% Create title
title('Filtered Electrons','FontSize',20);

% Create xlabel
xlabel('Energy (keV)','FontSize',20);

% Create ylabel
ylabel('Gamma Counts','FontSize',20);


annotation(figure3,'textbox',...
  [0.326555023923445 0.829932996976502 0.405581947743468
0.0609137055837563],...
  'String',{FitString},...
  'FontSize',20,...
  'LineStyle','none');
saveas(figure3,'figure3.eps','eps')
%%
Data2=Data-Filter;
for i=1:1:numel(Data2);
  if Data2(i)<=0;
    Data2(i)=0;
  end
end
%%% Plot Energy Data
% Create figure
figure2 = figure;

% Create axes
axes1 = axes('Parent',figure2,'FontSize',16);
box(axes1,'on');
hold(axes1,'all');

% Create plot
plot(EnergyBins,Data2)

% Create title
```

```matlab
title('Gamma Spectra from Counter 77 with background and compton continuum
removed','FontSize',20);

% Create xlabel
xlabel('Energy (keV)','FontSize',20);

% Create ylabel
ylabel('Gamma Counts','FontSize',20);


annotation(figure2,'textbox',...
    [0.326555023923445 0.829932996976502 0.405581947743468
0.0609137055837563],...
    'String',{FitString},...
    'FontSize',20,...
    'LineStyle','none');
saveas(figure2,'figure2.eps','eps')
%% Clear temporary variables
clearvars filename delimiter startRow endRow formatSpec fileID dataArray ans;
%% Efficiency Tables

Efffilename =
'/Users/kadelorm/Documents/Research/AustinSc47/Counter77EffTables.txt';
delimiter = ',';
format long
if Shelf==5
[~, ~, raw] =
xlsread('/Users/kadelorm/Documents/Research/AustinSc47/C77EfficiencyDat.xlsx
','Sheet1');
raw = raw(3:12,1:2);
data = reshape([raw{:}],size(raw));
ENERGY = data(:,1);
EFFICIENCY = data(:,2);
clearvars data raw cellVectors;
ShelfFitStr = 'Shelf 5';
Distance = .06; %cm
elseif Shelf==6
[~, ~, raw] =
xlsread('/Users/kadelorm/Documents/Research/AustinSc47/C77EfficiencyDat.xlsx
','Sheet1');
raw = raw(15:end,1:2);
data = reshape([raw{:}],size(raw));
ENERGY = data(:,1);
EFFICIENCY = data(:,2);
clearvars data raw cellVectors;
ShelfFitStr = 'Shelf 6';
```

```matlab
Distance =.05; %cm
end
%% Efficiency Interpolation
% Put them into proper format:
% http://www.mathworks.com/help/matlab/math/resizing-and-reshaping-
matrices.html
ENERGY_2 = reshape(ENERGY, 1, length(ENERGY));
EFFICIENCY_2 = reshape(EFFICIENCY, 1, length(EFFICIENCY));

%Must now interpolate the given numbers to match each of the energy groups
% used:
% Interpolation format: interp1(X,Y,xi) where xi is the number of
Interpdiv1 = (length(ENERGY_2)-1)/(length(EnergyBins(1:3668)));
xi = 1:Interpdiv1: (length(ENERGY_2))-2*Interpdiv1;
EffEnergy = interp1(1:length(ENERGY_2), ENERGY_2, xi);
EfficiencyInt = interp1(1:length(ENERGY_2), EFFICIENCY_2, xi);
%% Isolation of Peaks
hold off
% Sc47 Peak at 159.381 keV (68.3%)
figure2=figure(2);
Sc47PkFt = peakfit([EnergyBins(300:340)', Data2(300:340)])
GoodFit = 1;
%# ask for inputs
tmp = input(sprintf('If the fit looks good GoodFit=1; IF not GoodFit=2: ',GoodFit));
%# if the user hits 'return' without writing anything, tmp is empty and the default is
used
if ~isempty(tmp)
GoodFit = tmp;
end
if GoodFit ==1;
Sc47UpperBound = Sc47PkFt(2)+Sc47PkFt(4);
Sc47LowerBound = Sc47PkFt(2)-Sc47PkFt(4);
Sc47_159_Peaksum = sum(Data2(Sc47LowerBound*2:2*Sc47UpperBound));
elseif GoodFit==2;
delete(figure2);
figure2=figure(2);
plot(EnergyBins(300:340)',Data(300:340))
Sc47UpperBound = 320;
tmp = input(sprintf('Enter Upper Bound: ',Sc47UpperBound));
%# if the user hits 'return' without writing anything, tmp is empty and the default is
used
if ~isempty(tmp)
Sc47UpperBound = tmp;
end
Sc47LowerBound = 300;
%# ask for inputs
```

```matlab
tmp = input(sprintf('Enter Lower Bound: ',Sc47LowerBound));
%# if the user hits 'return' without writing anything, tmp is empty and the default is
used
if ~isempty(tmp)
Sc47LowerBound = tmp;
end
Cutoff1 = 0;
%# ask for inputs
tmp = input(sprintf('Enter Cutoff (default=0): ',Cutoff1));
%# if the user hits 'return' without writing anything, tmp is empty and the default is
used
if ~isempty(tmp)
Cutoff1 = tmp;
end
numbins=Sc47UpperBound-Sc47LowerBound;
Sc47_159_Peaksum = sum(Data(Sc47LowerBound*2:2*Sc47UpperBound))-
Cutoff1*numbins;
end
Sc47_159_intensity = 0.683;
Sc47halflife = 3.3492; %days
Sc47Lam = log(2)/Sc47halflife;
delete(figure2)
% Sc48 Peak at 983.526 keV (100.1%)
figure3 = figure(3);
Sc48PkFt1 = peakfit([EnergyBins(1950:1975)', Data2(1950:1975)])
%# ask for inputs
tmp = input(sprintf('If the fit looks good GoodFit=1; IF not GoodFit=2: ',GoodFit));
%# if the user hits 'return' without writing anything, tmp is empty and the default is
used
if ~isempty(tmp)
GoodFit = tmp;
end
if GoodFit ==1;
Sc48UpperBound1 = Sc48PkFt1(2)+Sc48PkFt1(4);
Sc48LowerBound1 = Sc48PkFt1(2)-Sc48PkFt1(4);
Sc48_983_Peaksum = sum(Data2(Sc48LowerBound1*2:2*Sc48UpperBound1));
elseif GoodFit==2;
delete(figure3);
figure3=figure(3);
plot(EnergyBins(1950:1975)',Data2(1950:1975))
 Sc48UpperBound1 = 1975;
%# ask for inputs
tmp = input(sprintf('Enter Upper Bound: ',Sc48UpperBound1));
%# if the user hits 'return' without writing anything, tmp is empty and the default is
used
if ~isempty(tmp)
```

```matlab
Sc48UpperBound1 = tmp;
end
Sc48LowerBound1 = 1950;
%# ask for inputs
tmp = input(sprintf('Enter Lower Bound: ',Sc48LowerBound1));
%# if the user hits 'return' without writing anything, tmp is empty and the default is
used
if ~isempty(tmp)
Sc48LowerBound1 = tmp;
end
Cutoff2 = 0;
%# ask for inputs
tmp = input(sprintf('Enter Cutoff (default=0): ',Cutoff2));
%# if the user hits 'return' without writing anything, tmp is empty and the default is
used
if ~isempty(tmp)
Cutoff2 = tmp;
end
numbins2=Sc48UpperBound1-Sc48LowerBound1;
Sc48_983_Peaksum = sum(Data2(Sc48LowerBound1*2:2*Sc48UpperBound1))-
Cutoff2*numbins2;
end
Sc48_983_intensity = 1.001;
Sc48halflife = 43.67/24; %days
Sc48Lam = log(2)/Sc48halflife;
delete(figure3)
% Sc48 Peak at 1312.120 keV (100.1%)
figure4 = figure(4)
Sc48PkFt2 = peakfit([EnergyBins(2600:2650)', Data2(2600:2650)])
%# ask for inputs
tmp = input(sprintf('If the fit looks good GoodFit=1; IF not GoodFit=2: ',GoodFit));
%# if the user hits 'return' without writing anything, tmp is empty and the default is
used
if ~isempty(tmp)
GoodFit = tmp;
end
if GoodFit ==1;
Sc48UpperBound2 = Sc48PkFt2(2)+Sc48PkFt2(4);
Sc48LowerBound2 = Sc48PkFt2(2)-Sc48PkFt2(4);
Sc48_1312_Peaksum = sum(Data2(Sc48LowerBound2*2:2*Sc48UpperBound2));
elseif GoodFit ==2;
delete(figure4);
figure4=figure(4);
plot(EnergyBins(2600:2650)',Data(2600:2650))
Sc48UpperBound2 = 2650;
%# ask for inputs
```

```matlab
tmp = input(sprintf('Enter Upper Bound: ',Sc48UpperBound2));
%# if the user hits 'return' without writing anything, tmp is empty and the default is
used
if ~isempty(tmp)
Sc48UpperBound2 = tmp;
end
Sc48LowerBound2 = 2600;
%# ask for inputs
tmp = input(sprintf('Enter Lower Bound: ',Sc48LowerBound2));
%# if the user hits 'return' without writing anything, tmp is empty and the default is
used
if ~isempty(tmp)
Sc48LowerBound2 = tmp;
end
Cutoff3 = 0;
%# ask for inputs
tmp = input(sprintf('Enter Cutoff (default=0): ',Cutoff3));
%# if the user hits 'return' without writing anything, tmp is empty and the default is
used
if ~isempty(tmp)
Cutoff3 = tmp;
end
numbins3=Sc48UpperBound2-Sc48LowerBound2;
Sc48_1312_Peaksum = sum(Data2(Sc48LowerBound2*2:2*Sc48UpperBound2))-
Cutoff3*numbins3;
end
Sc48_1312_intensity = 1.001;
delete(figure4)
% Sc46 Peak at 889.277 keV (99.98%)
figure5 = figure(5);
Sc46PkFt1 = peakfit([EnergyBins(1770:1790)', Data2(1770:1790)])
%# ask for inputs
tmp = input(sprintf('If the fit looks good GoodFit=1; IF not GoodFit=2: ',GoodFit));
%# if the user hits 'return' without writing anything, tmp is empty and the default is
used
if ~isempty(tmp)
GoodFit = tmp;
end
if GoodFit ==1;
Sc46UpperBound1 = Sc46PkFt1(2)+Sc46PkFt1(4);
Sc46LowerBound1 = Sc46PkFt1(2)-Sc46PkFt1(4);
Sc46_889_Peaksum = sum(Data2(Sc46LowerBound1*2:2*Sc46UpperBound1));
elseif GoodFit ==2;
delete(figure5);
figure5=figure(5);
plot(EnergyBins(1770:1790)',Data(1770:1790))
```

```
Sc46UpperBound1 = 1800;
%# ask for inputs
tmp = input(sprintf('Enter Upper Bound: ',Sc46UpperBound1));
%# if the user hits 'return' without writing anything, tmp is empty and the default is
used
if ~isempty(tmp)
Sc46UpperBound1 = tmp;
end
Sc46LowerBound1 = 1750;
%# ask for inputs
tmp = input(sprintf('Enter Lower Bound: ',Sc46LowerBound1));
%# if the user hits 'return' without writing anything, tmp is empty and the default is
used
if ~isempty(tmp)
Sc46LowerBound1 = tmp;
end
Cut0ff4 = 0;
%# ask for inputs
tmp = input(sprintf('Enter Cutoff (default=0): ',Cutoff4));
%# if the user hits 'return' without writing anything, tmp is empty and the default is
used
if ~isempty(tmp)
Cutoff4 = tmp;
end
numbins4=Sc46UpperBound1-Sc46LowerBound1;
Sc46_889_Peaksum = sum(Data2(Sc46LowerBound1*2:2*Sc46UpperBound1))-
Cutoff4*numbins4;
end
Sc46_889_intensity = .9989;
delete(figure5);
% Sc46 Peak at 1120.545 keV (99.98%)
figure6 = figure(6);
Sc46PkFt2 = peakfit([EnergyBins(2230:2250)', Data2(2230:2250)])
%# ask for inputs
tmp = input(sprintf('If the fit looks good GoodFit=1; IF not GoodFit=2: ',GoodFit));
%# if the user hits 'return' without writing anything, tmp is empty and the default is
used
if ~isempty(tmp)
GoodFit = tmp;
end
if GoodFit ==1;
Sc46UpperBound2 = Sc46PkFt2(2)+Sc46PkFt2(4);
Sc46LowerBound2 = Sc46PkFt2(2)-Sc46PkFt2(4);
else
delete(figure6);
figure6=figure(6);
```

```matlab
plot(EnergyBins(2230:2250)',Data(2230:2250))
Sc46UpperBound2 = 2260;
%# ask for inputs
tmp = input(sprintf('Enter Upper Bound: ', Sc46UpperBound2));
%# if the user hits 'return' without writing anything, tmp is empty and the default is
used
if ~isempty(tmp)
Sc46UpperBound2 = tmp;
end
Sc46LowerBound2 = 2220;
%# ask for inputs
tmp = input(sprintf('Enter Lower Bound: ', Sc46LowerBound2));
%# if the user hits 'return' without writing anything, tmp is empty and the default is
used
if ~isempty(tmp)
Sc46LowerBound2 = tmp;
end
Cutoff5 = 0;
%# ask for inputs
tmp = input(sprintf('Enter Cutoff (default=0): ',Cutoff5));
%# if the user hits 'return' without writing anything, tmp is empty and the default is
used
if ~isempty(tmp)
Cutoff5 = tmp;
end
numbins5=Sc46UpperBound2-Sc46LowerBound2;
Sc46_1120_Peaksum = sum(Data2(Sc46LowerBound2*2:2*Sc46UpperBound2))-
numbins5*Cutoff5;
end
Sc46_1120_Peaksum = sum(Data2(Sc46LowerBound2*2:2*Sc46UpperBound2));
Sc46_1120_intensity = 0.9989;
Sc46halflife = 83.79; %days
Sc46Lam = log(2)/Sc46halflife;
delete(figure6)
% Ca47 Peak at 1297.09 keV(67%)
figure7=figure(7);
Ca47PkFt = peakfit([EnergyBins(2585:2600)', Data2(2585:2600)])
%# ask for inputs
tmp = input(sprintf('If the fit looks good GoodFit=1; IF not GoodFit=2: ',GoodFit));
%# if the user hits 'return' without writing anything, tmp is empty and the default is
used
if ~isempty(tmp)
GoodFit = tmp;
end
if GoodFit ==1;
Ca47UpperBound = Ca47PkFt(2)+Ca47PkFt(4);
```

```matlab
Ca47LowerBound = Ca47PkFt(2)-Ca47PkFt(4);
Ca47_1297_Peaksum = sum(Data2(Ca47LowerBound*2:2*Ca47UpperBound));
else
delete(figure7);
figure7=figure(7);
plot(EnergyBins(2580:2610), Data2(2580:2610))
Ca47UpperBound = 2610;
%# ask for inputs
tmp = input(sprintf('Enter Lower Bound: ',Ca47UpperBound));
%# if the user hits 'return' without writing anything, tmp is empty and the default is
used
if ~isempty(tmp)
Ca47UpperBound = tmp;
end
Ca47LowerBound = 2580;
%# ask for inputs
tmp = input(sprintf('Enter Lower Bound: ',Ca47LowerBound));
%# if the user hits 'return' without writing anything, tmp is empty and the default is
used
if ~isempty(tmp)
Ca47LowerBound = tmp;
end
Cutoff6 = 0;
%# ask for inputs
tmp = input(sprintf('Enter Cutoff (default=0): ',Cutoff6));
%# if the user hits 'return' without writing anything, tmp is empty and the default is
used
if ~isempty(tmp)
Cutoff6 = tmp;
end
numbins6=Ca47UpperBound-Ca47LowerBound;
Ca47_1297_Peaksum = sum(Data2(Ca47LowerBound*2:2*Ca47UpperBound))-
Cutoff6*numbins6;
end

Ca47_1297_intensity = 0.67;
Ca47halflife = 4.536; %days
Ca47Lam = log(2)/Ca47halflife;
delete(figure7);
%% Accounting for efficiency
if Shelf == 6;
% Sc47 Peak at 159.381 keV (68.3%)
Eff159 = EfficiencyInt(1047);
Sc47_159Count = Sc47_159_Peaksum/(Sc47_159_intensity*Eff159*CL);
Sc47_159_PeaksumErr = sqrt(Sc47_159_Peaksum);
Sc47_159CountErr = Sc47_159_PeaksumErr/(Sc47_159_intensity*Eff159*CL);
```

```
% Sc48 Peak at 983.526 keV (100.1%)
Eff983 = EfficiencyInt(2683);
Sc48_983Count = Sc48_983_Peaksum/(Sc48_983_intensity*Eff983*CL);
Sc48_983_PeaksumErr = sqrt(Sc48_983_Peaksum);
Sc48_983CountErr = Sc48_983_PeaksumErr/(Sc48_1312_intensity*Eff983*CL);
% Sc48 Peak at 1312.120 keV (100.1%)
Eff1312 = EfficiencyInt(3256);
Sc48_1312Count = Sc48_1312_Peaksum/(Sc48_1312_intensity*Eff1312*CL);
Sc48_1312_PeaksumErr = sqrt(Sc48_1312_Peaksum);
Sc48_1312CountErr = Sc48_1312_PeaksumErr/(Sc48_1312_intensity*Eff1312*CL);
% Sc46 Peak at 889.277 keV (99.98%)
Eff889 = EfficiencyInt(2556);
Sc46_889Count = Sc46_889_Peaksum/(Sc46_889_intensity*Eff889*CL);
Sc46_889_PeaksumErr = sqrt(Sc46_889_Peaksum);
Sc46_889CountErr = Sc46_889_PeaksumErr/(Sc46_889_intensity*Eff889*CL);
% Sc46 Peak at 1120.545 keV (99.98%)
Eff1120 = EfficiencyInt(2865);
Sc46_1120Count = Sc46_1120_Peaksum/(Sc46_889_intensity*Eff1120*CL);
Sc46_1120_PeaksumErr = sqrt(Sc46_1120_Peaksum);
Sc46_1120CountErr = Sc46_1120_PeaksumErr/(Sc46_1120_intensity*Eff1120*CL);
% Ca47 Peak at 1297.09 keV(67%)
Eff1297 = EfficiencyInt(3221);
Ca47_1297Count = Ca47_1297_Peaksum/(Eff1297*Ca47_1297_intensity*CL);
Ca47_1297_PeaksumErr = sqrt(Ca47_1297_Peaksum);
Ca47_1297CountErr = Ca47_1297_PeaksumErr/(Ca47_1297_intensity*Eff1297*CL);
elseif Shelf ==5;
% Sc47 Peak at 159.381 keV (68.3%)
Eff159 = EfficiencyInt(1164);
Sc47_159Count = Sc47_159_Peaksum/(Sc47_159_intensity*Eff159*CL);
Sc47_159_PeaksumErr = sqrt(Sc47_159_Peaksum);
Sc47_159CountErr = Sc47_159_PeaksumErr/(Sc47_159_intensity*Eff159*CL);
% Sc48 Peak at 983.526 keV (100.1%)
Eff983 = EfficiencyInt(2702);
Sc48_983Count = Sc48_983_Peaksum/(Sc48_983_intensity*Eff983*CL);
Sc48_983_PeaksumErr = sqrt(Sc48_983_Peaksum);
Sc48_983CountErr = Sc48_983_PeaksumErr/(Sc48_983_intensity*Eff983*CL);
% Sc48 Peak at 1312.120 keV (100.1%)
Eff1312 = EfficiencyInt(3209);
Sc48_1312Count = Sc48_1312_Peaksum/(Sc48_1312_intensity*Eff1312*CL);
Sc48_1312_PeaksumErr = sqrt(Sc48_1312_Peaksum);
Sc48_1312CountErr = Sc48_1312_PeaksumErr/(Sc48_1312_intensity*Eff1312*CL);
% Sc46 Peak at 889.277 keV (99.98%)
Eff889 = EfficiencyInt(2628);
Sc46_889Count = Sc46_889_Peaksum/(Sc46_889_intensity*Eff889*CL);
Sc46_889_PeaksumErr = sqrt(Sc46_889_Peaksum);
Sc46_889CountErr = Sc46_889_PeaksumErr/(Sc46_889_intensity*Eff889*CL);
```

```
% Sc46 Peak at 1120.545 keV (99.98%);
Eff1120 = EfficiencyInt(2812);
Sc46_1120Count = Sc46_1120_Peaksum/(Sc46_889_intensity*Eff1120*CL);
Sc46_1120_PeaksumErr = sqrt(Sc46_1120_Peaksum);
Sc46_1120CountErr = Sc46_1120_PeaksumErr/(Sc46_1120_intensity*Eff1120*CL);
% Ca47 Peak at 1297.09 keV(67%);
Eff1297 = EfficiencyInt(3172);
Ca47_1297Count = Ca47_1297_Peaksum/(Eff1297*Ca47_1297_intensity*CL);
Ca47_1297_PeaksumErr = sqrt(Ca47_1297_Peaksum);
Ca47_1297CountErr = Ca47_1297_PeaksumErr/(Ca47_1297_intensity*Eff1297*CL);
end
%% Back Calculate to Activity at EoB
% Will give activities in Curies
Activity_Conversion = 2.22*(10^6); % 1 microCurie = 2.22e6 Decays/min
% Sc48 Peak at 983.526 keV (100.1%)
Sc48CountEoB1 = Sc48_983Count/exp(-Sc48Lam*DeltaT);
Sc48ActivityEoB1 = Sc48CountEoB1/Activity_Conversion
Sc48CountEoB1Err = Sc48_983CountErr/exp(-Sc48Lam*DeltaT);
Sc48ActivityEoB1Err = Sc48CountEoB1Err/Activity_Conversion
% Sc48 Peak at 1312.120 keV (100.1%)
Sc48CountEoB2 = Sc48_1312Count/exp(-Sc48Lam*DeltaT);
Sc48ActivityEoB2 = Sc48CountEoB2/Activity_Conversion
Sc48CountEoB2Err = Sc48_1312CountErr/exp(-Sc48Lam*DeltaT);
Sc48ActivityEoB2Err = Sc48CountEoB2Err/Activity_Conversion;
% Sc46 Peak at 889.277 keV (99.98%)
Sc46CountEoB1 = Sc46_889Count/exp(-Sc46Lam*DeltaT);
Sc46ActivityEoB1 = Sc46CountEoB1/Activity_Conversion
Sc46CountEoB1Err = Sc46_889CountErr/exp(-Sc46Lam*DeltaT);
Sc46ActivityEoB1Err = Sc46CountEoB1Err/Activity_Conversion
% Sc46 Peak at 1120.545 keV (99.98%)
Sc46CountEoB2 = Sc46_1120Count/exp(-Sc46Lam*DeltaT);
Sc46ActivityEoB2=Sc46CountEoB2/Activity_Conversion
Sc46CountEoB2Err = Sc46_1120CountErr/exp(-Sc46Lam*DeltaT);
Sc46ActivityEoB2Err = Sc46CountEoB2Err/Activity_Conversion
% Ca47 Peak at 1297.09 keV(67%)
Ca47CountEoB = Ca47_1297Count/exp(-Ca47Lam*DeltaT);
Ca47ActivityEoB=Ca47CountEoB/Activity_Conversion
Ca47CountEoBErr = Ca47_1297CountErr/exp(-Ca47Lam*DeltaT);
Ca47ActivityEoBErr = Ca47CountEoBErr/Activity_Conversion
% Sc47 Peak at 159.381 keV (68.3%)
Sc47CountEoB = ((Sc47_159Count-(Ca47CountEoB*(Ca47Lam/(Sc47Lam-
Ca47Lam))*exp(-Ca47Lam*DeltaT)))/exp(-Sc47Lam*DeltaT))-
(Ca47CountEoB*(Ca47Lam/(Ca47Lam-Sc47Lam)));
Sc47ActivityEoB = Sc47CountEoB/Activity_Conversion
```

```
Sc47CountEoBErr = ((Sc47_159CountErr-(Ca47CountEoBErr*(Ca47Lam/(Sc47Lam-
Ca47Lam))*exp(-Ca47Lam*DeltaT)))/exp(-Sc47Lam*DeltaT))-
(Ca47CountEoBErr*(Ca47Lam/(Ca47Lam-Sc47Lam)));
Sc47ActivityEoBErr = Sc47CountEoBErr/Activity_Conversion
%% Display
Isotope = char('Sc47', 'Sc46_889','Sc46_1120','Sc48_983', 'Sc48_1312', 'Ca47');
ActivityMicroCuries = [Sc47ActivityEoB, Sc46ActivityEoB1, Sc46ActivityEoB2,
Sc48ActivityEoB1, Sc48ActivityEoB2, Ca47ActivityEoB]';
ActivityError = [Sc47ActivityEoBErr, Sc46ActivityEoB1Err, Sc46ActivityEoB2Err,
Sc48ActivityEoB1Err, Sc48ActivityEoB2Err, Ca47ActivityEoBErr]';
Table = table(Isotope,ActivityMicroCuries,ActivityError)
writetable(Table, Output)
```

Bibliography

[1] Radioisotopes in Medicine, *World Nuclear Association*, April 2013. www.world-nuclear.org.

[2] Xu, J., Kenneth, M. D., Kochanek, D., Sherry, M. A., Murphy, L., *Deaths: final data for 2010*, 61(4): 31-33, 8 May 2013.

[3] M. Połosak, A. Piotrowska, S. Krajewski, and A. Bilewicz, Stability of 47 sc-complexes with acyclic polyamino-polycarboxylate ligands. *J Radioanal Nucl Chem*, 295(3):1867–1872, 2013.

[4] P. Rowshanfarzad, M. Sabet, A. Reza Jalilian, and M. Kamalidehghan, An overview of copper radionuclides and production of 61cu by proton irradiation of natzn at a medical cyclotron, *Applied Radiation and Isotopes*, 64(12):1563–1573, 12 2006.

[5] B. Bartoś, A. Majkowska, S. Krajewski, and A. Bilewicz, New separation method of no-carrier-added 47sc from titanium targets, *Radiochimica Acta*, 100(7):457–462, 2013/04/08 2012.

[6] T. Bokhari, A. Mushtaq, and I. Khan, Separation of no-carrier-added radioactive scandium from neutron irradiated titanium, *Journal of Radioanalytical and Nuclear Chemistry*, 283(2):389–393, 2010.

[7] L. F. Mausner, K. L. Kolsky, V. Joshi, and S. C. Srivastava, Radionuclide development at bnl for nuclear medicine therapy, *Applied Radiation and Isotopes*, 49(4):285–294, 4 1998.

[8] Isotope production and its application, *Los Alamos National Security*, 2010 http://isotopes.lanl.gov/isotopes.shtml

[9] W.D. Claus, *Radiation biology and medicine*, Reading, Massachusetts: Addison-Wesley, ch 7, pp 471-489, 1958.

[10] W. R. Hendee, *Radioactive isotopes in biological research*, Wiley, 1973, ch 7, pp 91-101, 1973.

[11] L. Pietrelli, L. Mausner, and K. Kolsky, Separation of carrier-free sc-47 from titanium targets, *Journal of Radioanalytical and Nuclear Chemistry*, 157(2):335–345, 03 1992.

[12] Mller, Cristina and Bunka, Maruta and Reber, Josefine and Fischer, Cindy and Zhernosekov, Konstantin and Trler, Andreas and Schibli, Roger, Promises of Cyclotron-Produced 44Sc as a Diagnostic Match for Trivalent -Emitters: In Vitro and In Vivo Study of a 44Sc-DOTA-Folate Conjugate, *Journal of Nuclear Medicine*, 54(12): 2168–2174, 2013.

[13] M. S. Gulley, H. Bach, F. M. Nortier, C. Pillai, L. J. Bitteker, K. D. John, F. O. Valdez, A. Seifter Exploring the energy/beam current parameter space for the isotope production facility (IPF) at LANSCE, *Los Alamos National Laboratory*, 2010.

[14] R. Garcia and I. Cohen, Evaluation of reactor induced (n, p) reactions for activation analysis of titanium in geological materials, *Journal of Radioanalytical and Nuclear Chemistry*, 82(2):353–361, 05 1984.

[15] Yagi, M., K Kondo Preparation of carrier-free 47Sc by the 48Ti (,p) reaction, *The International Journal of Applied Radiation and Isotopes*, Vol 28, Issue 5, May 1977, po 463-468, http://dx.doi.org/10.1016/0020-708X(77)90178-8.

[16] Schindewolf, U. and J. W. Irvine, Preparation of Carrer-Free Vanadium, Scandium, and Arsenic Activities from Cyclotron Targets by Ion Exchange, *Analytical Chemistry*, Vol 30: 906-8. 1958.

194

[17] J. T. Goorley, M. R. James, T. E. Booth, F. B. Brown, B. Forrest, J. S. Bull, L. J. Cox, J. W. Durkee, Jr., J. S. Elson, M. L. Fensin, M. Lorne, R. A. Forster, III, J. S. Hendricks, H. G. Hughes, III, R. C. Johns, B. C. Kiedrowski, R. L. Martz,S. G. Mashnik, G. W. McKinney, D. B. Pelowitz, R. E. Prael, J. E. Sweezy, L. S. Waters, T. Wilcox, A. J. Zukaitis, Initial MCNP6 Release Overview - MCNP6 Beta 3 *Los Alamos National Laboratory*, 2012.

[18] S. G. S. G. . Mashnik, A. J. A. J. . Sierk, and L. A. N. Laboratory, CEM2k - recent development in CEM, *Arxiv preprint nucl-th/0011064* (2000)

[19] S. G. Mashnik, K. K. Gudima, R. E. Prael, A. J. Sierk, M. I. Baznat, and N. V. Mokhov, CEM03.03 and laqgsm03.03 event generators for the MCNP6, MCNPX, and MARS15 transport codes, *arXiv preprint arXiv:0805.0751* (2008).

[20] J. S. Hendricks, G. W McKinney, L. S. Waters, T. L. Roberts, H. W Egdorf, J. P.Finch, H. R. Trellue, E. J. Pitcher, M. T. Swinhoe, S. T. Tobin, J. W. Durkee, MCNPX extensions: version 2.5.0, *Los Alamos National Laboratory*, 15 April 2005.

[21] D. P. Pelowitz, ed, MCNPX users manual: version 2.7.0, *Los Alamos National Laboratory*, 15 April 2011.

[22] J. W. Engle, M. R. James, S. G. Mashnik, C. T. Kelsey IV, L. E.Wolfsberg, D. A.Reass, M. A. Connors, H .T. Bach, M. E. Fassbender, K. D. John, E. R. Birnbaum, F. M.Nortier, *MCNPX characterization of the secondary neutron flux at the Los Alamos Isotope Production Facility*, *Los Alamos National Laboratory* New Mexico, USA, 2014.

[23] J. W. Engle, M. R. James, S. G Mashnik, C. T. Kelsey IV, L. E. Wolfsberg, D. A. Reass, M. A. Connors, H. T. Bach, M. E. Fassbender, K. D. John, E. R. Birnbaum, and F. M. Nortier. *MCNPX characterization of the secondary neutron*

195

flux at the Los Alamos Isotope Production Facility, *Lost Alamos National Laboratory* Los Alamos, 2014.

[24] D. W. McCarthy, R. E. Shefer, R. E. Klinkowstein, L. A. Bass, W. H. Margeneau, C. S. Cutler, C. J. Anderson, and M. J. Welch, Efficient production of high specific activity 64cu using a biomedical cyclotron, *Nuclear Medicine and Biology*, 24(1):35–43, 1 1997.

[25] S. Srivastava, Paving the way to personalized medicine: production of some theragnostic radionuclides at brookhaven national laboratory, *Seminars in Nuclear Medicine*, 99(10):635–640, 2011.

[26] G. Knoll. *Radiation Detection and Measurement*. John Wiley & Sons, Hoboken 2010.

[27] J. Taylor. *An Introduction to Error Analysis: The Study of Uncertainties in Physical Measurements*, A series of books in physics, University Science Books, ch 8, pp 181-209, South Orange, 1997.

[28] Titanium Dioxide, www.ffcr.or.jp.

[29] Aarnio, P. A., Ala-Heikkilae, J. J., Hakulinen, T. T., & Routti, J. T. 1994, Presented at the Conference on Methods and Applications of Radioanalytical Chemistry - 3, Kailua-Kona, Hawaii, 10-16 Apr. 1994, 10.

REPORT DOCUMENTATION PAGE

The public reporting burden for this collection of information is estimated to average 1 hour per response, including the time for reviewing instructions, searching existing data sources, gathering and maintaining the data needed, and completing and reviewing the collection of information. Send comments regarding this burden estimate or any other aspect of this collection of information, including suggestions for reducing the burden, to Department of Defense, Washington Headquarters Services, Directorate for Information Operations and Reports (0704-0188), 1215 Jefferson Davis Highway, Suite 1204, Arlington, VA 22202-4302. Respondents should be aware that notwithstanding any other provision of law, no person shall be subject to any penalty for failing to comply with a collection of information if it does not display a currently valid OMB control number.
PLEASE DO NOT RETURN YOUR FORM TO THE ABOVE ADDRESS.

1. REPORT DATE *(DD-MM-YYYY)*	2. REPORT TYPE	3. DATES COVERED *(From - To)*

4. TITLE AND SUBTITLE

5a. CONTRACT NUMBER

5b. GRANT NUMBER

5c. PROGRAM ELEMENT NUMBER

6. AUTHOR(S)

5d. PROJECT NUMBER

5e. TASK NUMBER

5f. WORK UNIT NUMBER

7. PERFORMING ORGANIZATION NAME(S) AND ADDRESS(ES)

**8. PERFORMING ORGANIZATION
REPORT NUMBER**

9. SPONSORING/MONITORING AGENCY NAME(S) AND ADDRESS(ES)

10. SPONSOR/MONITOR'S ACRONYM(S)

**11. SPONSOR/MONITOR'S REPORT
NUMBER(S)**

12. DISTRIBUTION/AVAILABILITY STATEMENT

13. SUPPLEMENTARY NOTES

14. ABSTRACT

15. SUBJECT TERMS

16. SECURITY CLASSIFICATION OF:			17. LIMITATION OF ABSTRACT	18. NUMBER OF PAGES	19a. NAME OF RESPONSIBLE PERSON
a. REPORT	b. ABSTRACT	c. THIS PAGE			
					19b. TELEPHONE NUMBER *(Include area code)*